By

Connor G. Hendrich

A dissertation submitted in partial fulfillment of the requirements for the degree of

Doctor of Philosophy

(Microbiology)

at the

UNIVERSITY OF WISCONSIN-MADISON

2021

Date of final oral examination: 12/2/2020

The dissertation is approved by the following members of the Final Oral Committee:

Caitilyn Allen, Professor, Plant Pathology
Andrew Bent, Professor, Plant Pathology
Mehdi Kabbage, Associate Professor, Plant Pathology
Laura Knoll, Professor, Medical Microbiology and Immunology
John-Demian Sauer, Associate Professor, Medical Microbiology and Immunology

Acknowledgements

I will start by thanking my advisor, Caitilyn Allen, for all of her mentorship and support. Besides all of your guidance on how to be a good scientist, I am extremely grateful for the time you spent to mentor me on outside skills like teaching, mentorship, and communication. I am lucky that you gave such a good 5-minute research talk during the first week of MDTP orientation. It introduced me to plant pathology and changed my life.

Thank you to all of my current and former labmates: April MacIntyre, Alicia Truchon, Corri Hamilton, Mariama Carter, Adam Bigot, Sanju Kunwar, Lavanya Babujee, Devanshi Khokhani, Madeline Hayes, Matt Pereyra, Jessica Prom, Olivia Steidl, Tiffany Lowe-Power, Beth Dalsing, Jon Jacobs, Jordan Weibel, Noah Kinscherf, and Yigeng Tan. All of you made it a joy to come to work, and I cannot think of a better group of people to have spent the past five years with. Especially thank you to Alicia Truchon for suffering with me through the crucible of RNA extractions for transcriptomics, Jon Jacobs for the excellent suggestion of said RNA-seq study, and Beth Dalsing for starting the nitric oxide project. Thank you to my undergrad, Yigeng Tan, for his patience as I spent the last half of his time in lab hunched in a corner writing this thesis.

Thank you to my committee: Laura Knoll, Andrew Bent, JD Sauer, and Mehdi Kabbage. I am grateful for all of your advice and guidance through my time at UW. I always left our meetings with much-needed focus, excitement, and direction.

Thank you to my long list of collaborators, especially André Xavier, Alessandra de Melo, Raka Mitra, Anjali Iyer-Pascuzzi, Valerian Meline, Sasha Kyrysyuk, Nina Denne, Alex Schultink, and Derrick Grunwald. All of you are proof that science is not only more effective when we work together, but it is also so much more enjoyable.

Thank you to my teaching mentors: Doug Rouse, Armila Aeilts, Amy Moser, Janet Batzli, Michelle Harris, Jae-Hyuk Yu, and John Roll.

Thank you to the MDTP and Plant Path communities, for providing two truly excellent homes at UW. Thank you to WEMP for letting me pretend to be a real plant pathologist and learn science outreach and communication.

Thank you to the Madison Area Jugglers, for throwing things at me until I felt at home.

Thank you to my family, especially to my parents for all of their love, their support, and for fostering a lasting love of learning in my brothers and I. I would not be where I am today without them.

Last, and most of all, thank you to Tayler for her love, her patience, and for always having my back.

ABSTRACT

Ralstonia solanacearum Secretion Systems: Critical virulence factors and points of vulnerability

Connor G. Hendrich

Under the supervision of Dr. Caitilyn Allen

University of Wisconsin-Madison

Ralstonia solanacearum (Rs) is a Gram-negative Betaproteobacterium that causes bacterial wilt disease on hosts like tomato, potato, and banana. Once established, it can be exceedingly difficult to treat. This, combined with its exceptionally wide host range, makes Rs a problem for agriculture around the world. Rs persists in the environment in the soil and enters the host through wounds and natural openings in the roots. From there, it travels to its preferred in-host niche, the xylem. Although Rs is slow-growing and sensitive to stress in vitro, Rs is well adapted to the xylem environment, where it grows to extremely high densities. Eventually, water flow is blocked, the host wilts, and Rs returns to the soil.

The xylem is not an especially nutrient-rich environment, and to thrive in this niche, *Rs* must influence its host. Secretion systems are essential virulence factors that allow bacteria to export virulence factors into their surroundings or into nearby host cells. While *Rs* relies on secretion systems, they can also be vulnerabilities, as when secreted effectors are recognized by the host immune system. This thesis examines the benefits and drawbacks of *Rs* secretion systems. First, I show how *Rs* links its virulence-promoting Type III Secretion System (T3SS) to

denitrifying respiration, which is important in the low-oxygen xylem sap. Because the T3SS is one of the most important *Rs* virulence factors, its regulation has been the subject of intense study. However, significant gaps remain in our understanding of how *Rs* coordinates the expression of the T3SS. Here, I show that a byproduct of denitrification, nitric oxide, activates the T3SS. My results indicate that *Rs* can use denitrification activity, to recognize that it is inside a host and turn on a key virulence factor. This result sheds light on the ongoing mystery of how *Rs* detects its in host environment.

I then describe a drawback to *Rs* secretion systems. *Rs* secretes several important virulence factors in through the Type II Secretion System (T2SS) and T2SS-defective *Rs* mutants cause little disease. We found that *Rs*-infecting phage phiAP1 uses the Type II Secretion System (T2SS) to enter cells of the bacterial host. Spontaneous phage-resistant mutants generally had inactivated T2SS. Further, I showed that the phage required T2SS activity, as targeted mutants that produce the T2SS complex, but cannot export cargo, were also resistant to the phage. This is useful because T2SS- *Rs* are avirulent, imposing a severe fitness cost on *Rs* that evolve resistance to the phage and suggesting that lytic phage phiAP1 has potential as a biocontrol agent to manage bacterial wilt disease. It also deepens our understanding of phage biology, and suggests a novel mechanism of phage infection using the T2SS.

Table of Contents

Acknowledgements	l
Abstract	iii
Table of Contents	v
List of Tables	viii
List of Figures	ix
Chapter 1: Introduction to virulence mechanisms and potential disease man	agement strategies
for bacterial wilts caused by the Ralstonia solanacearum species complex	1
Ralstonia solanacearum diversity and life cycle	2
Rs transitions between two distinct metabolic states during disease	3
Nitrogen metabolism plays an important role in the xylem	4
Rs secretion systems are key virulence factors	6
Type II Secretion	6
Type III Secretion	9
Type I and VI Secretion	11
Current management strategies for bacterial wilt disease	13
Chemical control of BWD	13
Host resistance	15
Biocontrol	17
Summary	20
Chapter 2: Nitric Oxide Regulates the <i>Ralstonia solanacearum</i> Type 3 Secret	t ion System 36
Abstract	37
Introduction	38
Results	40
Discussion	53
Methods	59
References	65

Chapter 3: A two-way street: the use of the Ralstonia solanacearum Type II Sec	retion System
during infection by the phage PhiAP1	80
Abstract	81
Introduction	81
Results	83
Discussion	98
Methods	103
References	108
Chapter 4: Summary and Future Directions	125
What is the mechanism of NO-mediated T3SS induction?	126
How do T2SS positive BIMs evade phiAP1?	134
Do divalent metal cation transports contribute to Rs survival in the xylem?	136
What are the <i>in planta</i> targets of the <i>Rs</i> Type III effectors RipAX1 and RipAX2	2? 138
Do Rs dehydrogenases contribute to anaerobic growth?	142
References	144
Appendix 1: Decoding tomato resistance to bacterial wilt disease using metatrar	nscriptomics
	151
Abstract	152
Introduction	152
Results	155
Discussion	167
Methods	169
References	171

Appendix 2: Characterization of seven new Ralstonia solanacearum infecting phages from	
Brazil	177
Abstract	178
Introduction	178
Results/Discussion	179
Methods	
References	187

List of Tables

Chapt	er 2	
	Supplementary Table 1: Bacterial strains, plasmids, and primers	73
Chapt	er 3	
	Table 1: Strain phenotypes	89
	Supplementary Table 1: Strains and plasmids	. 117
	Supplementary Table 2: Primers	. 119
	Supplementary Table 3: Unique BIM mutations	. 121
	Supplementary Table 4: Shared BIM mutations	. 123
Apper	ndix 1	
	Table 1: Experimental metadata	. 156
	Table 2: Percentage of differentially expressed genes shared between samples	. 163
Apper	ndix 2	
Дррсі		404
	Table 1: Host range panel details	. 181
	Table 2: Bp identity between phage genomes	. 184

List of Figures

Cha	pter	1
CHIA	ptei	_

	Figure 1: Rs life cycle
	Figure 2: Cross-section of tomato stems infected with green fluorescent protein (GFP)-
	expressing Rs strain GMI1000, visualized by fluorescence microscopy24
	Figure 3: Lytic vs lysogenic bacteriophage lifecycles
Chapt	er 2
	Figure 1: Nitric oxide affects expression of the <i>R. solanacearum</i> T3SS
	Figure 2: Nitric oxide causes broad changes in <i>R. solanacearum</i> gene expression 44
	Figure 3: Expression analysis of selected T3SS-related genes by qRT-PCR validated RNA-
	seq results
	Figure 4: Nitric oxide alters expression of T3SS-related genes both in vitro and in planta
	Supplementary Figure 1: Growth and NO levels of R. solanacearum strains under
	denitrifying conditions in culture75
	Supplementary Figure 2: In vitro cell densities and tomato stem colonization of samples
	used in RNA-seq76
	Supplementary Figure 3: General RNA-seq quality

Chapter 3

	Figure 1: Mutations in <i>gspL</i> and <i>pilD</i> confer resistance to PhiAP1
	Figure 2: Rs mutants BIM4 and BIM30 are both deficient in T2SS, but only BIM30 is
	deficient in Tfp-mediated twitching motility
	Figure 3: PhiAP1 infection depends on an active T2SS, and not the Tfp 92
	Figure 4: BIM4 and BIM 30 have reduced virulence on tomato
	Supplementary Figure 1: Targeted mutations in the T2SS reduce the export of pectir
	methylesterase
	Supplementary Figure 2: Introducing gspG under the control of the rpIM promoter
	increases gspG expression roughly ten-fold
	Supplementary Figure 3: Only T2SS positive BIMs retain virulence
Chapt	er 4
	Figure 1: The predicted S-nitrosylation site Cys112 of Rs GMI1000 hrpB is well-conserved
	among many HrpB homologues
	Figure 2: Mutating Cys112, a predicted S-nitrosylation (SNO) site, in hrpB alters Rs
	behaviors in planta
	Figure 3: RipAX1 and RipAX2 form discrete foci when expressed in tobacco leaves 141

Appendix 1

Fi	igure 1: Host range assay18	30
Appendix	x 2	
111	lay be involved in tomato defense against bwb	,,
m	nay be involved in tomato defense against BWD16	35
Fi	igure 3: MetaRNASeq revealed membrane-bound Pattern recognition receptors the	at
Fi	igure 2: Samples correlated more closely within experiments than within genotypes 16	52

Chapter 1

Introduction to virulence mechanisms and potential disease management strategies for bacterial wilts caused by the *Ralstonia solanacearum* species complex

Portions of this chapter will appear as:

Hendrich, C. G., Hamilton, C., MacIntyre A., Truchon, A. N., Allen, C. (2020). Metabolic strategies and adaptations of the *Ralstonia solanacearum* species complex. *MMBR*.

Contributions: CA contributed text related to *Rs* diversity and genome structure, ANT contributed text related to denitrification, AM contributed text related to cell wall breakdown products, CGH wrote the remainder of the text.

Ralstonia solanacearum diversity and life cycle

Members of the Ralstonia solanacearum (Rs) species complex (RSSC) cause bacterial wilt disease on a wide variety of plant hosts. A wide host range, an ability to persist in the environment, and a tremendous impact on crop yields make Rs is one of the most destructive bacterial plant pathogens in the world (1). Collectively, Rs strains can infect over 50 plant families and over 250 known plant species, many of which are economically important crops (2–4). These include a large number of solanaceous crops like tomato, potato, and eggplant, but also a diverse array of hosts from other families such as geranium, blueberry, peanut, and banana (5, 6). In addition, Rs can infect and persist in weeds and native plants. The RSSC encompasses a great deal of diversity. Rs strains have been categorized into four Phylotypes, each roughly corresponding to their geographic origin. Phylotype I strains originated in Asia, Phylotype II strains in the Americas, Phylotype III strains from Africa, and Phylotype IV strains are from Indonesia and Japan. While no individual Rs strain can infect the entire known diversity of RSSC hosts, individual strains can infect and cause disease on multiple hosts, sometimes plants as distantly related as tomato (a dicot) and banana (a monocot) (7). The Rs genome is composed of two circular replicons, with a chromosome of about 3.7 Mb and a megaplasmid that is roughly 2.1 Mb (8). Rs is naturally competent, and genomic analyses suggest that this group undergoes frequent gene losses, rearrangements, and horizontal gene transfer (9).

Despite the heterogeneity of both the RSSC and its known host range, most *Rs*-plant interactions follow a similar life cycle (Figure 1). *Rs* exist in the environment primarily in the soil and infested water. The bacteria can sense root exudates and travel using swimming motility

towards potential hosts (10). Once it encounters a host root, an *Rs* cell can enter through wounds or natural openings, such as the ones produced by the emergence of lateral roots (11). After entering the root cortex, the *Rs* makes its way to its major in-host niche, the water-transporting xylem tissue (12). By traveling through xylem vessels, *Rs* can spread throughout the host and grow to extremely high densities (13–15). Inside the xylem, *Rs* is able to extract nutrients from the host, evade host defenses, and thrive (16). Through the sheer mass of bacteria, the copious extracellular polymeric substances (EPS), and the action of cell wall degrading enzymes, the flow of water through infected xylem ceases, and the host wilts (14, 17, 18). *Rs* then escapes from the dying plant into the soil, where it is free to find other hosts and repeat the cycle. While most *Rs* strains follow this general life cycle, some Phylotype IV banana and clove strains are transmitted by insect vectors (19).

Rs transitions between two distinct metabolic states during disease

As for any organism, pathogenic or otherwise, the acquisition of nutrients is key to *Rs* success. The transition between a low cell density state in the rhizosphere and a high-density state during disease in the xylem shapes how *Rs* uses available nutrients. Density dependent quorum sensing (QS) regulates these processes by means of the regulator PhcA, which responds to the quorum signaling molecules 3-OH-MAME or 3-OH-PAME (20–22). Many *Rs* virulence factors, such as EPS, are metabolically expensive, so to conserve resources, *Rs* cells only produce these virulence factors after they have reached a threshold population size corresponding to around 1x10⁷ CFU/ml in broth culture, when PhcA is activated by accumulated QS signal. Additionally, a wide swath of metabolic genes respond to PhcA-dependent QS (23,

24). Transcriptomic analyses of $\Delta phcA$ mutants that are unable to transition into a high cell density state showed that the metabolic capacity of Rs is substantially greater at a low cell density than a high cell density. This means that Rs are highly adaptive scavengers in the soil and early in disease. However, once the cells reach a quorum in the xylem, they switch priorities from producing many enzymes to consume a wide array of nutrients to catabolizing a limited set of nutrients that are readily available *in planta*. This strategy conserves energy to invest in producing metabolically costly virulence factors that ensure success in the host.

Nitrogen metabolism plays an important role in the xylem

The xylem environment provides several challenges for microbial growth. One of these is a low availability of oxygen (13). However, the xylem does contain high levels of nitrate (13). Although Rs was initially described as an obligate aerobe, if nitrate is available Rs can grow anaerobically (25–27). Like many soil-dwelling proteobacteria, Rs can respire on nitrate, and some strains can completely denitrify NO_3^- to N_2 gas (28). Denitrification is the stepwise reduction of inorganic nitrate (NO_3^-) to nitrite (NO_2^-), then to nitric oxide (NO), followed by nitrous oxide (N_2O), and finally to di-nitrogen gas (N_2). In this process, the N molecule serves as a terminal electron acceptor to generate a proton gradient across the cytoplasmic membrane, which can be used to synthesize ATP. Rs gains most of the energy from this process from the reduction of nitrate to nitrite, and the remaining dissimilatory enzymes may function primarily to reduce the toxic cellular byproducts of previous reductions (13, 28). However, deletions of each enzyme in the denitrification pathway led to only minor virulence defects on tomato, suggesting that Rs has alternative means of producing energy in low-oxygen conditions (13).

During denitrification, Rs produces NO, a highly diffusible free radical that is the most consequential Reactive Nitrogen Species (RNS) (13, 29). NO reacts readily with transition metals, but NO itself is not particularly reactive (29, 30). However, NO can be activated by the presence of ROS, especially the radical superoxide (O_2). NO reacts extremely rapidly with (O_2) to form peroxynitrite (ONOO⁻) which, while not a radical, is a potent oxidant that can attack many cellular targets and is responsible for many of the toxic effects of RNS. In addition, NO can interact directly with O_2 to form nitrogen dioxide (N_2O), which can combine with another NO or N₂O molecule to form higher-order, more reactive nitrogen compounds like N₂O₃ or N₂O₄, which can readily attack free thiols. Nitrite can also be converted to N₂O₃ in acidic conditions (30). These byproducts of Rs denitrification, when combined with host-produced ROS and RNS, can destroy cell walls, enzymes, nucleic acids, and other vital cellular machinery. (29). This chemistry is significant for Rs behavior in planta for two reasons: the endogenous NOproducing denitrification pathway is highly expressed when the bacterium grows in the xylem, and Rs must manage exogenous host-produced ROS stress during infection (13, 31–33). To protect themselves from these destructive metabolites, Rs needs protective measures to export, breakdown, or otherwise neutralize the destructive threat created by denitrification. Rs encode multiple NO-detoxifying enzymes, including the NO reductase NorB (NO to NO₃-) and the oxido-reductase HmpX, which can convert NO to NO₃ using O₂ or, under anaerobic conditions, to N_2O .

Rs secretion systems are key virulence factors

While *Rs* are well-adapted to acquiring nutrients from their surroundings both inside a host and in the environment, additional virulence factors are required for disease. Gramnegative bacteria are defined by their complex cell wall, consisting of an inner and outer lipid bilayer membrane enclosing the periplasm and a thin layer of peptidoglycan (34). To influence their environment, bacteria have evolved sophisticated machinery to transport materials from the cell interior across the cell wall. These secretion systems are often key virulence factors for bacterial pathogens (35). All RSSC strains characterized to date encode both Type II and Type III secretion systems, which have been extensively studied with respect to their effects on virulence. *Rs* strains additionally encode a Type VI Secretion System and numerous Type I Secretion loci (36, 37).

Type II Secretion

The Type II Secretion System (T2SS) transports folded protein cargo from the periplasmic space across the outer membrane (38, 39). The T2SS is a complex structure, composed of linked inner and outer membrane complexes that form a channel across the outer membrane. Periplasmic cargo is loaded into the complex through interactions with the inner membrane protein GspC and the periplasmic domain of the outer membrane secretin GspD (40, 41). Once inside the complex, the cargo is pushed out of the cell by the extension of a pseudopilus. The pseudopilus is created by the action of the members of the inner membrane complex, with the cytoplasmic ATPase GspE providing the energy to add pseudopilin monomers to the growing pseudopilus (38).

Rs strain GMI1000 encodes two predicted T2SS loci. One of these, on the main chromosome, has been well studied and is critical for virulence. Although the complete repertoire of T2SS enzymes is not known, the complex is known to secrete plant cell wall degrading enzymes (pCWDEs) (42). pCWDEs are a common virulence factor of plant pathogens, allowing invading pathogens to break down the thick cell walls of host cells in order to invade, spread within the host, or to acquire nutrients (Figure 2). Rs encode six known pCWDEs: a cellobiohydrolase (cbhA), a pectin methylesterase (pme), three polygalacturonases (pehABC), and an endogluconase (egl) (42). PehABC and Pme all degrade pectin, whereas Egl and CbhA degrade cellulose (42–44). Of these, single mutants lacking cbhA, pehB, pehA, and egl all have slightly reduced virulence, with the egl and cbhA mutants having the largest defects. The virulence reductions caused by mutating multiple pCWDEs is generally additive, with the greatest effect seen in a mutant lacking all six genes. However, a completely T2SS negative mutant is significantly less virulent than the mutant lacking all six pCWDEs, suggesting that the T2SS secretes additional unknown virulence factors (42).

Curiously, pCWDEs that are secreted via the *Rs* T2SS do not seem to be used to generate nutrition for *Rs*. Galacturonic acid, the main sugar component of pectin, can be used as a sole carbon source by *Rs*, but a mutant that cannot import galacturonic acid or grow on this sugar as sole carbon source retains full virulence on tomato (45). Cellobiose, the main degradation product of cellulose, cannot be used as a sole carbon source by many *Rs* isolates, despite the fact that it is relatively abundant in xylem sap from infected tomatoes (16, 42, 46). Instead, the pCWDEs seem to be primarily used to facilitate pathogen spread within the stem. Degrading cell wall components may also help the bacteria escape detection by the plant. Many plant cell

wall breakdown components are potent Damage Associated Molecular Patterns (DAMPS) (47). A triple PehABC mutant was more virulent than a PehAB double mutant, suggesting that the product of PehC, an *exo*-polygalacturonase that releases mono- and di- galacturonate may trigger a host response (45).

In addition to the well-studied T2SS locus found on the main chromosome, Rs encodes a second T2SS locus on the megaplasmid. It is not unknown for bacteria to use multiple copies of secretion systems. For example, P. aeruginosa encodes two separate T2SS that have nonoverlapping functions, as one cannot complement mutants lacking the other (48). These systems secrete different cargo, and the T2SS proteins responsible for loading cargo cannot interact with enzymes secreted by the other system (40). The function of the second Rs T2SS is not known. It contains clear homologs for the outer membrane secretin, GspD, multiple pseudopilins, the inner membrane protein GspD, and the intracellular ATPase GspE. However, the locus does not contain obvious homologs for GspC, GspM, and GspL, three inner membrane proteins that help link inner and outer membrane complexes (38). Instead, the operon includes four predicted hypothetical membrane proteins that have only weak similarity to known T2SS proteins. It is unknown if these four genes function in the same way as GspC, GspM, and GspL. Published Rs transcriptomes suggest that the system is not well expressed in planta, is negatively regulated by the transcriptional virulence and host invasion regulators HrpG and HrpB, and is strongly repressed in the low-cell density mimicking ΔphcA mutant (23, 24, 49– 53). The locus appears to be well-conserved in genomes of strains from all four phylotypes, including insect vectored strains causing banana blood disease and Sumatra disease of cloves. It is unclear what function is driving the retention and conservation of this locus, although its lack of expression *in planta* could suggest it contributes to *Rs* survival in the environment.

Type III Secretion

The Type III Secretion System (T3SS) acts as a molecular syringe, injecting protein effectors directly into the cytoplasm of a neighboring eukaryotic cell through a modified pilus structure (35). The T3SS is a common virulence factor in many Gram-negative bacterial plant pathogens (54). Through a combination of *in silico* predictions, gene expression studies of T3SS regulator mutants, and secretion assays, over one hundred T3Es have been identified in the RSSC (8, 55–57). The number of T3E's encoded by individual strains vary, but the average number of effectors encoded is around 70 (58). Of these, only 16 are found in 95% of sequenced *Rs* genomes (59). This large repertoire of effectors may explain the very wide host range of most RSSC strains.

essential for successful plant infection (60). Even when T3SS- mutants are introduced in high numbers directly into the host xylem, they are unable to cause disease and their populations slowly drops below detectable levels (16). The function of T3Es has thus been a topic of intense study. However, because most *Rs* T3Es do not have known homologs and because many T3Es have redundant functions, determining their activity is challenging. The effectors whose functions have been elucidated generally have been shown to either interfere with host defense signaling pathways or alter host metabolism to favor the pathogen (58).

Because the T3SS is a complex and energetically expensive molecular machine, its expression is tightly controlled, with the major determinate of its expression being the presence of a host (See Chapter 2, Figure 1a) (52). Expression of most T3SS structural genes and effectors are directly activated by the AraC-type transcriptional regulator HrpB (53). HrpB expression is in turn controlled by two more transcriptional regulators, HrpG and PrhG (61). HrpG integrates at least three environmental factors. It is activated by a signaling cascade initiated by the cell surface receptor PrhA, which responds to the presence of plant cell wall material (62). Puzzlingly, a PrhA mutant retains full virulence, suggesting complex and possibly redundant regulatory mechanisms. However, HrpG also responds to an unknown soluble signal produced by plant cells, which was demonstrated by showing that HrpG is activated by plant cells even in the absence of PrhA (63). Finally, HrpG is repressed by the Rs QS regulator PhcA, but only in vitro (64). Outside of the plant, T3SS genes are repressed in rich media (52). This has led to the use of low-cell density Rs in minimal media as so-called "hrp inducing media" when studying the T3SS in vitro, although it is not known why rich media represses T3SS expression. Because of the QS-dependency of HrpG, it was predicted that the T3SS may be important only early in disease. However, the first transcriptomic studies of Rs in planta revealed that T3SS genes were highly expressed in planta even during late disease, when the cells were at a high density (49). This discrepancy was explained in part by the discovery of PrhG, which is a close homolog of HrpG that is activated by PhcA-dependent QS (61). The combined action of HrpG and PrhG may ensure sustained expression of the T3SS throughout disease. Several additional factors are required for T3SS gene expression. These include the three-gene operon prhKLM, which encodes two subunits of a predicted allophonate hydrolase and a LamB/YcsF family

protein (65). PrhKLM act via PrhG and is required for T3SS gene expression (65). Two other transcription factors, PrhO and PrhN, also positively regulate T3SS genes in *Rs* (66, 67). Despite intense study, many key questions remain about how the Rs T3SS is regulated. These include the identity of the cell wall component recognized by PrhA, the identity of the unknown soluble signal that activates HrpG in the presence of a host, the specific metabolic cues that affect T3SS gene expression in culture, and the exact function of PrhKLMNO during disease.

Despite their importance for virulence, T3Es can also represent vulnerabilities for the pathogen. Because they are injected directly into the host cytoplasm, they cannot be easily hidden from the host's system. Many plants have evolved resistance genes (R genes) that specifically recognize T3Es (68). Once an R gene product recognizes its cognate effector, the plant initiates an immediate and powerful counterattack, inducing a rapid targeted cell death response that kills host cells around the pathogen and limits their spread. This process is called the Hypersensitive Response (HR) and is a factor that limits the host range of individual *Rs* species (69). As discussed below, the speed and specificity of HR makes R genes an attractive way to design strategies to combat bacterial wilt disease, and some R genes specific to *Rs* have been discovered and employed in the field.

Type I and VI Secretion

In addition to Type II and Type III secretion systems, *Rs* also encodes a Type VI secretion system (T6SS). The T6SS is found in a wide array of Gram-negative bacteria and transports protein effectors from the cytoplasm directly into a neighboring bacterial or eukaryotic cell (35). T6SS loci are composed of at least thirteen different genes and may have evolved from a

T4-like bacteriophage (70). Because the T6SS can inject proteins across both prokaryotic and eukaryotic membranes, the T6SS can contribute to both virulence of pathogens and also to competition with other microbes. Both of these functions have been demonstrated for T6SSs of plant pathogenic bacteria (71). While the functions of T6SS secreted cargo in Rs have not yet been described, a few studies have begun to examine the role the system play in the Rs life cycle. Zhang, et al. showed that the predicted T6SS genes are active and that T6SS- mutants had reduced motility and biofilm production (72). These deficiencies were enough to delay disease development on tomato. T6SS components were also overproduced by two cold-tolerant Rs strains while they grew on tomato seedlings at the cool temperature of 18°C (73). It is not clear what role the T6SS might play during cool virulence, although a similar temperaturedependence was seen in the T6SS of the root nodulating bacterium Rhizobium leguminosarum (74). However, a transcriptomic study of the cool-virulent strain UW551 did not find any significant difference in T6SS gene expression between 20°C and 28°C when the strain grew in either rich media or tomato stems (75). In the same study, the non-cool virulent strain GMI1000 had lower expression of three T6SS genes at cool temperatures in rich media. Examining the potential roles of the T6SS in both virulence and inter-microbe competition in Rs may be a fruitful area of future study.

Type I Secretion Systems (T1SS) are a diverse category of exporters that span both membranes and export a variety of different cargo into the extracellular space, including small molecules like antibiotics and divalent cations (35). *Rs* encode multiple copies and types of these secretions systems, most of which have not been specifically studied (37). Brown, et al. examined the role of the RND MDR exporter AcrAB-TolC in the Phylotype II strain K60. This

efflux pump system is highly expressed *in planta*, and mutants lacking the exporter had slightly reduced virulence on tomato (76). The authors found that the $\Delta acrA$ mutant had increased sensitivity to several chemicals including plant-produced antimicrobial compounds such as caffeic acid, esculentin, tomatine, and berberine. Other T1SS loci may provide Rs with the ability to resist other chemical stressors and may be a promising area of future study.

Current management strategies for bacterial wilt disease

The destructiveness and global distribution of BWD means that effective control of *Rs* is an important goal. A range of management techniques have been employed, with various degrees of efficacy. Cultural practices such as preventing the introduction of the pathogen to a field or greenhouse, the proper disinfection of farm equipment, and the production of clean seed are important first steps for combating the disease (77). If a field or region is already infested, more direct approaches can include chemical treatment, genetic resistance, and biocontrol.

Chemical control of BWD

Chemical pesticides have long been studied and used to combat BWD (77). One technique is soil fumigation, where large areas of soil are treated with toxic compounds to directly kill a pathogen (78). Fumigants included methyl bromide, metam sodium, chloropicrin, and sodium azide (78, 79). The effectiveness of these treatments varied widely, and often did not lead to complete control of the disease. Besides incomplete effectiveness, many of these chemical treatments have negative environmental and human health effects (80, 81). Methyl

stratospheric ozone layer (82). Other concerns over effects on the native soil microbiota and the potential for resistant pathogen isolates are also drawbacks to chemical fumigation (77). Less toxic pesticides such as phosphorous acid or the heat treatment of soil by solarization have also been studied for their ability to control *Rs* in the soil (77, 83).

Rather than directly attacking the pathogen, recent attempts to chemically control BWD have focused on priming the host and rhizosphere to fight against *Rs*. A range of chemicals including acibenzolar-S-methyl, silicon, the chitin derivative chitosan, and Validamycin A can all induce host resistance to *Rs* (84–87). Typically these chemicals trigger plant systemic acquired resistance, which primes the plant to respond more quickly to invading pathogens (77). Validamycin A may also have direct antibacterial activity due to its ability to inhibit the *Rs* trehalase enzyme, which make a potential carbon source unavailable to *Rs* (86). While induced resistance can be effective, its use should be weighed against the yield cost of maintaining a constant low-level immune response, although these drawbacks depend on the identity of the host and abundance of the pathogen (88).

Long-term cultivation of susceptible crops in regions where *Rs* is endemic has allowed researchers to examine the interplay between bulk soil properties and BWD incidence. Two long-term studies of soil chemistry in tomato and tobacco fields in southern China found a link between a lower soil pH and increased BWD severity (89, 90) Li et al. further showed that soil amendments that increase soil pH, like wood ash and lime, significantly reduced BWD incidence (89). However, the exact mechanism of this interaction is unclear, as pH can be both a cause and consequence of a variety of biological factors. Altered soil pH was associated with different

rates of *Rs* growth, different rates of expression of both bacterial virulence genes and host resistance genes, nutrient availability in the soil, and different compositions of non-pathogenic soil microbes (89, 90). Teasing apart these interactions could facilitate development of more specific BWD treatments. Other attempts to modify bulk soil properties have increased available carbon in the soil through soil amendments like biochar and other organic matter such as plant waste (77, 91).

Host resistance

One of the most common and most effective strategies for combating plant pathogens is planting genetically resistant hosts. Farmers have selected for genetic disease resistance for thousands of years, long before we had any knowledge of the mechanisms involved. The plant immune system has two main layers. The first layer, called pattern triggered immunity (PTI), depends on the detection of conserved Microbial Associated Molecular Pathogens (MAMPs) (92). Common bacterial MAMPs include surface exposed components like flagellin or LPS and cytoplasmic components like EF-Tu. After a host pattern recognition receptor detects a microbial MAMP, several innate immune responses are triggered, such as reinforcement of cell walls with callose or production of antimicrobial compounds like ROS. While this first layer of immunity is sufficient for the vast majority of microbes, successful pathogens can overcome these defenses, either by disguising or hiding potential MAMPs or by deploying secreted effectors that specifically block parts of the PTI signaling cascade. *Rs*, for example, encodes a modified version of flagellin that does not elicit host responses and also deploys several T3Es such as RipAD and RipAR that are known to suppress innate immunity (93–95). Host genes

involved in triggering PTI have been successfully manipulated to create transgenic crop lines that are more resistant to *Rs*. For example, the Ef-Tu receptor EFR from *Arabidopsis thaliana* can be introduced into tomato to significantly reduce the severity of both BWD and bacterial spot caused by *Xanthomonas spp* (96).

The second layer of plant defense often takes advantage of the same secreted effectors that help pathogens colonize their hosts. As described above, products of plant resistance genes (R genes) recognize specific pathogen effectors (68). Once recognition occurs, the HR is rapidly induced to kill tissue around the pathogen and isolate it. This highly effective way of controlling pathogen growth is called Effector Triggered Immunity (ETI). Because of the specificity of the recognition, the speed of the response, and the severity of the response, R genes have been an area of intense study for combating plant diseases. R genes from several hosts can recognize Rs. Tobacco, for example, can recognize three Rs effectors: RipAA, RipP1, and RipB; both wild and cultivated eggplant can recognize the effector RipAX2; and Arabidopsis can recognize RipP2 (97–100). As with EFR, the transfer of R genes between hosts either by conventional breeding or using biotechnology can be an effective way of creating new resistant crop varieties. For example, it was recently shown that the tobacco R gene Roq1, which recognizes the Rs effector RipB, can expressed in tomato to significantly reduce BWD symptoms (101).

Although gene for gene resistance mediated by R genes is effective for controlling *Rs*, many important crop hosts lack this type of immunity. For example, tomato, one of the world's most important vegetable crops, has no known R genes against *Rs*. Instead, tomato bacterial wilt resistance is quantitative, depends on several different loci, and may rely on PTI (69). The

presence of multiple loci involved in resistance can make it hard to introduce these traits into commercially viable varieties (102). For example, one *Rs* resistance locus in the widely used tomato breeding line Hawaii7996 is so tightly linked to small fruit size that breeders have been unable to separate the two traits. These problems can be circumvented by grafting a resistant rootstock to the aboveground portion (scion) of a commercially desirable but susceptible variety (103). Although these grafted plants are more expensive to produce, this process is commonly used around the world, and can be an economically viable way of growing crops in areas with high pressure from BWD (104).

Biocontrol

Biocontrol is a less environmentally destructive way to control *Rs*. It offers several potential benefits, including a reduced danger of toxicity to farm workers and ecosystems, reduced need for repeated applications when agents can replicate in the field, and high specificity (77). As with chemical treatments, the exact mechanism of control depends on the particular biocontrol agent (BCA), but can include passively increasing host health, priming host innate defenses, competition for niches in the rhizosphere or inside the host, or direct bactericidal effects (77, 105–108). Many bacterial and fungal BCAs have been proposed and tested against *Rs*, including non-pathogenic *Ralstonia* species (77).

Bacteriophages are promising BCAs. The appeal of these viruses lies in their diversity and abundance, their high degree of specificity and lethality against *Rs* and the fact that they replicate in the environment only if the target pathogen is present (109). Phage-based biocontrol products have already been registered and produced to combat other plant

diseases, including bacterial speck, fire blight, and potato soft rot (109, 110). Although many attempts have been made to isolate *Rs*-specific phages, there are as yet no commercially available products to combat BWD (111). Several factors must be considered in choosing phages and designing biocontrol protocols. For example, while a phage isolate may be effective at killing *Rs in vitro*, its activity in the field may be reduced or altered due to factors such as limited spread due to adsorption to soil particles or damage from the UV radiation in sunlight (109). In addition, bacteria have an arsenal of immune mechanisms to combat phages, including restriction enzymes, abortive infection systems, toxin-antitoxin systems, CRISPR, and the ability to mutate surface receptors of phages (109, 112). Although most *Rs* strains do encode a CRISPR system, a recent study found it is not functional in culture (113). However, the choice of antiphage-mechanism depends on external environmental pressures, and CRISPR could play a role when *Rs* must compete with diverse microbial competitors in the environment (112).

Regardless of the mechanism, treating *Rs* with phages in the laboratory quickly drives evolution of resistant mutants (113, 114). Wang et al. tested the ability of a cocktail of up to four phages to control bacterial wilt on tomato in greenhouse and field experiments (115). While the cocktail significantly reduced disease and *Rs* density in the rhizosphere, resistant mutants were easily isolated even from soil treated with combinations of phages. Interestingly, these isolates had broad resistance to the phage cocktail, but they also had a significantly slower growth rate, so the implication of anti-viral resistance for long-term use of phage therapy to control BWD in the field remains unclear.

The dynamics and infection mechanisms may also affect the utility of specific phages as BCAs. Fujiwara et al. studied a panel of lytic *Rs*-infecting phages both in culture and on tomato seedlings. One phage had a significantly slower replication cycle and did not completely suppress *Rs* growth in culture (116). Other, more aggressive phages isolates exerted strong selection pressure that led to *Rs* phage resistance and eventually allowed rapid bacterial growth. In contrast the less aggressive isolate kept bacterial populations at a consistent, low level over a period of 150 hours. The slow-growing isolate was effective at reducing *Rs* infection of tomato seedlings, suggesting that the lower aggression of the isolate kept *Rs* populations low enough to reduce disease while not providing enough selection pressure to allow resistance to take over the population.

An additional aspect of phage biology to consider is the choice of a lytic vs lysogenic phage (Figure 3). In general, studies have focused on lytic phages that killing their host (109). Yet *Rs* is readily infected by lysogenic phages, and temperate phages from the genus Inoviridae can be found in the genomes of *Rs* isolates (117, 118). Some of these may be useful in controlling BWD because they reduce the expression of virulence factors like motility and T3SS (119, 120). However, an opposite dynamic is equally possible, and Addy et al. found that the presence of a prophage actually increased virulence by altering the regulation of density dependent QS and allowing the infected strain to grow more aggressively *in planta* (121).

It is clear that while phages are promising biocontrol candidates, more work is needed to understand the complex dynamics between phage, bacteria, host, and the environment.

While several phages have been patented for use against BWD, none are commercially available (111). In the future, they may play a vital role in a BWD control regimen, perhaps

combined with other strategies. For example, combining phages with another BCA, an avirulent strain of *Rs*, was more effective at controlling disease on tobacco than the bacterial BCA alone (122). Gaining a nuanced understanding of phage biology and modes of resistance may help us design long-lasting phage biocontrol strategies.

Summary

Members of the RSSC are effective pathogens on a wide variety of plant hosts due to their arsenal of virulence factors and their metabolic adaptation to the xylem environment. While these adaptations are vital to the pathogen's ability to cause disease, their very importance makes them points of vulnerability. Secreted T3Es can be recognized by the host, triggering powerful immune responses, and phages can co-opt different molecular machinery in *Rs*, subverting the bacterium from the inside. Humans can take advantage of these interactions to design resilient BWD management practices. In this thesis, I will describe two advances in our knowledge of *Rs* virulence factors.

In Chapter 2, I describe a previously unknown link between nitrogen metabolism and the T3SS, adding to the complex picture of T3SS regulation in *Rs*. We showed that NO produced as a byproduct of denitrifying metabolism induced the expression of the T3SS. In culture, we found that increasing NO levels either through chemical NO donors or using a *Rs* mutant that overproduces NO increased the expression of T3SS genes. *In planta*, a *Rs* mutant that cannot produce NO had reduced T3SS gene expression. This additional layer of regulation, tied to a foundational element of *Rs* metabolism, highlights the importance of the T3SS for *Rs* fitness.

Chapter 3 describes the mechanism of infection of the an *Rs*-specific bacteriophage phiAP1. Our experiments show that phiAP1 requires a functioning T2SS to infect *Rs*. This means that evolving phage resistance can force the pathogen to give up a major element of its virulence arsenal. I will be co-first author of a paper describing this work, which is the product of a collaboration with phage biologists.

These chapters demonstrate both the importance of bacterial secretion systems for *Rs* during BWD and how they can be used by humans to combat BWD. The appendix describes an initial genetic characterization of seven new *Rs*-infecting phages and how transcriptomics can be used to better understand genetic resistance to *Rs* in tomato.

In addition, during my Ph.D. I also contributed work that earned me authorship on the following papers:

Lowe-Power TM, Hendrich CG, von Roepenack-Lahaye E, Li B, Wu D, Mitra R, Dalsing BL, Ricca
P, Naidoo J, Cook D, Jancewicz A, Masson P, Thomma B, Lahaye T, Michael AJ, Allen C.
2018. Metabolomics of tomato xylem sap during bacterial wilt reveals *Ralstonia*solanacearum produces abundant putrescine, a metabolite that accelerates wilt disease.
Environ Microbiol 20:1330–1349.

Thomas, N. C., Hendrich, C. G., Gill, U. S., Allen, C., Hutton, S. F., Schultink, A. (2020) 'Roq1 confers resistance to *Xanthomonas, Pseudomonas syringae* and *Ralstonia solanacearum* in tomato', *Frontiers in Plant Science*, 11(463).

- Hamilton, C.D., Steidl, O.R., Macintyre, A.M., Hendrich, C.G. and Allen, C. (2020) *Ralstonia* solanacearum depends on catabolism of myo-inositol, sucrose, and trehalose for virulence in an infection stage-dependent manner. *MPMI*.
- Truchon, A. N., Dalsing, B. D., Khokhani, D., Lowe-Power, T., MacIntyre, A., Hendrich, C. G., McDonald, B., Ailloud, F., Anex, R., Klassen, J., Gonzalez-Orta, E., Currie, C., Prior, P., Allen, C. Subgroups in the *Ralstonia solanacearum* species complex use divergent respiratory strategies to grow in tomato xylem

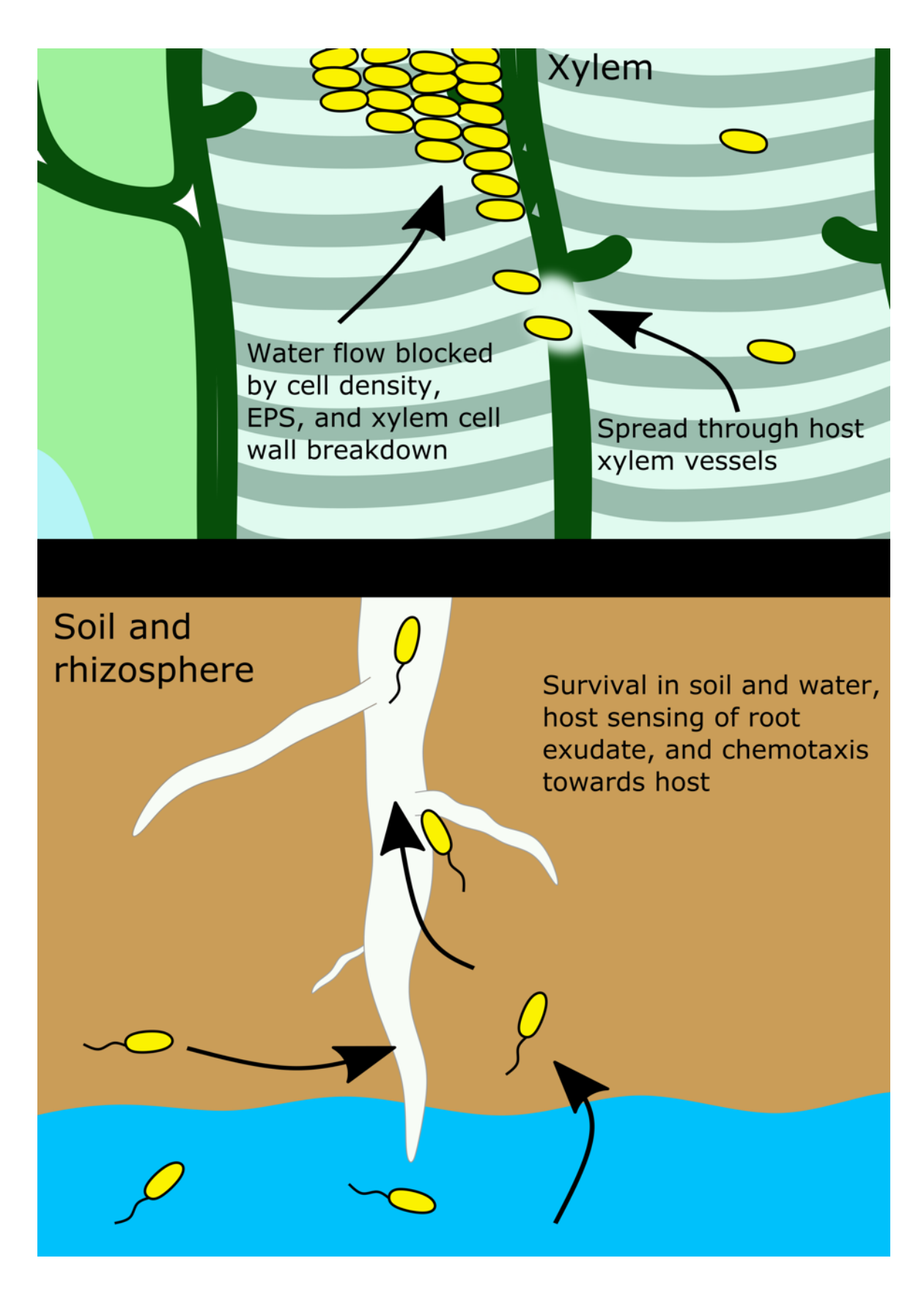


Figure 1. Rs life cycle

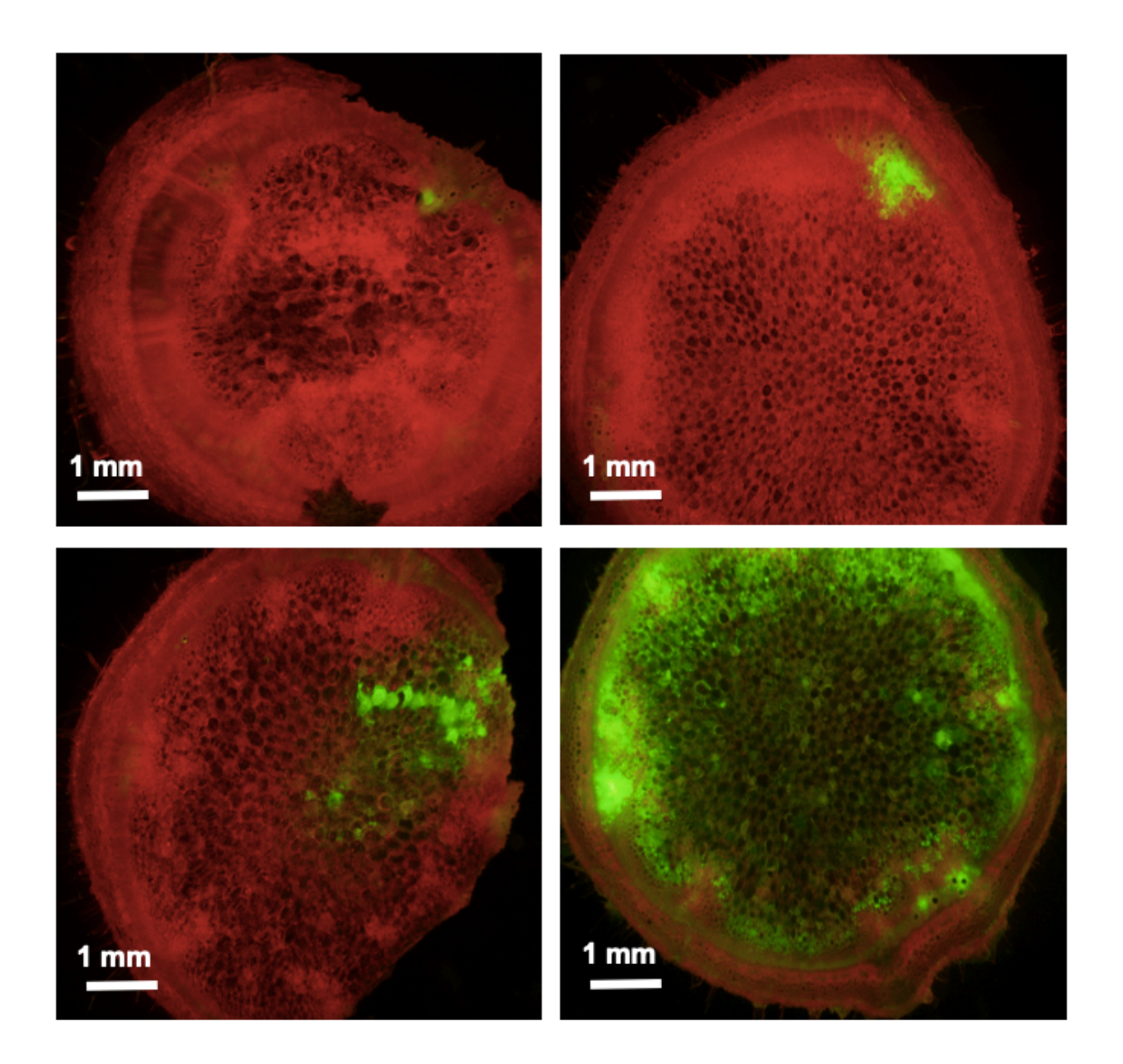


Figure 2. Cross-section of tomato stems infected with green fluorescent protein (GFP)-expressing *Rs* strain GMI1000, visualized by fluorescence microscopy. Lateral spread out of xylem vessels is enabled by pathogen-produced plant cell wall-degrading enzymes. Photo credit: Connor G. Hendrich.

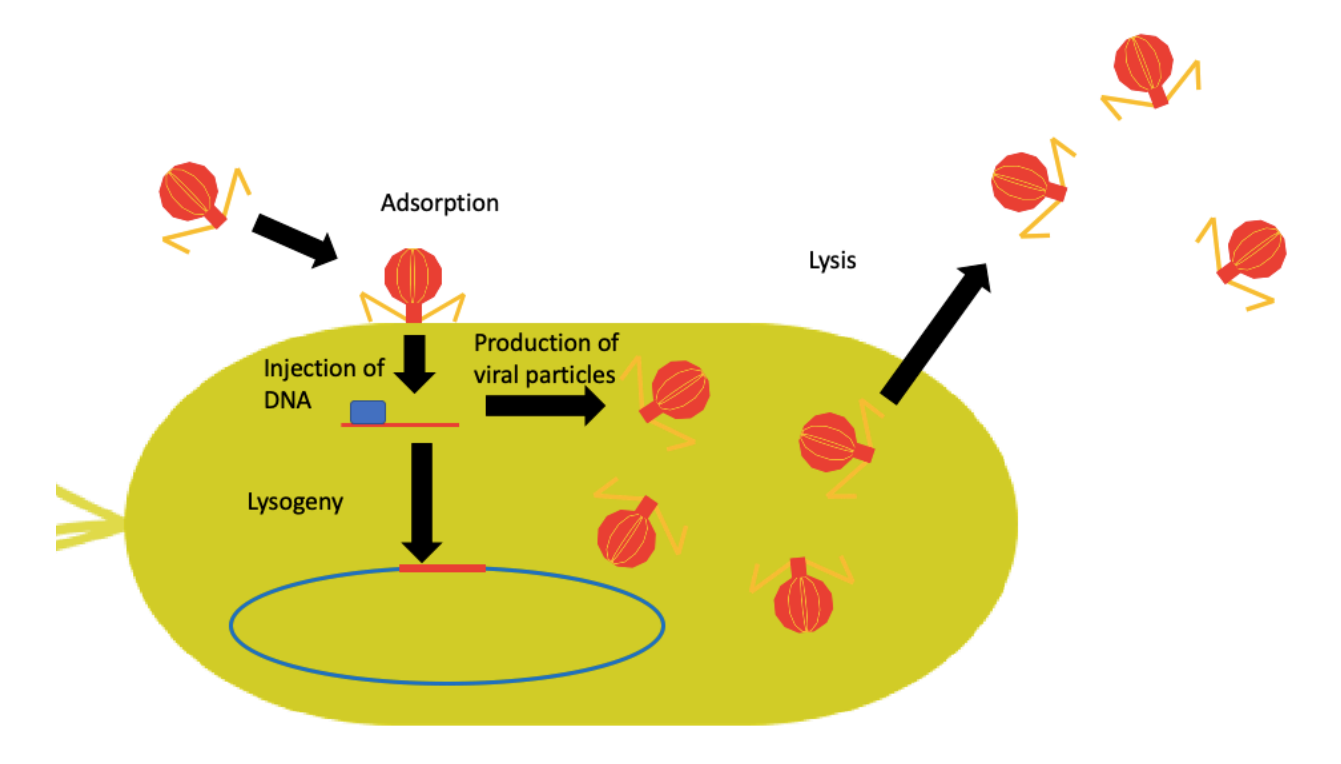


Figure 3. Lytic vs lysogenic bacteriophage lifecycles

References

- Mansfield J, Genin S, Magori S, Citovsky V, Sriariyanum M, Ronald P, Dow M, Verdier V, Beer S V., Machado MA, Toth I, Salmond G, Foster GD. 2012. Top 10 plant pathogenic bacteria in molecular plant pathology. Mol Plant Pathol 13:614–629.
- 2. Hayward AC, Hartman GL. 1994. The hosts of *Pseudomonas solanacearum*, p. 9–24. *In*Bacterial Wilt: The Disease and its Causative Agent, Pseudomonas solanacearum, 1st ed.
 Wallingford, UK.
- 3. Betney R, de Silva E, Krishnan J, Stansfield I. 2010. Autoregulatory systems controlling translation factor expression: thermostat-like control of translational accuracy. RNA 16:655–63.
- 4. Buddenhagen I, Kelman A. 1964. Biological and physiological aspects of bacterial wilt caused by *Pseudomonas solanacearum*. Annu rev Phytopathol 2:203–230.
- 5. Strider DL, Jones RK, Haygood RA. 1981. Southern bacterial wilt of geranium caused by *Pseudomonas solanacearum*. Plant Dis 65:52–53.
- 6. Bocsanczy AM, Espindola AS, Norman DJ. 2019. Whole-Genome Sequences of *Ralstonia solanacearum* Strains P816, P822, and P824, Emerging Pathogens of Blueberry in Florida. Microbiol Resour Announc 8:1–2.
- 7. Ailloud F, Lowe TM, Robène I, Cruveiller S, Allen C, Prior P. 2016. In planta comparative transcriptomics of host-adapted strains of *Ralstonia solanacearum*. PeerJ 2016.
- 8. Salanoubat M, Genin S, Artiguenave F, Gouzy J, Mangenot S, Arlat M, Billault A, Brottier P, Camus JC, Cattolico L, Chandler M, Choisne N, Claudel-Renard C, Cunnac S, Demange N, Gaspin C, Lavie M, Moisan A, Robert C, Saurin W, Schiex T, Siguier P, Thébault P, Whalen M, Wincker P, Levy M, Weissenbach J, Boucher C a. 2002. Genome sequence of the plant pathogen *Ralstonia solanacearum*. Nature 415:497–502.
- 9. Genin S, Denny TP. 2012. Pathogenomics of the *Ralstonia solanacearum* species complex. Annu Rev Phytopathol 50:67–89.
- 10. Yao J, Allen C. 2006. Chemotaxis Is required for virulence and competitive fitness of the bacterial wilt pathogen *Ralstonia solanacearum* 188:3697–3708.
- 11. Vasse J, Frey P, Trigalet A. 1994. Microscopic studies of intercellular infection and protoxylem invasion of tomato roots by *Pseudomonas solanacearum*. MPMI 8:241–251.
- 12. Caldwell D, Kim B, Iyer-Pascuzzi AS. 2017. *Ralstonia solanacearum* differentially colonizes roots of resistant and susceptible tomato plants. Phytopathology 107:528–536.
- 13. Dalsing BL, Truchon AN, Gonzalez-Orta ET, Milling AS, Allen C. 2015. Ralstonia

- solanacearum uses inorganic nitrogen metabolism for virulence, ATP production, and detoxification in the oxygen-limited host xylem environment. MBio 6:1–13.
- 14. Tran T, MacIntyre A, Khokhani D, Hawes MC, Allen C. 2016. Extracellular DNases of *Ralstonia solanacearum* modulate biofilms and facilitate bacterial wilt virulence. Environ Microbiol Environ Microbiol Reports 00:1–15.
- 15. Monteiro F, Genin S, van Dijk I, Valls M. 2012. A luminescent reporter evidences active expression of *Ralstonia solanacearum* type III secretion system genes throughout plant infection. Microbiol (United Kingdom) 158:2107–2116.
- 16. Lowe-Power TM, Hendrich CG, von Roepenack-Lahaye E, Li B, Wu D, Mitra R, Dalsing BL, Ricca P, Naidoo J, Cook D, Jancewicz A, Masson P, Thomma B, Lahaye T, Michael AJ, Allen C. 2018. Metabolomics of tomato xylem sap during bacterial wilt reveals *Ralstonia solanacearum* produces abundant putrescine, a metabolite that accelerates wilt disease. Environ Microbiol 20:1330–1349.
- 17. Kao CC, Barlow E, Sequeira L. 1992. Extracellular polysaccharide is required for wild-type virulence of *Pseudomonas solanacearum*. J Bacteriol 174:1068–1071.
- 18. Liu H, Zhang S, Schell MA, Denny TP. 2005. Pyramiding unmarked deletions in *Ralstonia solanacearum* shows that secreted proteins in addition to plant cell-wall-degrading enzymes contribute to virulence. Mol Plant Microbe Interact 18:1296–1305.
- 19. Safni I, Subandiyah S, Fegan M. 2018. Ecology, epidemiology and disease management of *Ralstonia syzygii* in Indonesia. Front Microbiol 9:1–11.
- 20. Lowe-Power TM, Khokhani D, Allen C. 2018. How *Ralstonia solanacearum* Exploits and Thrives in the Flowing Plant Xylem Environment. Trends Microbiol.
- 21. Flavier AB, Clough SJ, Schell MA, Denny TP. 1997. Identification of 3-hydroxypalmitic acid methyl ester as a novel autoregulator controlling virulence in *Ralstonia solanacearum*. Mol Microbiol 26:251–259.
- 22. Kai K, Ohnishi H, Shimatani M, Ishikawa S, Mori Y, Kiba A, Ohnishi K, Tabuchi M, Hikichi Y. 2015. Methyl 3-Hydroxymyristate, a diffusible signal mediating *phc* quorum sensing in *Ralstonia solanacearum*. ChemBioChem 16:2309–2318.
- 23. Khokhani D, Lowe-Power TM, Tran TM, Allen C. 2017. A Single Regulator Mediates Strategic Switching between Attachment / Spread and Growth / Virulence in the Plant Pathogen *Ralstonia solanacearum*. MBio 8:1–20.
- 24. Perrier A, Barlet X, Peyraud R, Rengel D, Guidot A, Genin S. 2018. Comparative transcriptomic studies identify specific expression patterns of virulence factors under the control of the master regulator PhcA in the *Ralstonia solanacearum* species complex. Microb Pathog 116:273–278.

- 25. Hayward AC, El-Nashaar HM, Nydegger U, de Lindo L. 1990. Variation in nitrate metabolism in biovars of *Pseudomonas soalanacearum*. J Appl Bacteriol 269–280.
- 26. Yabuuchi E, Kawumura Y, Ezaki T. 2015. *Ralstonia*, p. . *In* Whitman, WB (ed.), Bergey's Manual of Systematics of Archaea and Bacteria. Springer, New York.
- 27. Prior P, Ailloud F, Dalsing BL, Remenant B, Sanchez B, Allen C. 2016. Genomic and proteomic evidence supporting the division of the plant pathogen *Ralstonia solanacearum* into three species. BMC Genomics 17:1–11.
- 28. Zumft WG. 1997. Cell biology and molecular basis of denitrification. Microbiol Mol Biol Rev 61:533–616.
- 29. Beckman JS, Koppenol WH. 1996. Nitric oxide, superoxide, and peroxynitrite: the good, the bad, and ugly. Am J Physiol 271:C1424-37.
- 30. Van Faassen E, Vanin AF. 2007. Nitric oxide radicals and their reactionsRadicals for Life: The Various Forms of Nitric Oxide. Elsevier B.V.
- 31. Colburn-Clifford JM, Scherf JM, Allen C. 2010. *Ralstonia solanacearum* Dps contributes to oxidative stress tolerance and to colonization of and virulence on tomato plants. Appl Environ Microbiol 76:7392–9.
- 32. Flores-Cruz Z, Allen C. 2009. *Ralstonia solanacearum* Encounters an Oxidative Environment During Tomato Infection. MPMI.
- 33. Lamb C, Dixon RA. 1997. The oxidative burst in plant disease resistance. Annu Rev Plant Physiol Plant Mol Biol 48:251–275.
- 34. Beveridge TJ. 1999. Structures of gram-negative cell walls and their derived membrane vesicles. J Bacteriol 181:4725–4733.
- 35. Costa TRD, Felisberto-Rodrigues C, Meir A, Prevost MS, Redzej A, Trokter M, Waksman G. 2015. Secretion systems in Gram-negative bacteria: structural and mechanistic insights. Nat Rev Microbiol 13:343–59.
- 36. Guidot A, Prior P, Schoenfeld J, Carrère S, Genin S, Boucher C. 2007. Genomic structure and phylogeny of the plant pathogen *Ralstonia solanacearum* inferred from gene distribution analysis. J Bacteriol 189:377–387.
- 37. Genin S, Boucher C. 2004. Lessons learned from the genome analysis of *Ralstonia solanacearum*. Annu Rev Phytopathol 42:107–134.
- 38. Mclaughlin LS, Haft RJF, Forest KT. 2012. Structural insights into the Type II secretion nanomachine. Curr Opin Struct Biol 22:208–216.

- 39. Yan Z, Yin M, Xu D, Zhu Y, Li X. 2017. Structural insights into the secretin translocation channel in the type II secretion system. Nat Struct Mol Biol 24:177–183.
- 40. Douzi B, Ball G, Cambillau C, Tegoni M, Voulhoux R. 2011. Deciphering the Xcp *Pseudomonas aeruginosa* Type II Secretion machinery through multiple interactions with substrates. J Biol Chem 286:40792–40801.
- 41. Korotkov K V., Johnson TL, Jobling MG, Pruneda J, Pardon E, Héroux A, Turley S, Steyaert J, Holmes RK, Sandkvist M, Hol WGJ. 2011. Structural and functional studies on the interaction of GspC and GspD in the Type II Secretion System. PLoS Pathog 7.
- 42. Liu H, Zhang S, Schell M a, Denny TP. 2005. Pyramiding unmarked deletions in *Ralstonia solanacearum* shows that secreted proteins in addition to plant cell-wall-degrading enzymes contribute to virulence. Mol Plant Microbe Interact 18:1296–1305.
- 43. Denny TP, Carney BF, Schell MA. 1990. Inactivation of multiple virulence genes reduces the ability of *Pseudomonas solanacearum* to cause wilt symptoms. Mol Plant Microbe Interact 3:293–300.
- 44. Huang Q, Allen C. 2000. Polygalacturonases are required for rapid colonization and full virulence of *Ralstonia solanacearum* on tomato plants. Physiol Mol Plant Pathol 57:77–83.
- 45. González ET, Allen C. 2003. Characterization of a *Ralstonia solanacearum* operon required for polygalacturonate degradation and uptake of galacturonic acid. Mol Plant-Microbe Interact 16:536–544.
- 46. Hayward AC. 1964. Characteristics of *Pseudomonas solanacearum*. J Appl Bacteriol 27:265–277.
- 47. Hou S, Liu Z, Shen H, Wu D. 2019. Damage-associated molecular pattern-triggered immunity in plants. Front Plant Sci 10.
- 48. Ball G, Durand É, Lazdunski A, Filloux A. 2002. A novel type II secretion system in *Pseudomonas aeruginosa*. Mol Microbiol 43:475–485.
- 49. Jacobs JM, Babujee L, Meng F, Milling AS, Allen C. 2012. The *in planta* transcriptome of *Ralstonia solanacearum*: conserved physiological and virulence strategies during bacterial wilt of tomato. MBio 3:e00114-12.
- 50. Mori Y, Ishikawa S, Ohnishi H, Shimatani M, Morikawa Y, Hayashi K, Ohnishi K, Kiba A, Kai K, Hikichi Y. 2017. Involvement of ralfuranones in the quorum sensing signalling pathway and virulence of *Ralstonia solanacearum* strain OE1-1. Mol Plant Pathol 1–10.
- 51. Hayashi K, Senuma W, Kai K, Kiba A, Ohnishi K, Hikichi Y. 2019. Major exopolysaccharide, EPS I, is associated with the feedback loop in the quorum sensing of *Ralstonia*

- solanacearum strain OE1-1. Mol Plant Pathol 20:1740–1747.
- 52. Valls M, Genin S, Boucher C. 2006. Integrated Regulation of the Type III Secretion System and Other Virulence Determinants in *Ralstonia solanacearum*. PLoS Pathog 2:e82.
- 53. Occhialini A, Cunnac S, Reymond N, Genin S, Boucher C. 2005. Genome-wide analysis of gene expression in *Ralstonia solanacearum* reveals that the *hrpB* gene acts as a regulatory switch controlling multiple virulence pathways 18:938–949.
- 54. Büttner D, Bonas U. 2006. Who comes first? How plant pathogenic bacteria orchestrate type III secretion. Curr Opin Microbiol 9:193–200.
- 55. Genin S, Gough CL, Zischek C, Boucher CA. 1992. Evidence that the *hrpB* gene encodes a positive regulator of pathogenicity genes from *Pseudomonas solanacearum*. Mol Microbiol 6:3065–3076.
- 56. Cunnac S, Occhialini A, Barberis P, Boucher C, Genin S. 2004. Inventory and functional analysis of the large Hrp regulon in *Ralstonia solanacearum*: identification of novel effector proteins translocated to plant host cells through the type III secretion system. Mol Microbiol 53:115–128.
- 57. Mukaihara T, Tamura N, Iwabuchi M. 2010. Genome-wide identification of a large repertoire of *Ralstonia solanacearum* Type III effector proteins by a new functional screen. Mol Plant Microbe Interact 23:251–62.
- 58. Landry D, González-Fuente M, Deslandes L, Peeters N. 2020. The large, diverse, and robust arsenal of *Ralstonia solanacearum* Type III effectors and their in planta functions. Mol Plant Pathol 1–12.
- 59. Sabbagh CRR, Carrere S, Lonjon F, Vailleau F, Macho AP, Genin S, Peeters N. 2019. Pangenomic Type III effector database of the plant pathogenic *Ralstonia* spp. PeerJ 7:e7346.
- 60. Boucher CA, Barberis PA, Trigalet AP, Demery DA. 1985. Transposon mutagenesis of *Pseudomonas solanacearum*: Isolation of Tn5-induced avirulent mutants. J Gen Microbiol 131:2449–2457.
- 61. Zhang Y, Chen L, Yoshimochi T, Kiba A, Hikichi Y, Ohnishi K. 2013. Functional analysis of *Ralstonia solanacearum* PrhG regulating the *hrp* regulon in host plants. Microbiol (United Kingdom) 159:1695–1704.
- 62. Aldon D, Brito B, Boucher C, Genin S. 2000. A bacterial sensor of plant cell contact controls the transcriptional induction of *Ralstonia solanacearum* pathogenicity genes. Embo J 19:2304–2314.
- 63. Zuluaga AP, Puigvert M, Valls M. 2013. Novel plant inputs influencing Ralstonia

- *solanacearum* during infection. Front Microbiol 4:1–7.
- 64. Génin S, Brito B, Denny TP, Boucher C. 2005. Control of the *Ralstonia solanacearum* Type III secretion system (Hrp) genes by the global virulence regulator PhcA. FEBS Lett 579:2077–2081.
- 65. Zhang Y, Kiba A, Hikichi Y, Ohnishi K. 2011. prhKLM genes of *Ralstonia solanacearum* encode novel activators of hrp regulon and are required for pathogenesis in tomato. FEMS Microbiol Lett 317:75–82.
- 66. Zhang Y, Li J, Zhang W, Shi H, Luo F, Hikichi Y, Shi X, Ohnishi K. 2018. A putative LysR-type transcriptional regulator PrhO positively regulates the type III secretion system and contributes to the virulence of *Ralstonia solanacearum*. Mol Plant Pathol 1–12.
- 67. Zhang Y, Luo F, Wu D, Hikichi Y, Kiba A, Igarashi Y, Ding W, Ohnishi K. 2015. PrhN, a putative marR family transcriptional regulator, is involved in positive regulation of type III secretion system and full virulence of *Ralstonia solanacearum*. Front Microbiol 6:1–12.
- 68. Jones J, Dangl J. 2006. The plant immune system. Nature 444:323–329.
- 69. Kim BS, French E, Caldwell D, Harrington EJ, Iyer-Pascuzzi AS. 2015. Bacterial wilt disease: Host resistance and pathogen virulence mechanisms. Physiol Mol Plant Pathol 95:37–43.
- 70. Records AR. 2011. The type VI secretion system: A multipurpose delivery system with a phage-like machinery. Mol Plant-Microbe Interact 24:751–757.
- 71. Ryu C-M. 2015. Against friend and foe: type 6 effectors in plant-associated bacteria. J Microbiol 53:201–8.
- 72. Zhang L, Xu J, Xu J, Zhang H, He L, Feng J. 2014. TssB is essential for virulence and required for Type VI secretion system in *Ralstonia solanacearum*. Microb Pathog 74:1–7.
- 73. Bocsanczy AM, Achenbach UCM, Mangravita-Novo A, Chow M, Norman DJ. 2014. Proteomic comparison of *Ralstonia solanacearum* strains reveals temperature dependent virulence factors. BMC Genomics 15:280.
- 74. Bladergroen MR, Badelt K, Spaink HP. 2003. Infection-blocking genes of a symbiotic *Rhizobium leguminosarum* strain that are involved in temperature-dependent protein secretion. Mol Plant-Microbe Interact 16:53–64.
- 75. Meng F, Babujee L, Jacobs JM, Allen C. 2015. Comparative transcriptome analysis reveals cool virulence factors of *Ralstonia solanacearum* Race 3 Biovar 2. PLoS One 10:1–22.
- 76. Brown DG, Swanson JK, Allen C. 2007. Two host-induced *Ralstonia solanacearum* genes, *acrA* and *dinF*, encode multidrug efflux pumps and contribute to bacterial wilt virulence. Appl Environ Microbiol 73:2777–2786.

- 77. Yuliar, Nion YA, Toyota K. 2015. Recent trends in control methods for bacterial wilt diseases caused by *Ralstonia solanacearum*. Microbes Environ 30:1–11.
- 78. Enfinger JM, McCarter SM, Jaworski CA. 1979. Evaluation of Chemicals and Application Methods for Control of Bacterial Wilt of Tomato Transplants. Phytopathology 69:637–640.
- 79. Santos BM, Gilreath JP, Motis TN, Noling JW, Jones JP, Norton JA. 2006. Comparing methyl bromide alternatives for soilborne disease, nematode and weed management in fresh market tomato. Crop Prot 25:690–695.
- 80. Park M-G, Choi J, Hong Y-S, Park CG, Kim B-G, Lee S-Y, Lim H-J, Mo H, Lim E, Cha W. 2020. Negative effect of methyl bromide fumigation work on the central nervous system. PLoS One 15.
- 81. Warwick NJ, Pyle JA, Shallcross DE. 2006. Global modeling of the atmospheric methyl bromide budget. J Atmos Chem 54:133–159.
- 82. 2018. Scientific Assessment of Ozone Depletion. Geneva, Switzerland.
- 83. Norman DJ, Chen J, Yuen JMF, Mangravita-Novo A, Byrne D, Walsh L. 2006. Control of bacterial wilt of geranium with phosphorous acid. Plant Dis 90:798–802.
- 84. Pradhanang PM, Ji P, Momol MT, Olson SM, Mayfield JL, Jones JB. 2005. Application of acibenzolar-S-methyl enhances host resistance in tomato against *Ralstonia solanacearum*. Plant Dis 89:989–993.
- 85. Jiang N, Fan X, Lin W, Wang G, Cai K. 2019. Transcriptome analysis reveals new insights into the bacterial wilt resistance mechanism mediated by silicon in tomato. Int J Mol Sci 20:5–10.
- 86. Ishikawa R, Fujimori K, Matsuura K. 1996. Antibacterial activity of Validamycin A against *Pseudomonas solanacearum* and its efficacy against tomato bacterial wilt. Ann Phytopathol Soc Jpn 62:478–482.
- 87. Kiirika LM, Stahl F, Wydra K. 2013. Phenotypic and molecular characterization of resistance induction by single and combined application of chitosan and silicon in tomato against *Ralstonia solanacearum*. Physiol Mol Plant Pathol 81:1–12.
- 88. Vallad GE, Goodman RM. 2004. Systemic acquired resistance and induced systemic resistance in conventional agriculture. Crop Sci 44:1920–1934.
- 89. Li S, Liu Y, Wang J, Yang L, Zhang S, Xu C, Ding W. 2017. Soil acidification aggravates the occurrence of bacterial wilt in south China. Front Microbiol 8:1–12.
- 90. Qi G, Ma G, Chen S, Lian C, Zhao X. 2019. Microbial network and soil properties are

- changed in bacterial wilt susceptible soil. Appl Environ Microbiol 1–35.
- 91. Chen S, Qi G, Ma G, Zhao X. 2020. Biochar amendment controlled bacterial wilt through changing soil chemical properties and microbial community. Microbiol Res 231:126373.
- 92. Song W, Forderer A, Yu D, Chai J. 2020. Structural biology of plant defence. New Phytol.
- 93. Pfund C, Tans-Kersten J, Dunning FM, Alonso JM, Ecker JR, Allen C, Bent AF. 2004. Flagellin is not a major defense elicitor in *Ralstonia solanacearum* cells or extracts applied to *Arabidopsis thaliana*. Mol Plant-Microbe Interact 17:696–706.
- 94. Nakano M, Oda K, Mukaihara T. 2017. *Ralstonia solanacearum* novel E3 ubiquitin ligase (NEL) effectors RipAW and RipAR suppress pattern-triggered immunity in plants. Microbiol (United Kingdom) 163:992–1002.
- 95. Jeon H, Kim W, Kim B, Lee S, Jayaraman J, Jung G, Choi S, Sohn KH, Segonzac C. 2020. *Ralstonia solanacearum* Type III effectors with predicted nuclear localization signal localize to various cell compartments and modulate immune responses in *Nicotiana* spp. Plant Pathol J 36:303.
- 96. Kunwar S, Iriarte F, Fan Q, Da Silva EE, Ritchie L, Nguyen NS, Freeman JH, Stall RE, Jones JB, Minsavage G V., Colee J, Scott JW, Vallad GE, Zipfel C, Horvath D, Westwood J, Hutton SF, Paret ML. 2018. Transgenic expression of EFR and Bs2 genes for field management of bacterial wilt and bacterial spot of tomato. Phytopathology 108:1402–1411.
- 97. Poueymiro M, Cunnac S, Barberis P, Deslandes L, Peeters N, Cazale-Noel A-C, Boucher C, Genin S. 2009. Two Type III Secretion System Effectors from *Ralstonia solanacearum* GMI1000 Determine Host-Range Specificity on Tobacco. Mol Plant-Microbe Interact 22:538–550.
- 98. Nakano M, Mukaihara T. 2019. The Type III effector RipB from *Ralstonia solanacearum* RS1000 acts as a major avirulence factor in *Nicotiana benthamiana* and other *Nicotiana* species. Mol Plant Pathol 20:1237–1251.
- 99. Nahar K, Matsumoto I, Taguchi F, Inagaki Y, Yamamoto M, Toyoda K, Shiraishi T, Ichinose Y, Mukaihara T. 2014. *Ralstonia solanacearum* type III secretion system effector Rip36 induces a hypersensitive response in the nonhost wild eggplant *Solanum torvum*. Mol Plant Pathol 15:297–303.
- 100. Morel A, Guinard J, Lonjon F, Sujeen L, Barberis P, Genin S, Vailleau F, Daunay MC, Ditinger J, Poussier S, Peeters N, Wicker E. 2018. The Type III effector RipAX2 enables the control of the *Ralstonia solanacearum* species complex (RSSC) by eggplant AG91-25 carrying the resistance locus EBWR9. Mol Plant Pathol 19:2459–2472.
- 101. Thomas NC, Hendrich CG, Gill US, Allen C, Hutton SF, Schultink A. 2020. Roq1 confers resistance to *Xanthomonas*, *Pseudomonas syringae* and *Ralstonia solanacearum* in

- tomato. Front Plant Sci 11.
- 102. Moose SP, Mumm RH. 2008. Molecular plant breeding as the foundation for 21st century crop improvement. Plant Physiol 147:969–977.
- 103. Kunwar S, Paret ML, Olson SM, Ritchie L, Rich JR, Freeman J, McAvoy T. 2014. Grafting using rootstocks with resistance to *Ralstonia solanacearum* against *Meloidogyne incognita* in tomato production. Plant Dis 99:119–124.
- 104. Planas-Marquès M, Kressin JP, Kashyap A, Panthee DR, Louws FJ, Coll NS, Valls M. 2019. Four bottlenecks restrict colonization and invasion by the pathogen *Ralstonia* solanacearum in resistant tomato. J Exp Bot 71:2157–2171.
- 105. Thanh DT, Tarn LTT, Hanh NT, Tuyen NH, Bharathkumar S, Lee SY, Park K-S. 2009. Biological control of soilborne diseases on tomato, potato, and black pepper by selected PGPR in the greenhouse and field in Vietnam. Plant Pathol J 25:263–269.
- 106. Xue QY, Chen Y, Li SM, Chen LF, Ding GC, Guo DW, Guo JH. 2009. Evaluation of the strains of *Acinetobacter* and *Enterobacter* as potential biocontrol agents against *Ralstonia* wilt of tomato. Biol Control 48:252–258.
- 107. Wei Z, Huang J, Tan S, Mei X, Shen Q, Xu Y. 2013. The congeneric strain *Ralstonia pickettii* QL-A6 of *Ralstonia solanacearum* as an effective biocontrol agent for bacterial wilt of tomato. Biol Control 65:278–285.
- 108. Ramesh R, Phadke GS. 2012. Rhizosphere and endophytic bacteria for the suppression of eggplant wilt caused by Ralstonia solanacearum. Crop Prot 37:35–41.
- 109. Buttimer C, McAuliffe O, Ross RP, Hill C, O'Mahony J, Coffey A. 2017. Bacteriophages and bacterial plant diseases. Front Microbiol 8:1–15.
- 110. Mikiciński A, Sobiczewski P, Puławska J, Maciorowski R. 2016. Control of fire blight (*Erwinia amylovora*) by a novel strain 49M of *Pseudomonas graminis* from the phyllosphere of apple (*Malus* spp.). Eur J Plant Pathol 145:265–276.
- 111. Álvarez B, Biosca EG. 2017. Bacteriophage-based bacterial wilt biocontrol for an environmentally sustainable agriculture. Front Plant Sci 8:1–7.
- 112. Alseth EO, Pursey E, Lujan A, McLeod I, Rollie C, Westra E. 2019. Bacterial biodiversity drives the evolution of CRISPR-based phage resistance in *Pseudomonas aeruginosa*. Nature 574:586115.
- 113. da Silva Xavier A, de Almeida JCF, de Melo AG, Rousseau GM, Tremblay DM, de Rezende RR, Moineau S, Alfenas-Zerbini P. 2019. Characterization of CRISPR-Cas systems in the *Ralstonia solanacearum* species complex. Mol Plant Pathol 0:223–239.

- 114. Álvarez B, López MM, Biosca EG. 2019. Biocontrol of the Major Plant Pathogen *Ralstonia solanacearum* in Irrigation Water and Host Plants by Novel Waterborne Lytic Bacteriophages 10:1–17.
- 115. Wang X, Wei Z, Yang K, Wang J, Jousset A, Xu Y, Shen Q, Friman VP. 2019. Phage combination therapies for bacterial wilt disease in tomato. Nat Biotechnol 37:1513–1520.
- 116. Fujiwara A, Fujisawa M, Hamasaki R, Kawasaki T, Fujie M, Yamada T. 2011. Biocontrol of *Ralstonia solanacearum* by treatment with lytic bacteriophages. Appl Environ Microbiol 77:4155–4162.
- 117. Yamada T. 2013. Filamentous phages of *Ralstonia solanacearum*: Double-edged swords for pathogenic bacteria. Front Microbiol 4:1–7.
- 118. Murugaiyan S, Bae JY, Wu J, Lee SD, Um HY, Choi HK, Chung E, Lee JH, Lee SW. 2011. Characterization of filamentous bacteriophage PE226 infecting *Ralstonia solanacearum* strains. J Appl Microbiol 110:296–303.
- 119. Addy HS, Askora A, Kawasaki T, Fujie M, Yamada T. 2012. Loss of Virulence of the Phytopathogen *Ralstonia solanacearum* Through Infection by φRSM Filamentous Phages. Phytopathology 102:469–477.
- 120. Ahmad AA, Stulberg MJ, Mershon JP, Mollov DS, Huang Q. 2017. Molecular and biological characterization of φRs551, a filamentous bacteriophage isolated from a race 3 biovar 2 strain of *Ralstonia solanacearum*. PLoS One 12:1–19.
- 121. Addy HS, Askora A, Kawasaki T, Fujie M, Yamada T. 2012. The filamentous phage φrSS1 enhances virulence of phytopathogenic *Ralstonia solanacearum* on tomato. Phytopathology 102:244–251.
- 122. Tanaka H, Negishi H, Maeda H. 1990. Control of tobacco bacterial wilt by an avirulent strain of *Pseudomonas solanacearum* M4S and its bacteriophage. Japanese J Phytopathol 56:243–246.

Chapter 2

Nitric Oxide Regulates the Ralstonia solanacearum Type 3 Secretion System

This chapter is a modified version of the following manuscript submitted to Molecular Plant Pathology:

Hendrich, C. G., Truchon, A. N., Dalsing, B. L., & Allen, C. Nitric Oxide Regulates the *Ralstonia* solanacearum Type 3 Secretion System.

Contributions: CGH and BLD collected Lux reporter growth curves. CGH and ANT designed RNA-seq study, collected and sequenced RNA, and analyzed transcriptome data. CGH conducted all other experiments. CGH, BLD, and CA all contributed to NO-T3SS experimental design. CGH wrote the text and made the figures.

Abstract

Ralstonia solancearum causes bacterial wilt disease on diverse plant hosts. R. solanacearum cells enter a host from soil or infested water through the roots, then multiply and spread in the water-transporting xylem vessels. Despite the low nutrient content of xylem sap, R. solanacearum grows extremely well inside the host, using denitrification to respire in this hypoxic environment. R. solanacearum growth in planta also depends on the successful deployment of protein effectors into host cells using a Type III Secretion System (T3SS). The T3SS is absolutely required for R. solanacearum virulence, but it is metabolically costly and can trigger host defenses. Thus, the pathogen's success depends on optimized regulation of the T3SS. We found that a byproduct of denitrification, the toxic free-radical nitric oxide (NO), positively regulates the R. solanacearum T3SS both in vitro and in planta. Using chemical treatments and R. solanacearum mutants with altered NO levels, we show that the expression of a key T3SS regulator is induced by NO in culture. Analyzing the transcriptome of R. solanacearum responding to varying levels of NO both in culture and in planta revealed that the T3SS and effectors were broadly upregulated with increasing levels of NO. This regulation was specific to the T3SS and was not shared by other stressors. Our results suggest that R. solanacearum experiences an NO-rich environment in the plant host and may use this NO as a signal to activate T3SS during infection.

Introduction

Ralstonia solancearum (Rs) is a Gram-negative soil-borne betaproteobacterium that causes bacterial wilt disease on a wide range of plant hosts, including important crops like tomato, potato, and banana (1). The bacteria survive in and are spread through infected soil and water, infecting host roots through wounds and natural openings (2). Once inside, R. solanacearum cells move to the xylem, where they can grow and spread throughout the plant. Although this bacterium is slow growing and sensitive to stress when grown in vitro, in plant xylem vessels R. solanacearum is a formidable force. R. solanacearum quickly grows to high cell densities in xylem even though this habitat is low in oxygen and nutrients, and accessible to host defenses (3). As it grows, R. solanacearum produces an arsenal of virulence factors, including highly mucoid extracellular polymeric substances (EPS), a consortium of cell wall degrading enzymes, and dozens of protein effectors that are injected into host cells via the Type III Secretion System (T3SS) (3). Water transport in infected plants is eventually blocked by a combination of host-produced gels and tyloses, degradation of vessel walls, EPS, and the sheer mass of bacterial cells. Without sufficient water, plants wilt and die while R. solanacearum cells escape back into the soil, where they can find another host (4).

The lethality of bacterial wilt disease combined with its wide host range and a lack of effective treatments make *R. solanacearum* an important agricultural problem around the world (1, 5). Successful disease management depends on understanding *R. solanacearum* biology, but the pathogen behaves very differently in culture than it does in its natural environment (6). In particular, the T3SS, which is absolutely essential for virulence and subject to a complex regulatory cascade, is affected by the plant environment in ways that remain

poorly understood (7). The PhcA quorum sensing system upregulates T3 secretion in culture, but not *in planta* (6, 8–10). An unidentified 'diffusible factor' increases T3SS expression *in planta* via the HrpG global regulator (3).

We have discovered that the diffusible free radical nitric oxide (NO) plays a role in *R. solanacearum* life inside plants. Xylem sap is rich in nitrate, which *R. solanacearum* uses as an alternate electron acceptor to respire in the hypoxic xylem environment (11). The *R. solanacearum* strain GMI1000 reduces nitrate completely to dinitrogen gas by means of denitrifying respiration. The genes required for this process are highly expressed during infection (6, 10). However, denitrifying respiration produces NO as an intermediate. In large quantities, NO is toxic and strongly inhibits *R. solanacearum* growth. The pathogen manages this threat by detoxifying NO with the nitric oxide reductase NorB and the flavohemoglobin HmpX, which are both highly expressed *in planta* and required for full virulence (6, 11). Plants use NO extensively for both signaling and defense, and can produce NO through multiple different pathways (12–16). Thus, *R. solanacearum* likely encounters NO during plant pathogenesis.

In this study, we identify a link between NO and regulation of the *R. solanacearum* T3SS. We first show that T3SS gene expression increases when *R. solanacearum* is actively denitrifying. We then show that this effect depends specifically on the presence of NO. Based on these results, we conducted a transcriptomics experiment to determine the effects of NO on *R. solanacearum* gene expression in culture and *in planta* and show that levels of many transcripts, including 107 T3SS-related genes, are altered by changes in NO levels.

Results

Nitric oxide changes expression of the R. solanacearum T3SS

Regulation of the T3SS in *R. solanacearum* is multi-layered and incompletely understood (Figure 1a). Because *R. solanacearum* actively denitrifies *in planta*, we wondered if this pathway or its products affect T3SS expression during plant infection (6, 11). To test this hypothesis, we used an *R. solanacearum* reporter strain carrying a fusion of the *lux* operon to the promoter of *hrpB*, which encodes a key T3SS regulator (3). Transcription of *hrpB* increased >3-fold when the bacterium was denitrifying in culture (Figure 1b). We therefore further explored how denitrification and NO specifically affect *hrpB* expression. We incubated a *hrpB::lux* cell suspension with tomato seedlings for 24 hours with or without the NO scavenger cPTIO (17). As expected, the presence of a host plant activated *hrpB* gene expression but adding cPTIO to the mixture completely reversed this effect (Figure 1c). This indicated that the denitrifying respiration-dependent increase in *hrpB* expression that we observed in culture is specifically triggered by NO. Further, this result suggests that NO could be the unknown soluble signal that increases *hrp* regulon expression *in planta*.

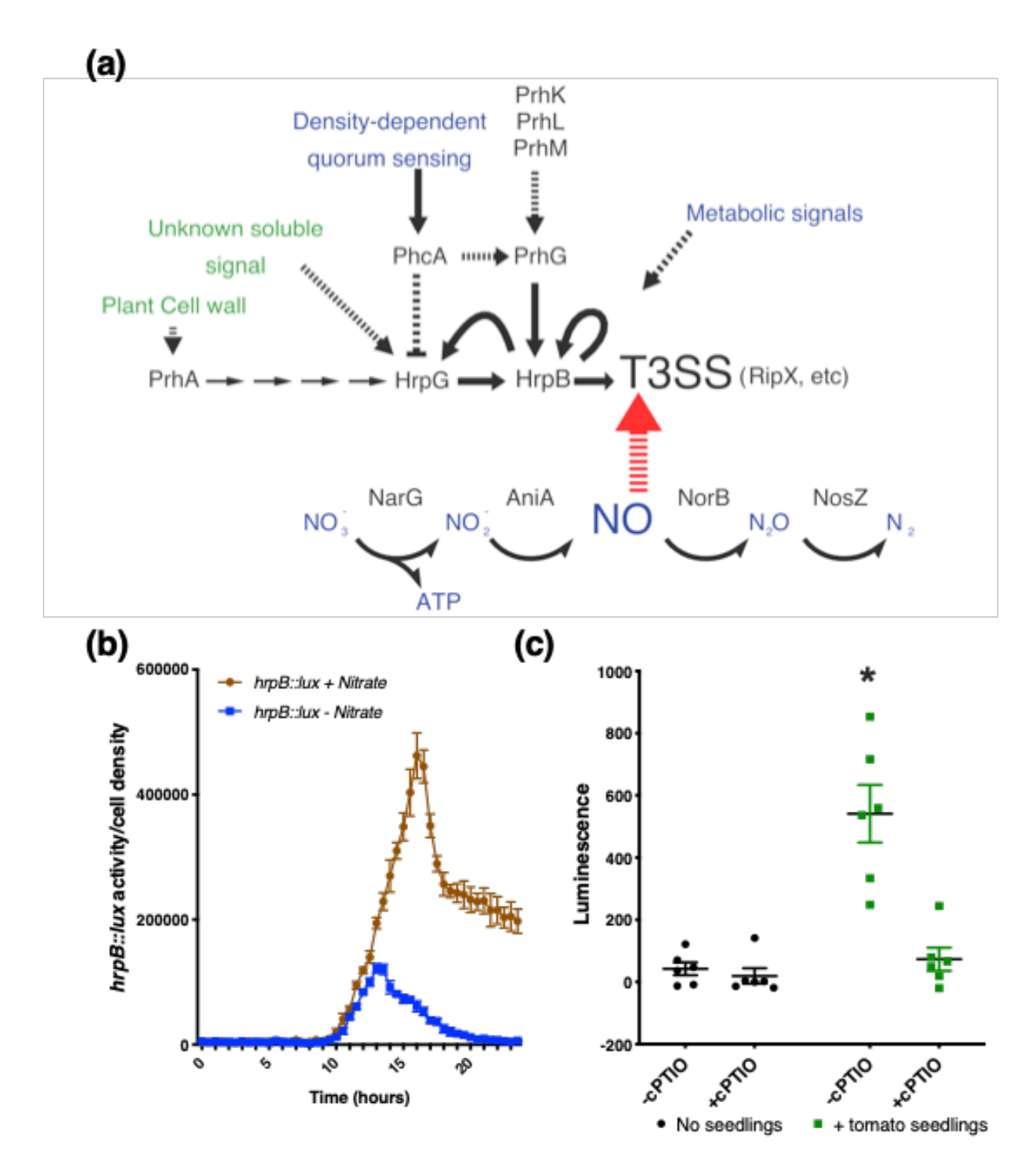
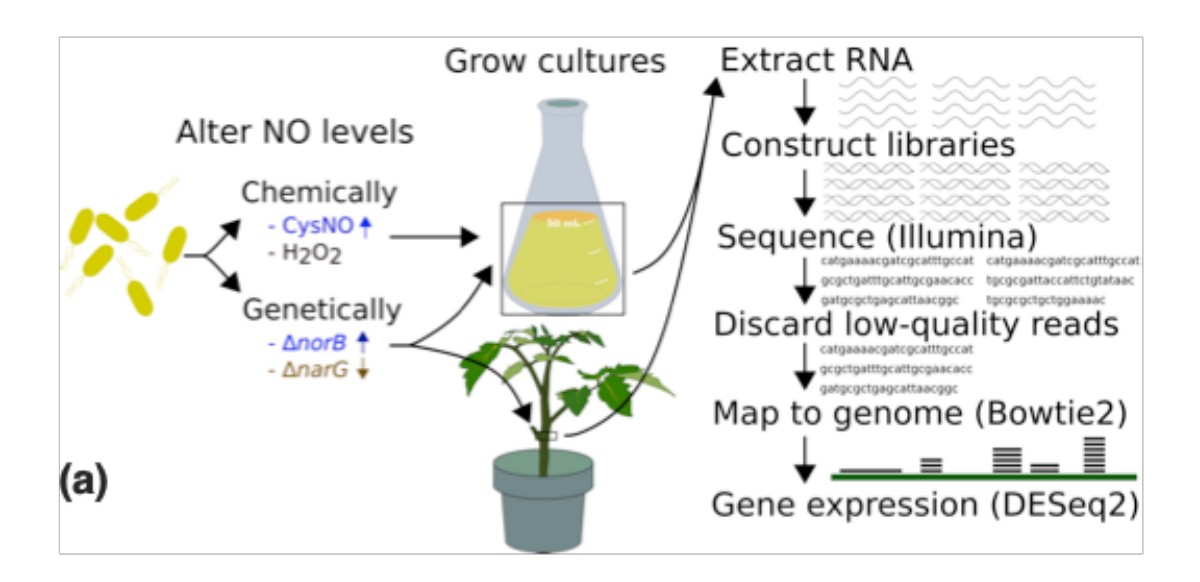


Figure 1. Nitric oxide affects expression of the *R. solanacearum* T3SS. (a) Summary of known T3SS regulation in *R. solanacearum* strain GMI1000. Arrows indicate positive regulation, barred lines indicate repression, dashed lines indicate an unknown or uncharacterized mechanism,

green text indicates plant-derived signals, and blue text indicates metabolites. T3SS genes, such as the T3 effector ripX, are controlled by the transcriptional regulator HrpB. HrpB is transcriptionally activated by HrpG and PrhG, which are themselves controlled by the quorumsensing regulator PhcA, but only in vitro. PrhG activity also depends on three uncharacterized proteins, PrhK, PrhL, and PrhM, through an unknown mechanism. HrpG is activated by the contact-dependent plant cell wall sensor PrhA as well as by an unknown soluble signal present during plant infection. (b) Expression of a bacterial luciferase transcriptional reporter of HrpB. R. solanacearum strain GMI1000 hrpB::lux was grown in denitrification-inducing conditions with or without 30 mM nitrate. Both culture density (OD600) and luminescence were measured every 30 min, and luminescence was normalized to culture density. Error bars represent standard error of the mean. Cultures grown with nitrate had significantly increased hrpB expression (2way ANOVA, P=0.0003). (c) The NO scavenger cPTIO decreased T3SS activity in the presence of a host. Luminescence of R. solanacearum hrpB::lux was measured after 24 h incubation in water with or without five day-old tomato seedlings, and with or without 1 mM cPTIO, an NOscavenger. Exposure to tomato seedlings induced hrpB::lux expression (P=0.004, students T test). R. solanacearum cells exposed to both tomato seedlings and cPTIO had luminescence indistinguishable from that of cells without tomato seedlings. Error bars represent standard error of the mean.

Denitrifying metabolism causes broad changes in R. solanacearum gene expression.

To better understand the effects of NO on Rs biology, we sequenced the transcriptomes of R. solanacearum cells grown with varying levels of NO both in culture and in infected tomato plants (Figure 2a). In culture, we grew the cells in 0.1% O₂ in a modified Van den Mooter medium (VDM), which promotes denitrifying respiration (11). We manipulated intracellular R. solanacearum NO levels genetically by using mutants lacking either the NarG nitrate reductase (the $\Delta narG$ mutant cannot denitrify and does not produce NO), or the NorB nitric oxide reductase (the ΔnorB mutant accumulates NO, see Supplementary Figure 1). Exogenous NO levels were manipulated by treating cells with CysNO, a nitrosothiol NO donor. Because high NO levels are toxic to R. solanacearum, we controlled for general stress responses by also profiling transcriptomes of cultures treated with H₂O₂, a non-NO source of stress. After about 18 h, growth of the $\Delta norB$ mutant was inhibited by accumulating NO, so we sampled cultures 16 hpi, when $\Delta narG$, $\Delta norB$, and the wild-type strain were at similar densities (Supplementary Figure 1). CysNO or H₂O₂ treatments were added 4 h before sampling, at the highest concentrations that did not significantly alter culture growth (Supplementary Figure 2a). Total RNA was extracted from bacteria in planta 3 days after tomato plants were inoculated with ~2000 CFU of *R. solanacearum* through a cut petiole (10). This method synchronized the infection process better than root inoculation. Bacterial colonization in sampled tissue was standardized by extracting RNA only from stems containing between 5x10⁷ and 10⁹ CFU/g stem, as determined by dilution plating a ground stem section (Supplementary Figure 2B). Each of the three biological replicates contained pooled RNA from 4 or 5 plants.



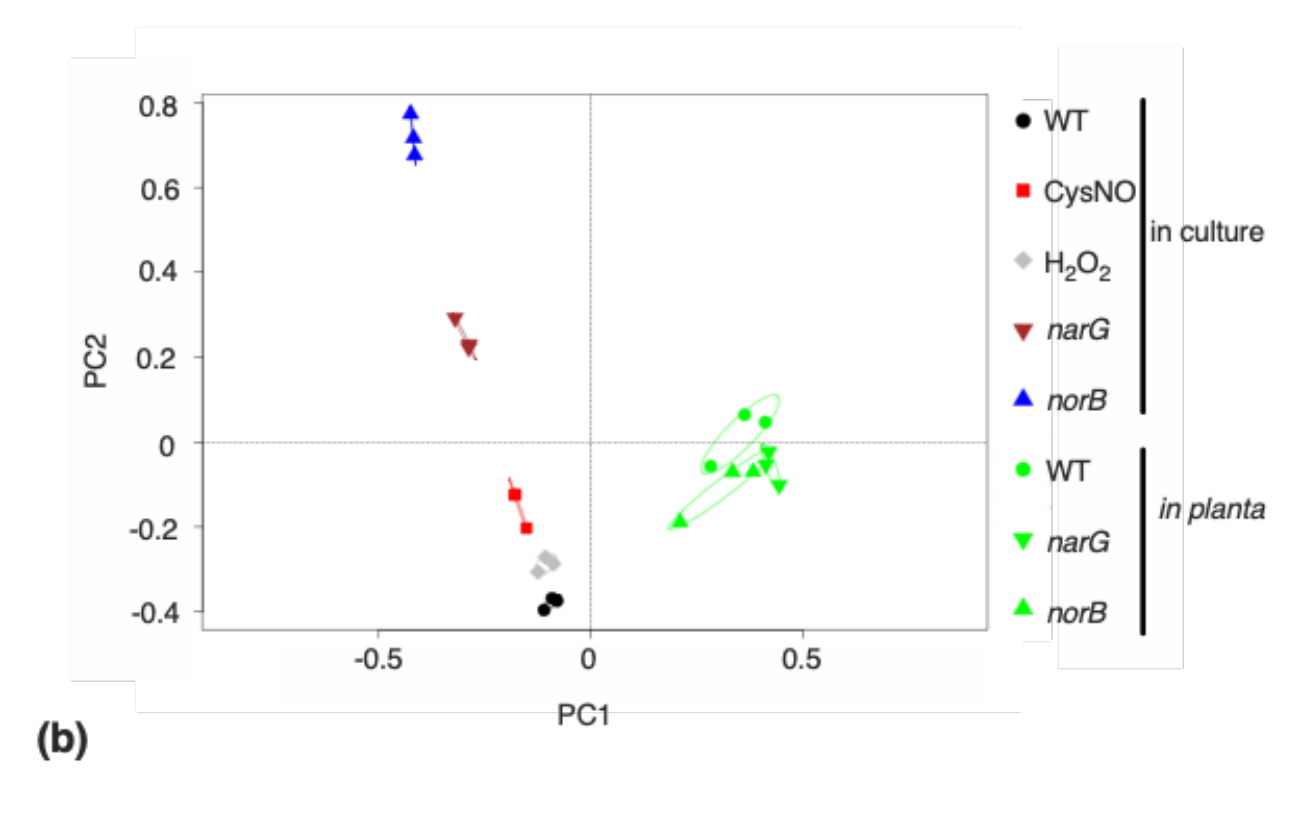


Figure 2. Nitric oxide causes broad changes in *R. solanacearum* gene expression. (a) Design of RNA-seq experiment. We extracted RNA from *R. solanacearum* grown with altered NO levels from stems of infected tomato plants (*in planta*) and from denitrifying VDM medium (in culture) and NO levels were increased chemically by adding the NO donor CysNO to wild type

(WT) and increased genetically by using a NO-accumulating Δ norB mutant. The Δ narG mutant has reduced levels of NO. H₂O₂ -treated WT was included as a control for non-nitrosative general stress responses. **(b)** Whole-transcriptome datasets were used for principal component analysis; plot created in R with the package Vegan (18). Each data point represents one biological replicate, with three replicates per condition. Ellipses represent a 95% confidence interval for each condition (some ellipses are so small that they appear as lines).

Around 97% of RNA-seq reads from *in vitro* samples mapped to the *R. solanacearum* genome (Supplementary Figure 3A). Because tomato stem slices also included host RNA, only 9.2% of the *in planta* RNA reads mapped to the *R. solanacearum* genome. However, the absolute number of bacterial transcripts from the *in planta* samples still exceeded 10⁶ reads per replicate. Principal component analysis clustered the *in vitro* samples together based on treatment, and the *in planta* samples were even more tightly clustered, reflecting less variation in gene expression than the culture samples (Figure 2b). Genes were considered differentially expressed if they had an adjusted P-value <0.05. A full list of gene expression values can be found in the supplementary materials.

We validated our transcriptomic results by using qRT-PCR to measure the expression of two regulators of T3SS, hrpB and hrpG, and one well-expressed T3E, ripX. Expression levels of each of these genes in the $\Delta narG$ and $\Delta norB$ mutants closely matched those obtained from RNA-seq analysis (Figure 3). As with hrpB expression, hrpG and ripX were both activated by NO, whether it was produced endogenously or exogenously.

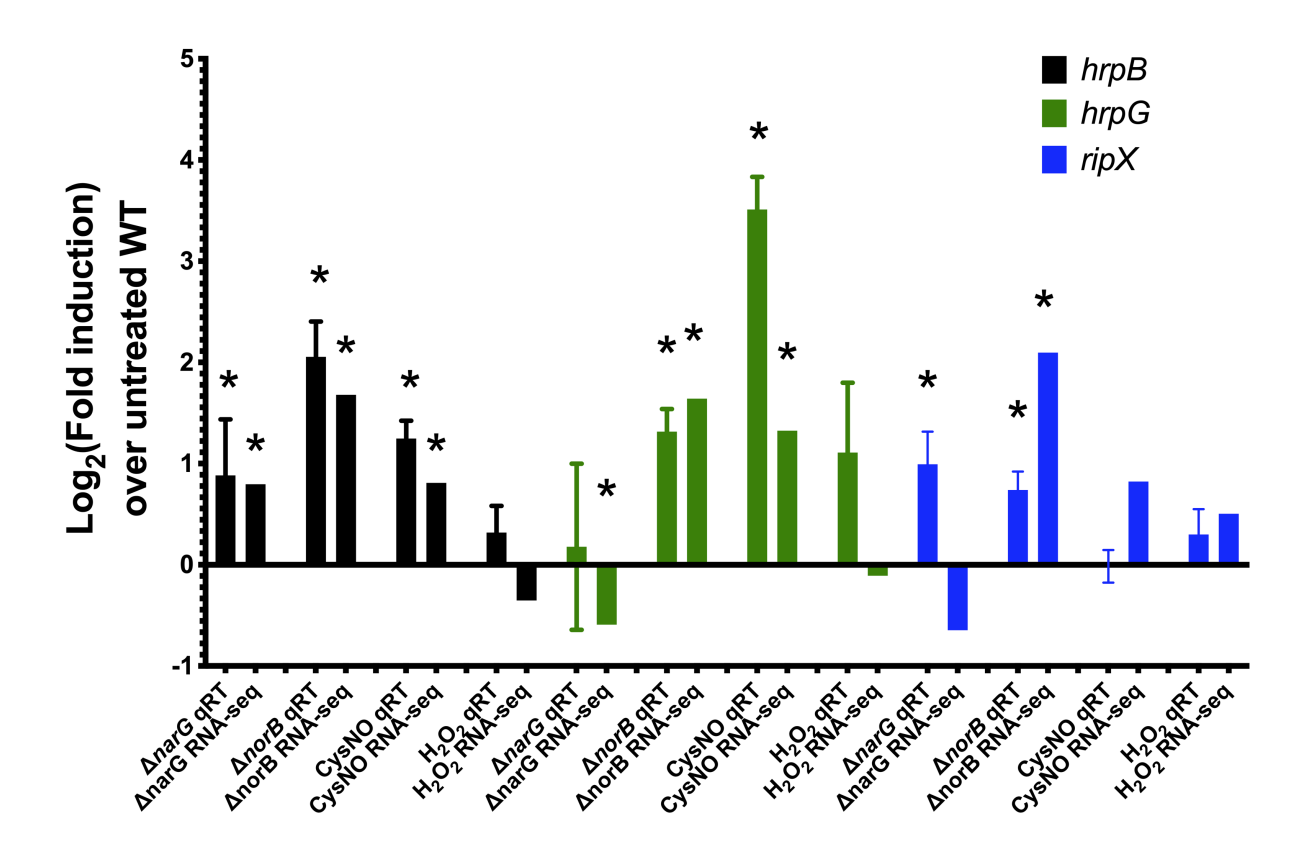


Figure 3. Expression analysis of selected T3SS-related genes by qRT-PCR validated RNA-seq results. RNA was extracted from *R. solanacearum* cultured in VDM media at 0.1% oxygen for 16 hours for both qRT-PCR and RNA-seq analysis. *R. solanacearum* samples were: wild type strain GMI1000 (WT, untreated control reference), non-denitrifying low-NO mutant ($\Delta narG$) and NO-accumulating mutant ($\Delta norB$), and WT treated for 4h with exogenous NO (CysNO). Gene expression levels in all samples were normalized using *serC* (6). Error bars indicate standard error of the mean. Black bars, \log_2 fold-change expression of T3SS regulatory gene *hrpB*; green bars, \log_2 fold-change expression of Type 3-secreted effector gene *ripX*. * *P*<0.05, for qRT, student's t-test compared to gene expression level in untreated WT bacteria; for RNA-seq, FDR using Benjamini-Hochberg.

Denitrifying conditions in culture do not replicate in planta conditions

Because xylem fluid contains relatively small amounts of nutrients, minimal media has often been considered to mimic the xylem environment (19, 20). Because VDM is a minimal medium and *R. solanacearum* experiences low-oxygen conditions and uses denitrifying respiration during tomato infection, we asked if anaerobic growth in VDM would better mimic the tomato xylem environment than rich media (11). However, when we examined expression of *R. solanacearum* genes in tomato stems compared to in VDM, we found a total of 1038 genes were differentially regulated in these conditions (Supplementary materials). Most genes involved in denitrification were expressed at a higher level in VDM than *in planta*. Other broad categories that were altered include sugar metabolism, flagellar motility, amino acid transporters, iron uptake genes, and ribosomal proteins. In line with previous results, T3SS-related genes were among the most highly upregulated genes *in planta* (6). Overall, growth in VDM did not closely replicate the *in planta* environment and the bacterium seemed more reliant on denitrifying metabolism in VDM.

Altering denitrification and NO levels changes expression of denitrification and virulencerelated genes *in planta*

To determine if the effects of NO on the T3SS were specific or a part of a general response, we examined genes differentially regulated by altering NO levels genetically *in* planta. In the stem, 187 genes were significantly altered by blocking denitrification and NO production in $\Delta narG$ while only 49 genes were altered in the NO accumulating $\Delta norB$. In $\Delta narG$, nine of the most significantly upregulated genes were directly involved in nitrate sensing and

uptake or were components of the nitrate reductase protein, though expression of sulfur metabolic and flagellar assembly genes and the alkanesulfonate uptake protein ssuB were also decreased (Supplementary materials). When the $\Delta norB$ mutant grew in planta, expression of ssuB and some genes involved in chemotaxis and flagellar assembly were decreased relative to the wild-type strain. This muted response highlights the robust regulatory state of R. solanacearum growing in planta and shows that even changes in fundamental aspects of its biology can tolerated (21).

Consistent with the observation that the entire transcriptome of WT R. solanacearum was very different $in\ planta$ than in culture (Figure 2a) the transcriptomic profiles of the denitrification mutants grown in culture were much more divergent, with 3,145 significantly altered genes in $\Delta narG$ and 3,976 altered in $\Delta norB$. In the non-denitrifying $\Delta narG$, the bacterium showed changes in many metabolic pathways, some of which suggested reduced growth and metabolic activity. Down-regulated genes were enriched in KEGG pathways like purine and pyrimidine metabolism, oxidative phosphorylation, and tRNA synthetases (Supplementary materials). As also observed $in\ planta$, $\Delta narG$ had reduced expression in genes involved in sulfate and alkanesulfonate uptake and sulfate reduction. $\Delta narG$ also had increased expression of flagellar assembly and chemotaxis genes and decreased expression of genes associated with the Sec-dependent secretion and the Type II secretion systems.

Genes up-regulated in the NO-accumulating $\Delta norB$ mutant were enriched in the KEGG pathways of flagellar assembly, sulfur relay system and fatty acid degradation (Supplementary materials). Downregulated genes were enriched in central metabolic KEGG pathways like oxidative phosphorylation, pyrimidine metabolism, biosynthesis of amino acids, and fatty acid

biosynthesis. Many of the most highly induced genes were annotated as being involved in either siderophore synthesis or iron uptake, a trend that was also observed in CysNO-treated cells. CysNO-treated R. solanacearum cells and $\Delta norB$ also saw reduction in expression of Types I, II, and VI secretion systems.

R. solanacearum encounters more nitrosative stress in VDM than in planta

To determine the overlap between oxidative and nitrosative stress responses, we examined the expression of genes known to be involved in ROS and RNS responses in R. solanacearum and E. coli. General ROS-responsive genes included oxyR, katEG, sodBC, groEL, groES, dnaK, recA, ahpF and ahpC1, ndh, icsA, zwf, trxA, and gor (22, 23). To search for a purely nitrosative response, we looked at the expression of norB and hmpX, which directly detoxify NO in R. solanacearum (11, 24). Transcriptomes of R. solanacearum cells grown in tomato stems indicated increased oxidative stress in planta relative to when growing in VDM. Expression of the katE catalase increased 35-fold in wild type bacteria growing in tomato, but norB and hmpX expression decreased 5-fold and 20-fold, suggesting lower nitrosative stress levels. In planta, neither the non-denitrifying $\Delta narG$ strain nor the NO overproducing $\Delta norB$ strain showed significant changes any known oxidative stress response genes or in *norB* or *hmpX* expression. In culture, our oxidative stress control treatment with H₂O₂ increased expression of katE. The H₂O₂ treated cells also had increased expression of NO detoxifying genes hmpX and norB. The non-denitrifying $\Delta narG$ mutant showed changes in most oxidative stress response genes, with decreased expression of a few key genes, such as superoxide dismutase. The NO accumulating $\Delta norB$ saw an overall similar trend to $\Delta narG$ in its expression of oxidative stress response genes, except it had decreased expression of the chaperones *groES* and *groEL* and increased expression of the iron-sulfur protein *sufA*. As expected, the Δ*norB* mutant transcriptome suggested NO stress, with an 11-fold up-regulation of the NO-detoxifying *hmpX*. Overall, these results showed some overlap in the response to ROS and RNS stress in culture and suggested that *R. solanacearum in planta* experienced less nitrosative stress in tomato xylem than denitrifying in VDM.

Nitric oxide induced expression of T3SS-related genes both in vitro and in planta.

To determine if in addition to hrpB, other T3SS-associated genes are induced by NO in culture, we measured relative expression of all 107 known R. solanacearum T3SS genes under each tested condition. These genes encode T3SS structural elements, regulators, secreted effectors, and chaperones (Figure 4) (8, 25–35). Cells of the NO-accumulating $\Delta norB$ mutant grown in culture had broadly increased T3SS gene expression relative to wild type, with nine of sixteen structural elements significantly increased. Only one structural element, hrpF, trended non-significantly towards reduced expression (Figure 4a). Five out of thirteen known regulators of T3SS were significantly upregulated in $\Delta norB$, although expression of the prhA, prhG, prhO, and the prhKLM operon were all reduced. Two out of the four T3E chaperones had significantly elevated expression in $\Delta norB$, as did most T3Es. The differential expression of effectors did not seem to correlate with their known interactions with chaperones (Supplementary materials). The expression of T3SS genes in CysNO-treated cells largely mirrored that of norB, with 80% of tested genes having a similar trend. However, the magnitude of the effect was lower. T3SS gene expression in $\Delta narG$ was more varied, with fewer significantly differentially regulated genes

than $\Delta nor B$. In contrast to $\Delta nor B$, $\Delta nar G$, and CysNO-treated cultures, H_2O_2 -treated cultures had only eight significantly changed T3SS genes (Figure 4a). Overall, we saw a greater induction of T3SS genes in culture by our high-NO conditions than low-NO conditions.

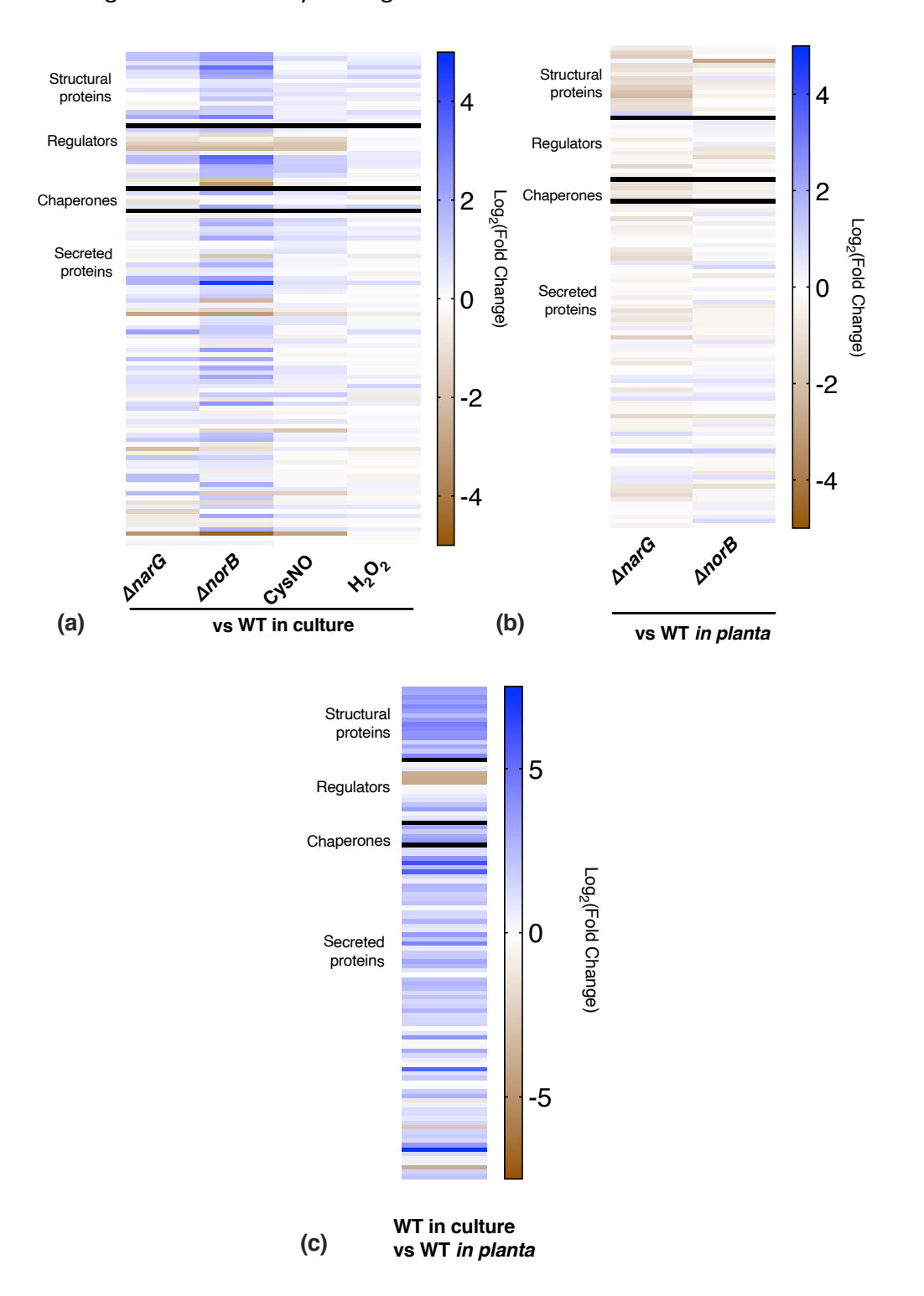


Figure 4. Nitric oxide alters expression of T3SS-related genes both in vitro and in planta. (a) Heatmap showing relative expression levels of 107 T3SS-associated genes in R. solanacearum cells growing in rich medium with varying NO levels. All fold-change numbers are compared to levels in untreated wild-type (WT) cells. Gene annotations, fold change, and significance levels can be found in the supplementary materials. NO levels were modified genetically using mutants lacking narG (deleting this nitrate reductase reduces endogenous NO) and norB (deleting this nitric oxide reductase increases endogenous NO). NO levels were increased chemically by adding 1 mM CysNO. Cells treated with 100 μ M hydrogen peroxide (H_2O_2) were a non-NO control to show general stress responses. (b) Relative expression levels of 107 T3SSassociated genes in R. solanacearum cells growing in planta. About 2000 CFU of WT R. solanacearum, ΔnarG, or ΔnorB were introduced into 17-day old Bonny Best tomato plants through a cut petiole and RNA was harvested from a stem slice 3 days after inoculation. (c) Expression of most T3SS-associated genes in R. solanacearum strain GMI1000 was enhanced when the bacterium grew in tomato plants relative to when R. solanacearum cells multiplied in vitro under denitrifying conditions (VDM medium, 0.1% O₂).

To determine if altering NO levels affects R. solanacearum T3SS gene expression in a biologically relevant environment with all natural T3SS regulating inputs, we examined changes in T3SS gene expression in $\Delta narG$ and $\Delta norB$ in planta. Compared to R. solanacearum grown in culture, wild type R. solanacearum in planta had much higher expression of almost every T3SS-associated gene (Figure 3c). When growing in tomato stems, $\Delta norB$ grown in planta had no significantly differentially regulated T3SS genes, possibly because relatively high levels of NO

are already present in the plant environment (Figure 3b). In contrast, the non-denitrifying ΔnarG mutant showed an overall trend of lower T3SS gene expression, with expression of nine genes significantly reduced (Figure 3b). These included two components of the T3SS structure, hrpF and hrcN, the regulators hrpB and prhG, the effector chaperone hpaG, and four T3SS effectors. Even in the highly T3SS-inducing in planta environment, reducing R. solanacearum-produced NO was sufficient to reduce T3SS gene expression in tomato xylem.

Discussion

The T3SS is essential for *R. solanacearum* virulence, as it is for many Gram-negative pathogenic bacteria. Involving at least 16 structural proteins, this secretion system is metabolically expensive to synthesize and operate, so the bacterium is under strong selection pressure to express it only when it increases fitness (36, 37). Many factors contribute to the regulation of T3SS in *R. solanacearum*, including the presence of undefined host cell wall materials, unknown soluble factors, unknown metabolic cues, and (in culture) quorum sensing (3, 33–35, 38–40). While many T3SS regulators have been described, open questions remain, such as why T3SS is repressed in rich media and whether specific host cell wall components activate PrhA. In addition, many genes that affect T3SS gene expression do so via unknown mechanisms (32–34). The results presented here suggests that NO participates in this complex regulatory network.

Despite its toxicity at high concentrations, NO is widely used as a signaling molecule in all domains of life (41–43). Many effects of NO are mediated by NO-dependent protein post-translational modifications, including binding transition metals, S-nitrosylation of cysteine, and

tyrosine nitration (16, 43–48). While most well-characterized mechanisms of NO signaling have been described in eukaryotes, examples of NO signaling in bacteria have also been identified. Species in Legionella, Shewanella, Vibrio, and Silicibacter have been shown to use H-NOX proteins to sense NO and regulate biofilm formation (49-53). NO also contributes to biofilm regulation in Pseudomonas aeruginosa via the protein NosP (54). Both H-NOX proteins and NosP bind NO using iron centers, but no orthologues of these genes are apparent in the R. solanacearum genome. The first example of S-nitrosylation in bacteria was the oxidative stress response protein OxyR in E. coli (55). OxyR regulates a distinct set of genes when a key cysteine is nitrosylated rather than oxidized. In addition to this, nitrosative stress damage triggers Snitrosylation of the Salmonella enterica redox sensor SsrB and affects the S-nitroso proteome of Mycobacterium tuberculosis (56, 57). Although we show NO activates a key virulence factor in R. solanacearum, its specific mechanism of action is not yet known. Using in silico predictions of NO-dependent post-translational modifications, we could identify and selectively modify potentially important residues in T3SS regulatory proteins to determine the mechanism of NOdependent T3SS activation (58, 59).

To explore the possibility that the up-regulation by NO of T3SS-associated genes in *R*. *solanacearum* is mediated by S-nitrosylation, we searched for potential S-nitrosylation sites in T3SS regulatory proteins using GPS-SNO (58). The strain GMI1000 HrpB protein contains a predicted S-nitrosylation site at cysteine 112 that is conserved across the RSSC and in the corresponding regulatory protein HrpX in plant pathogenic Xanthomonads. However, we were unable to conclusively test this hypothesis since mutating this residue yield ambiguous results (as might be expected for a function regulated by many factors), and we were unable to purify

sufficient HrpB protein to chemically measure S-nitrosylation. Thus, this mechanism remains possible but unproven.

We found that expression of T3SS-associated genes was enhanced by the presence of a plant host and by exogenous NO released by the NO donor CysNO, and the plant-mediated induction was suppressed by the NO scavenger cPTIO (Figure 1c). T3SS gene expression also increased in response to nitric oxide produced by R. solanacearum itself, both at natural levels generated by denitrifying respiration and at enhanced levels caused by deleting norB. As previously reported (6, 9, 10), R. solanacearum cells infecting tomato plants highly expressed most T3SS genes, but reducing R. solanacearum-produced NO by preventing denitrifying respiration with a $\triangle narG$ mutation significantly decreased expression of some T3SS-related genes in planta. These included genes encoding structural components, HrpF and HrcN, key regulators HrpB and PrhG, the chaperone HpaG, and four T3-secreted effectors (Figure 4b). This was especially striking because overall gene expression in $\Delta narG$ was otherwise very similar to that of wild type. These results raise the possibility that R. solanacearum uses the presence of NO as an indirect indicator of the host xylem environment. There was no increase in T3SS gene expression in the NO-overproducing ΔnorB mutant, which may indicate that T3SS genes are already so highly expressed in planta that the addition of more NO does not further increase this elevated level of expression.

Besides its effects on the T3SS, altering NO concentrations in culture elicited broad changes in gene expression. We reduced NO levels using the non-denitrifying mutant $\Delta narG$. However, preventing the cells from using the denitrification pathway has significant effects on the biology and metabolic state of the cells, making the interpretation of these results

challenging. For example, the $\Delta narG$ cells grown in culture showed evidence of decreases in growth rate and metabolic activity, indicated by decreased expression in the biosynthetic pathways of nucleotides, reduced expression of the oxidative phosphorylation system, and decreased production of many tRNAs. Treating the cells with NO, either with exogenously applied CysNO or with the NO-overproducing $\Delta norB$, caused similar changes in many metabolic pathways in culture. However, a primary force in culture was the stress caused by increased NO concentrations. This manifested in decreased expression of denitrification and nitrate uptake functions and an increased expression of the NO-detoxifying enzyme hmpX. This stress was associated with decreased expression of most R. solanacearum secretion systems. However, expression of the T3SS showed the opposite trend, indicating the specificity of NO-dependent T3SS regulation.

When denitrification mutants grew *in planta* they had far fewer alterations in gene expression relative to wild type than when the mutants grew in culture. This suggests that inputs from the plant host help *R. solanacearum* control its metabolism and behaviors. Overall, the cells grown *in planta* seem to encounter less nitrosative stress than cells grown in denitrifying conditions in culture. This could mean that NO stress is not as important *in planta* than in culture, but it does not take into account differences in the microenvironments of the xylem environment. Bacteria grown in culture experience a uniform environment with consistent NO stress. In contrast, *R. solanacearum* cells colonizing plant stems occupy multiple different microenvironments, which likely contain varying NO levels.

A previous study compared gene expression between *R. solanacearum* grown in rich media and *R. solanacearum* living in tomato xylem (6). Although there were methodological

present between that experiment and this one, we saw many similarities in the DEGs present between in culture and *in planta R. solanacearum*. In both experiments, many of the most highly upregulated genes are involved in the T3SS. Of the genes that were upregulated *in planta* in both experiments, 31 out of 141 (~22%) encoded structural components, regulators, or effectors of the T3SS. Three exceptions to this trend were *prhKLM*. Mutating any of these genes leads to a loss of T3SS gene expression, yet all three were highly downregulated *in planta* compared to either CPG or VDM (Supplementary materials) (6, 34). Several other genes that were highly upregulated *in planta* in both experiments encode metabolism of sucrose or myoinositol, two carbon sources important for *R. solanacearum* during infection (60–62). Additionally, genes involved in flagellar motility were upregulated in both experiments. A similar number of genes (137) were downregulated *in planta* in both experiments. These included several genes predicted to be involved in amino acid transport and metabolism and the superoxide dismutase genes *sodB* and *sodC*.

Components of the denitrification pathway were among the most highly upregulated *R*. solanacearum genes in planta compared to in rich medium. Consistent with this observation, *R*. solanacearum mutants unable to denitrify were reduced in growth in planta and in bacterial wilt virulence (11). However, the same genes were around 20-fold more highly expressed in denitrifying culture than in planta. Further, the RNS-responsive NO-detoxifying genes norB and hmpX were upregulated in planta compared to rich media but were expresses much less in planta than in denitrifying conditions in culture. This indicates that *Rs* experiences more nitrosative stress when growing in denitrifying culture conditions than when growing in the plant host, which in turn is more nitrosatively stressful than aerobic growth in rich media. These

data add to the strong evidence that *R. solanacearum* gene expression and metabolism are very different in the biologically realistic host environment than in culture. This may be due to the complex structure of the xylem environment, where host inputs modulate *R. solanacearum* gene expression, the ability to form defensive biofilms and multiple microenvironments with different nutrient or oxygen concentrations, or because the xylem is a flowing environment, constantly bringing new nutrients into the bacterial habitat. The bacterium's behavior in culture should be regarded as artifactual unless proven otherwise.

We attempted to directly measure the concentrations of NO in healthy and infected tomato xylem collected from fluid pooling on a cut stem using the NO-reactive fluorescent dye DAF-FM, electro paramagnetic resonance (EPR), and an NO-sensitive microsensor (63–66). While a fluorescent signal was observed when DAF-FM was added to xylem sap, no signal was detected through EPR using the NO spin trap cPTIO or with the microsensor (Unisense, Aarhus, Denmark), suggesting that the DAF-FM fluorescence was not specific to NO. These results highlight the need to measure NO using multiple methods in biological systems (67). This failure to detect NO in tomato xylem may not reflect true levels of NO in an intact plant. We collected xylem sap by de-topping tomato plants just above the cotyledons and allowing root pressure to force xylem fluid to pool on the cut stem. Any material exuded in the first two minutes after cutting was removed in an attempt to limit the amount of cellular debris and phloem in the collected material. This method, while useful for obtaining sap to analyze for stable metabolites may not work with a transient metabolite like NO (20). Cutting the stems stimulates production of reactive oxygen species, which quickly react with NO to form other reactive nitrogen species, potentially diluting any NO signal (68-70). Furthermore, this approach can only measure NO

levels in bulk xylem sap. The xylem is a dynamic and physically heterogenous environment.

Xylem flow, xylem structure, and *R. solanacearum*-produced biofilms may all create gradients or microenvironments with altered NO concentrations in the xylem of intact plants

(Zimmermann, 1983; Kim *et al.*, 2016; Tran *et al.*, 2016; Lowe-Power, Khokhani and Allen,

2018). These factors complicate direct measurement of xylem NO. Confocal microscopy of intact infected stems using fluorescent markers to visualize *R. solanacearum*, biofilms, and NO may eventually give a more complete understanding of this challenging landscape.

Overall, these results reveal a strong connection between NO levels and expression of the *R. solanacearum* T3SS. They suggest that *R. solanacearum* regulates virulence in part by using denitrifying metabolism and the resulting NO as a signal of the hypoxic high-nitrogen host xylem environment. Ongoing work is exploring how *R. solanacearum* manages nitrosative stress and identify additional effects of NO on biology of both host plant and bacterial pathogen.

Materials and Methods

Bacterial strains and culture conditions.

All strains, plasmids, and primers used in this study are listed in Supplementary Table 1. *R. solanacearum* was cultured in either CPG or a modified VDM medium at 28° C (11, 74). *E. coli* was grown in Luria-Bertani (LB) media at 37° C. As needed, cultures were supplemented with antibiotics: $25 \,\mu\text{g/mL}$ kanamycin or $15 \,\mu\text{g/mL}$ gentamicin.

Strain construction.

An R. solanacearum GMI1000 mutant lacking hrpB (RSp0873) was created using a modified sacB-dependent positive selection vector, pUFR80 (75). The regions directly upstream and downstream of hrpB were amplified using the $\Delta hrpBup/dwn$ primer pairs. These fragments were then inserted into pUFR80 digested with HindIII using Gibson assembly (76). The resulting plasmid, pUFR80- $\Delta hrpB$ was transformed into R. solanacearum GMI1000 and successful plasmid integrations were selected for kanamycin resistance. The resulting colonies were then counter selected on CPG + 5% w/v sucrose. Successful deletions were confirmed using PCR, sequencing, and a functional screen for the ability to induce HR on the incompatible host N. tabacum (77).

The $\Delta hrpB$ mutation was complemented by inserting a DNA fragment encoding hrpB and hrcC with the ~600 bp upstream containing their native promoter into the selectively neutral att site in the R. solanacearum chromosome using pRCK (78). The fragment was amplified using hrpBcomp_F/R and inserted into AvRII/XbaI-digested pRCK using Gibson assembly. This vector was then transformed into $\Delta hrpB$ and selected on CPG+kan.

Plant growth conditions.

Wilt-susceptible tomato cv. Bonny Best were germinated and grown in BM2 all-purpose germination and propagation mix (Berger, Saint-Modeste, QC). Plants were grown at 28°C with a 12 hr photoperiod. Seedlings were transplanted after 14 days. After transplanting, plants were watered on alternate days with 1/2 strength Hoagland solution. Tomato seeds for axenic seedling production were sterilized by washing with 10% bleach for ten minutes, followed by

two five-minute washes in 70% ethanol, then rinsed five times with water and germinated on water agar plates.

Lux reporter assays.

To test the effect of denitrification on T3SS gene expression, *R. solanacearum* strain GMI1000 carrying a *hrpB::lux* reporter gene fusion was grown in denitrifying conditions as follows (9). Overnight cultures grown in CPG were resuspended in VDM with or without 30 mM potassium nitrate to an initial OD₆₀₀ of 0.001. These cultures were grown in 200 μL volumes in clear-bottomed white-walled 96 well plates at 28°C in 0.1% O₂ with shaking. Every half hour, the Abs₆₀₀ and luminescence was measured using a BioTek SynergyHT microplate reader (BioTek, Winooski, VT, USA). To determine the effects of the NO scavenger cPTIO on T3SS gene expression, *hrpB::lux* cultures were resuspended in 24-well plates in 1 mL of water, either with or without two five day-old sterile tomato seedlings. As appropriate, cPTIO was added to a final concentration of 1 mM. The plates were incubated at 28°C with shaking for ~24 hours. The pigmented liquid was removed from the seedlings and transferred to 1.5 mL Eppendorf tubes, after which the bacteria were pelleted by centrifugation. The pigmented supernatant was removed, and the pellets resuspended in 200 μL of water. These suspensions were transferred to a new plate and the Abs₆₀₀ and luminescence was measured as detailed above.

RNA extraction for sequencing.

To profile gene expression of *R. solanacearum* at various levels of NO stress, we extracted RNA from *R. solanacearum* grown in culture and *in planta*. For each in condition, we

used R. solanacearum from three separate overnight cultures as biological replicates. For the in vitro samples, overnight cultures grown in CPG were resuspended to a final OD₆₀₀ of 0.01 in 50 mL of VDM + 30 mM potassium nitrate in conical tubes. These cultures were incubated without shaking for 12 hours at 28°C in 0.1% O₂. Four hours before harvesting, CysNO or H₂O₂ were added to the relevant cultures to a final concentration of 1 mM and 100 μM, respectively. CysNO was synthesized by adding HCl to a solution containing 200 mM L-cysteine and 200 mM sodium nitrite. The solution was incubated in the dark for ten minutes before it was neutralized by adding sodium hydroxide to a final concentration of 200 mM. The molarity of the solution was determined using the absorbance at 334 nm and the extinction coefficient 90/M*cm. After 16h total incubation, sub-samples were collected for dilution plating to determine CFU/ml and the tubes were capped and centrifuged at room temperature for 5 min at 8000 rpm. The supernatant was removed and pellets were frozen in liquid nitrogen. RNA extractions were carried out using a modified version of the Quick-RNATM MiniPrep kit (Zymo Research, Irvine, CA, USA), as follows. Pellets were resuspended in 400 µL of ice cold TE pH 8 with 1 mg/mL lysozyme, 0.25 μL Superase Inhibitor (Ambion, Austin, TX, USA), and 80 μL of 10% SDS, vortexed for 10s, transferred to a new 2 mL tube, and shaken at ~300 rpm for 2 min. 800 μL of RNA-Lysis lysis buffer was added, the tubes were vortexed again for 10 s, cleaned according to the kit manufacturer's instructions, and eluted in 100 μL of water. Nucleic acid concentrations were estimated using a nanodrop, normalized to 200 ng/uL, and cleaned using the DNA-free DNAse kit (Invitrogen, Carlsbad, CA, USA). Samples were incubated at 37C for 1 hour, with 2 μL more of DNAse added at 30 min. After DNAse inactivation, samples were further cleaned by chloroform extraction, then precipitated overnight at -20 $^{\circ}$ C with 100 μ M Sodium Acetate pH 5.5 and 66 $^{\circ}$

ethanol. Samples were checked for concentration on a Nanodrop, for DNA contamination by PCR using the qRT-PCR primers *serC_F/R*, and for RNA integrity (RIN) using an Agilent Bioanalyzer 21000 (Agilent, Santa Clara, CA, USA). All samples had RIN values above 7.3.

The *in planta* samples were harvested after 21 day old Bonny Best tomatoes were inoculated with ~2000 CFU of each bacteria strain through the cut petiole of the first true leaf. At 3 dpi, approximately 0.1 g of stem tissue was collected from the site of inoculation, immediately frozen in liquid nitrogen, and stored at -80°C. Another ~0.1 g of tissue was collected from directly below the inoculation site and was ground in bead beater tubes using a PowerLyzer (Qiagen, Hilden, Germany) for two cycles of 2200 rpm for 90 s in each with a 4 min rest between cycles. This material was then dilution plated to measure bacterial colonization.

From each biological replicate, we chose six plants with the most similar level of colonization.

RNA was extracted from these using a modified hot phenol-chloroform method (6). Between 4 and 5 individual plants were pooled per biological replicate. Nucleic acid sample quality was checked using a nanodrop, Agilent bioanalyzer, and qRT-PCR primers Actin_F/R. All samples had RIN values of above 7.2.

RNA sequencing and data analysis.

All RNA was sent to Novogene (Beijing, China) for library preparation, sequencing, and analysis. rRNA depletion, fragmentation, and library construction were done using NEBNext® $\mu Ltra^{TM}$ Directional RNA Library Prep Kit for Illumina® (NEB, Ipswitch, MA, USA) following the manufacturer's recommendation and starting with 3 μg of RNA per sample. After the libraries were constructed, their quality was assessed using an Agilent Bioanalyzer 21000 system and

sequenced using an Illumina platform to generate paired-end reads. Between 19,000,000 and 40,000,000 reads were produced per sample. Raw reads were converted to FASTQ files using Illumina CASAVA v1.8, and then filtered for quality, removing reads with adaptor contamination, greater than 10% uncertain nucleotides, or more than 50% of nucleotides with a Q_{pred} less than or equal to 5. Over 95% of reads were of good quality, and were mapped to the *R. solanacearum* GMI1000 genome

(https://www.ncbi.nlm.nih.gov/assembly/GCF_000009125.1) using Bowtie2 -2.2.3 (79). From this, gene expression was calculated using HTseq v0.6.1 and differential gene expression was calculated using DESeq 1.18.0. P-values calculated by DESeq were adjusted to control for the false discovery rate (FDR) using the Benjamini-Hochberg approach. Gene Ontology enrichment was analyzed using GOseq Release2.12 and KEGG enrichment was calculated using KOBAS v2.0 software.

Measuring T3SS expression with qRT-PCR.

Expression of T3SS genes was measured in denitrification mutants grown in 40 mL of VDM + 30 mM nitrate grown in GasPakTM EZ microaerobic pouches (BD, Franklin Lakes, NJ, USA) at 28° C with shaking for 18 hours starting from an OD₆₀₀ of 0.001. RNA extractions were carried out using a hot phenol-chloroform method(6). Extractions were carried out using the Quick-RNATM MiniPrep kit (Zymo Research, Irvine, CA, USA). cDNA synthesis was done using the Superscript VILO cDNA synthesis kit (Invitrogen, Carlsbad, CA, USA). qPCR reactions were carried out in 10 μ L volumes using 5 ng of total template using PowerUp Syber Green Master) in a QuantStudio 5 Real-Time PCR System Mix (Applied Biosystems, Foster City, CA, USA).

Acknowledgments

The authors would like to thank Jon Jacobs for discussion and advice throughout the project and Max Miao for his expertise and discussion about statistics and R. This work was funded by National Sciences Foundation grant IOS 1258082. CGH and BLD were supported by NSF predoctoral fellowships. This material is based upon work supported by the National Science Foundation Graduate Research Fellowship Program under Grant No. DGE-1747503. Any opinions, findings, and conclusions or recommendations expressed in this material are those of the author(s) and do not necessarily reflect the views of the National Science Foundation. The authors declare no competing financial interests

Data Availability Statement

The data supporting this research are openly available in the Gene Expression Omnibus at https://www.ncbi.nlm.nih.gov/geo/query/acc.cgi?acc=GSE160024, GEO accession: GSE160024.

References

- 1. Elphinstone J. 2005. The current bacterial wilt situation: a global overview., p. 9–28. *In* Allen, C, Prior, P, Hayward, AC (eds.), Bacterial Wilt: The Disease and the *Ralstonia solanacearum* Species Complex. Society, American Phytopathological, St Paul, MN.
- 2. Vasse J, Frey P, Trigalet A. 1994. Microscopic studies of intercellular infection and protoxylem invasion of tomato roots by *Pseudomonas solanacearum*. MPMI 8:241–251.
- 3. Genin S, Denny TP. 2012. Pathogenomics of the *Ralstonia solanacearum* species complex. Annu Rev Phytopathol 50:67–89.

- 4. Swanson JK, Montes L, Mejia L, Allen C. 2007. Detection of latent infections of *Ralstonia* solanacearum race 3 biovar 2 in geranium. Plant Dis 91:828–834.
- 5. Yuliar, Nion YA, Toyota K. 2015. Recent trends in control methods for bacterial wilt diseases caused by *Ralstonia solanacearum*. Microbes Environ 30:1–11.
- 6. Jacobs JM, Babujee L, Meng F, Milling AS, Allen C. 2012. The *in planta* transcriptome of *Ralstonia solanacearum*: conserved physiological and virulence strategies during bacterial wilt of tomato. MBio 3:e00114-12.
- 7. Poueymiro M, Genin S. 2009. Secreted proteins from *Ralstonia solanacearum*: a hundred tricks to kill a plant. Curr Opin Microbiol 12:44–52.
- 8. Génin S, Brito B, Denny TP, Boucher C. 2005. Control of the *Ralstonia solanacearum* Type III secretion system (Hrp) genes by the global virulence regulator PhcA. FEBS Lett 579:2077–2081.
- 9. Monteiro F, Genin S, van Dijk I, Valls M. 2012. A luminescent reporter evidences active expression of *Ralstonia solanacearum* type III secretion system genes throughout plant infection. Microbiol (United Kingdom) 158:2107–2116.
- 10. Khokhani D, Lowe-Power TM, Tran TM, Allen C. 2017. A Single Regulator Mediates Strategic Switching between Attachment / Spread and Growth / Virulence in the Plant Pathogen *Ralstonia solanacearum*. MBio 8:1–20.
- 11. Dalsing BL, Truchon AN, Gonzalez-Orta ET, Milling AS, Allen C. 2015. *Ralstonia solanacearum* uses inorganic nitrogen metabolism for virulence, ATP production, and detoxification in the oxygen-limited host xylem environment. MBio 6:1–13.
- 12. Scheler C, Durner J, Astier J. 2013. Nitric oxide and reactive oxygen species in plant biotic interactions. Curr Opin Plant Biol 16:534–539.
- 13. Delledonne M, Xia Y, Dixon R a, Lamb C. 1998. Nitric oxide functions as a signal in plant disease resistance. Nature 394:585–588.
- 14. Simontacchi M, Galatro A, Ramos-Artuso F, Santa-María GE. 2015. Plant Survival in a Changing Environment: The Role of Nitric Oxide in Plant Responses to Abiotic Stress. Front Plant Sci 6:977.
- 15. Wilson ID, Neill SJ, Hancock JT. 2008. Nitric oxide synthesis and signalling in plants. Plant, Cell Environ 31:622–631.
- 16. Leitner M, Vandelle E, Gaupels F, Bellin D, Delledonne M. 2009. NO signals in the haze. Nitric oxide signalling in plant defence. Curr Opin Plant Biol 12:451–458.
- 17. Pfeiffer S, Leopold E, Hemmens B, Schmidt K, Werner ER, Mayer B. 1997. Interference of

- carboxy-PTIO with nitric oxide-and peroxynitrite- mediated reactions. Free Radic Biol Med 22:787–794.
- 18. Oksanen J, Blanchet G, Friendly M, Kindt R, Legendre P, McGlinn D, Minchin PR, O'Hara RB, Simpson GL, Solymos P, Stevens MHH, Szoecs E, Wagner H. 2019. vegan: Community Ecology Package. R package version 2.5-6.
- 19. Arlat M, Gough CL, Zischek C, Barberis P a, Trigalet A, Boucher C a. 1992. Transcriptional organization and expression of the large hrp gene cluster of *Pseudomonas solanacearum*. Mol Plant Microbe Interact.
- 20. Lowe-Power TM, Hendrich CG, von Roepenack-Lahaye E, Li B, Wu D, Mitra R, Dalsing BL, Ricca P, Naidoo J, Cook D, Jancewicz A, Masson P, Thomma B, Lahaye T, Michael AJ, Allen C. 2018. Metabolomics of tomato xylem sap during bacterial wilt reveals *Ralstonia solanacearum* produces abundant putrescine, a metabolite that accelerates wilt disease. Environ Microbiol 20:1330–1349.
- 21. Peyraud R, Cottret L, Marmiesse L, Genin S. 2018. Control of primary metabolism by a virulence regulatory network promotes robustness in a plant pathogen. Nat Commun 9:418.
- 22. Flores-Cruz Z, Allen C. 2009. *Ralstonia solanacearum* Encounters an Oxidative Environment During Tomato Infection. MPMI.
- 23. Flores-Cruz Z, Allen C. 2011. Necessity of OxyR for the hydrogen peroxide stress response and full virulence in *Ralstonia solanacearum*. Appl Environ Microbiol 77:6426–6432.
- 24. Farr SB, Kogoma T. 1991. Oxidative stress responses in *Escherichia coli* and *Salmonella typhimurium*. Microbiol Rev 55:561–585.
- 25. Cunnac S, Occhialini A, Barberis P, Boucher C, Genin S. 2004. Inventory and functional analysis of the large Hrp regulon in *Ralstonia solanacearum*: identification of novel effector proteins translocated to plant host cells through the type III secretion system. Mol Microbiol 53:115–128.
- 26. Marc Marenda, Callard BBD, Genin S, Barberis P, Boucher C, Arlat M. 1998. PrhA controls a novel regulatory pathway required for the specific induction of *Ralstonia solanacearum hrp* genes in the presence of plant cells. Mol Microbiol 27:437–453.
- 27. Lonjon F, Turner M, Henry C, Rengel D, Lohou D, van de Kerkhove Q, Cazale A-C, Peeters N, Genin S, Vailleau F. 2015. Comparative Secretome Analysis of *Ralstonia solanacearum* Type 3 Secretion-Associated Mutants Reveals a Fine Control of Effector Delivery, Essential for Bacterial Pathogenicity. Mol Cell Proteomics.
- 28. Peeters N, Carrère S, Anisimova M, Plener L, Cazalé A-C, Genin S. 2013. Repertoire, unified nomenclature and evolution of the Type III effector gene set in the *Ralstonia*

- solanacearum species complex. BMC Genomics 14:859.
- 29. Van Gijsegem F, Gough C, Zischek C, Niqueux E, Arlat M, Genin S, Barberis P, German S, Castello P, Boucher C. 1995. The hrp gene locus of *Pseudomonas solanacearum*, which controls the production of a type III secretion system, encodes eight proteins related to components of the bacterial flagellar biogenesis complex. Mol Microbiol 15:1095–1114.
- 30. Plener L, Manfredi P, Valls M, Genin S. 2010. PrhG, a transcriptional regulator responding to growth conditions, is involved in the control of the type III secretion system regulon in *Ralstonia solanacearum*. J Bacteriol 192:1011–1019.
- 31. Lonjon F, Lohou D, Cazalé AC, Büttner D, Ribeiro BG, Péanne C, Genin S, Vailleau F. 2017. HpaB-Dependent Secretion of Type III Effectors in the Plant Pathogens *Ralstonia solanacearum* and *Xanthomonas campestris* pv. *vesicatoria*. Sci Rep 7:1–14.
- 32. Zhang Y, Luo F, Wu D, Hikichi Y, Kiba A, Igarashi Y, Ding W, Ohnishi K. 2015. PrhN, a putative marR family transcriptional regulator, is involved in positive regulation of type III secretion system and full virulence of *Ralstonia solanacearum*. Front Microbiol 6:1–12.
- 33. Zhang Y, Li J, Zhang W, Shi H, Luo F, Hikichi Y, Shi X, Ohnishi K. 2018. A putative LysR-type transcriptional regulator PrhO positively regulates the type III secretion system and contributes to the virulence of *Ralstonia solanacearum*. Mol Plant Pathol 1–12.
- 34. Zhang Y, Kiba A, Hikichi Y, Ohnishi K. 2011. prhKLM genes of *Ralstonia solanacearum* encode novel activators of hrp regulon and are required for pathogenesis in tomato. FEMS Microbiol Lett 317:75–82.
- 35. Brito B, Marenda M, Barberis P. 1999. *prhJ* and *hrpG*, two new components of the plant signal-dependent regulatory cascade controlled by PrhA in *Ralstonia solanacearum*. Mol Microbiol 31:237–251.
- 36. Genin S, Gough CL, Zischek C, Boucher CA. 1992. Evidence that the hrpB gene encodes a positive regulator of pathogenicity genes from *Pseudomonas solanacearum*. Mol Microbiol 6:3065–3076.
- 37. Boucher CA, Barberis PA, Trigalet AP, Demery DA. 1985. Transposon mutagenesis of *Pseudomonas solanacearum*: Isolation of Tn5-induced avirulent mutants. J Gen Microbiol 131:2449–2457.
- 38. Zuluaga AP, Puigvert M, Valls M. 2013. Novel plant inputs influencing *Ralstonia* solanacearum during infection. Front Microbiol 4:1–7.
- 39. Aldon D, Brito B, Boucher C, Genin S. 2000. A bacterial sensor of plant cell contact controls the transcriptional induction of *Ralstonia solanacearum* pathogenicity genes. Embo J 19:2304–2314.

- 40. Senuma W, Takemura C, Hayashi K, Ishikawa S, Kiba A, Ohnishi K, Kai K, Hikichi Y. 2020. The putative sensor histidine kinase PhcK is required for the full expression of *phcA* encoding the global transcriptional regulator to drive the quorum-sensing circuit of *Ralstonia solanacearum* strain OE1-1. Mol Plant Pathol 1–15.
- 41. Asgher M, Per TS, Masood A, Fatma M, Freschi L, Corpas FJ, Khan NA. 2017. Nitric oxide signaling and its crosstalk with other plant growth regulators in plant responses to abiotic stress. Environ Sci Pollut Res 24:2273–2285.
- 42. Astuti RI, Nasuno R, Takagi H. 2018. Nitric Oxide Signalling in Yeast. Adv Microb Physiol 72:29–63.
- 43. Simmonds MJ, Detterich JA, Connes P. 2014. Nitric oxide, vasodilation and the red blood cell. Biorheology 51:121–134.
- 44. Cooper CE. 1999. Nitric oxide and iron proteins. Biochim Biophys Acta Bioenerg 1411:290–309.
- 45. Wünsche H, Baldwin IT, Wu J. 2011. S-Nitrosoglutathione reductase (GSNOR) mediates the biosynthesis of jasmonic acid and ethylene induced by feeding of the insect herbivore *Manduca sexta* and is important for jasmonate-elicited responses in *Nicotiana attenuata*. J Exp Bot 62:4605–4616.
- 46. Kolbert Z, Feigl G, Bordé Á, Molnár Á, Erdei L. 2017. Protein tyrosine nitration in plants: Present knowledge, computational prediction and future perspectives. Plant Physiol Biochem 113:56–63.
- Zhang R, Hess DT, Qian Z, Hausladen A, Fonseca F, Chaube R, Reynolds JD, Stamler JS.
 2015. Hemoglobin βCys93 is essential for cardiovascular function and integrated response to hypoxia. Proc Natl Acad Sci U S A 112:6425–6430.
- 48. Russwurm M, Koesling D. 2004. NO activation of guanylyl cyclase. EMBO J 23:4443–4450.
- 49. Rao M, Smith BC, Marletta MA. 2015. Nitric Oxide mediates biofilm formation and symbiosis in *Silicibacter* sp. strain TrichCH4B. MBio 6:1–10.
- 50. Henares BM, Higgins KE, Boon EM. 2012. Discovery of a Nitric Oxide Responsive Quorum Sensing Circuit in *Vibrio harveyi*. ACS Chem Biol 7:1331–1336.
- 51. Liu N, Xu Y, Hossain S, Huang N, Coursolle D, Gralnick JA. 2012. Nitric Oxide Regulation of Cyclic di-GMP Synthesis and Hydrolysis in *Shewanella woodyi*. Biochemistry 51:2087–2099.
- 52. Network CS, Plate L, Marletta MA. 2012. Article Nitric Oxide Modulates Bacterial Biofilm Formation through a Multicomponent. Mol Cell 46:449–460.

- 53. Carlson HK, Vance RE, Marletta MA. 2010. H-NOX Regulation of c-di-GMP Metabolism and Biofilm Formation in *Legionella pneumophila*. Mol Microbiol 77:930–942.
- 54. Hossain S, Boon EM. 2017. Discovery of a Novel Nitric Oxide Binding Protein and Nitric-Oxide-Responsive Signaling Pathway in *Pseudomonas aeruginosa*. ACS Infect Dis 3:454–461.
- 55. Seth D, Hausladen A, Wang Y-J, Stamler JS. 2012. Endogenous Protein S-Nitrosylation in *E. coli*: Regulation by OxyR. Science (80-) 336:470–3.
- 56. Rhee KY, Erdjument-Bromage H, Tempst P, Nathan CF. 2005. S-nitroso proteome of *Mycobacterium tuberculosis*: Enzymes of intermediary metabolism and antioxidant defense. Proc Natl Acad Sci U S A 102:467–72.
- 57. Husain M, Jones-carson J, Song M, Mccollister BD, Bourret TJ. 2010. Redox sensor SsrB Cys 203 enhances *Salmonella* fitness against nitric oxide generated in the host immune response to oral infection. Proc Natl Acad Sci U S A 107:4–13.
- 58. Xue Y, Liu Z, Gao X, Jin C, Wen L, Yao X, Ren J. 2010. GPS-SNO: Computational prediction of protein s-nitrosylation sites with a modified GPS algorithm. PLoS One 5:1–7.
- 59. Liu Z, Cao J, Ma Q, Gao X, Ren J, Xue Y. 2011. GPS-YNO2: computational prediction of tyrosine nitration sites in proteins. Mol Biosyst 7:1197.
- 60. Lowe-Power TM, Khokhani D, Allen C. 2018. How *Ralstonia solanacearum* Exploits and Thrives in the Flowing Plant Xylem Environment. Trends Microbiol.
- 61. Hamilton CD, Steidl OR, Macintyre AM, Hendrich CG, Allen C. 2020. *Ralstonia solanacearum* depends on catabolism of myo-inositol, sucrose, and trehalose for virulence in an infection stage-dependent manner. MPMI.
- 62. Xian L, Yu G, Wei Y, Rufian JS, Li Y, Zhuang H, Xue H, Morcillo RJL, Macho AP. 2020. A Bacterial Effector Protein Hijacks Plant Metabolism to Support Pathogen Nutrition. Cell Host Microbe 1–10.
- 63. Namin SM, Nofallah S, Joshi MS, Kavallieratos K, Tsoukias NM. 2013. Kinetic analysis of DAF-FM activation by NO: Toward calibration of a NO-sensitive fluorescent dye. Nitric Oxide Biol Chem 28:39–46.
- 64. Kleschyov AL, Wenzel P, Munzel T. 2007. Electron paramagnetic resonance (EPR) spin trapping of biological nitric oxide. J Chromatogr B Anal Technol Biomed Life Sci.
- 65. Yoshioka T, Iwamoto N, Ito K. 1996. An application of electron paramagnetic resonance to evaluate nitric oxide and its quenchers. J Am Soc Nephrol 7:961–965.
- 66. Schreiber F, Polerecky L, De Beer D. 2008. Nitric oxide microsensor for high spatial

- resolution measurements in biofilms and sediments. Anal Chem 80:1152–1158.
- 67. Gupta KJ, Igamberdiev AU. 2013. Recommendations of using at least two different methods for measuring NO. Front Plant Sci 4:2–5.
- 68. Milling AS, Babujee L, Allen C. 2011. *Ralstonia solanacearum* extracellular polysaccharide is a specific elicitor of defense responses in wilt-resistant tomato plants. PLoS One 6.
- 69. Beckman JS, Koppenol WH. 1996. Nitric oxide, superoxide, and peroxynitrite: the good, the bad, and ugly. Am J Physiol 271:C1424-37.
- 70. Van Faassen E, Vanin AF. 2007. Nitric oxide radicals and their reactionsRadicals for Life: The Various Forms of Nitric Oxide. Elsevier B.V.
- 71. Kim MK, Ingremeau F, Zhao A, Bassler BL, Stone HA. 2016. Local and global consequences of flow on bacterial quorum sensing. Nat Microbiol 1:15005.
- 72. Tran T, MacIntyre A, Khokhani D, Hawes MC, Allen C. 2016. Extracellular DNases of *Ralstonia solanacearum* modulate biofilms and facilitate bacterial wilt virulence. Environ Microbiol Environ Microbiol Reports 00:1–15.
- 73. Zimmermann MH. 1983. Xylem Structure and the Ascent of Sap. Springer-Verlag, Berlin.
- 74. Hendrick CA, Sequeira L. 1984. Lipopolysaccharide-defective mutants of the wilt pathogen *Pseudomonas solanacearum*. Appl Environ Microbiol 48:94–101.
- 75. Castañeda A, Reddy J, El-Yacoubi B, Gabriel D. 2005. Mutagenesis of all eight *avr* genes in *Xanthomonas campestris* pv. *campestris* had no detected effect on pathogenicity, but one *avr* gene affected race specificity. Mol Plant-Microbe Interact 18:1306–1317.
- 76. Sievers F, Wilm A, Dineen D, Gibson TJ, Karplus K, Li W, Lopez R, McWilliam H, Remmert M, Soding J, Thompson JD, Higgins DG. 2011. Fast, scalable generation of high-quality protein multiple sequence alignments using Clustal Omega. Mol Syst Biol 7:539–545.
- 77. Poueymiro M, Cunnac S, Barberis P, Deslandes L, Peeters N, Cazale-Noel A-C, Boucher C, Genin S. 2009. Two Type III Secretion System Effectors from *Ralstonia solanacearum* GMI1000 Determine Host-Range Specificity on Tobacco. Mol Plant-Microbe Interact 22:538–550.
- 78. Monteiro F, Solé M, van Dijk I, Valls M. 2012. A chromosomal insertion toolbox for promoter probing, mutant complementation, and pathogenicity studies in *Ralstonia solanacearum*. Mol Plant Microbe Interact 25:557–68.
- 79. Langmead B, Trapnell C, Pop M, Salzberg SL. 2009. Ultrafast and memory-efficient alignment of short DNA sequences to the human genome. Genome Biol 10.

- 80. Hanahan D. 1983. Studies on Transformation of *Escherichia coli* with Plasmids. J Mol Biol 166:557–580.
- 81. Ge SX, Son EW, Yao R. 2018. iDEP: An integrated web application for differential expression and pathway analysis of RNA-Seq data. BMC Bioinformatics 19:1–24.

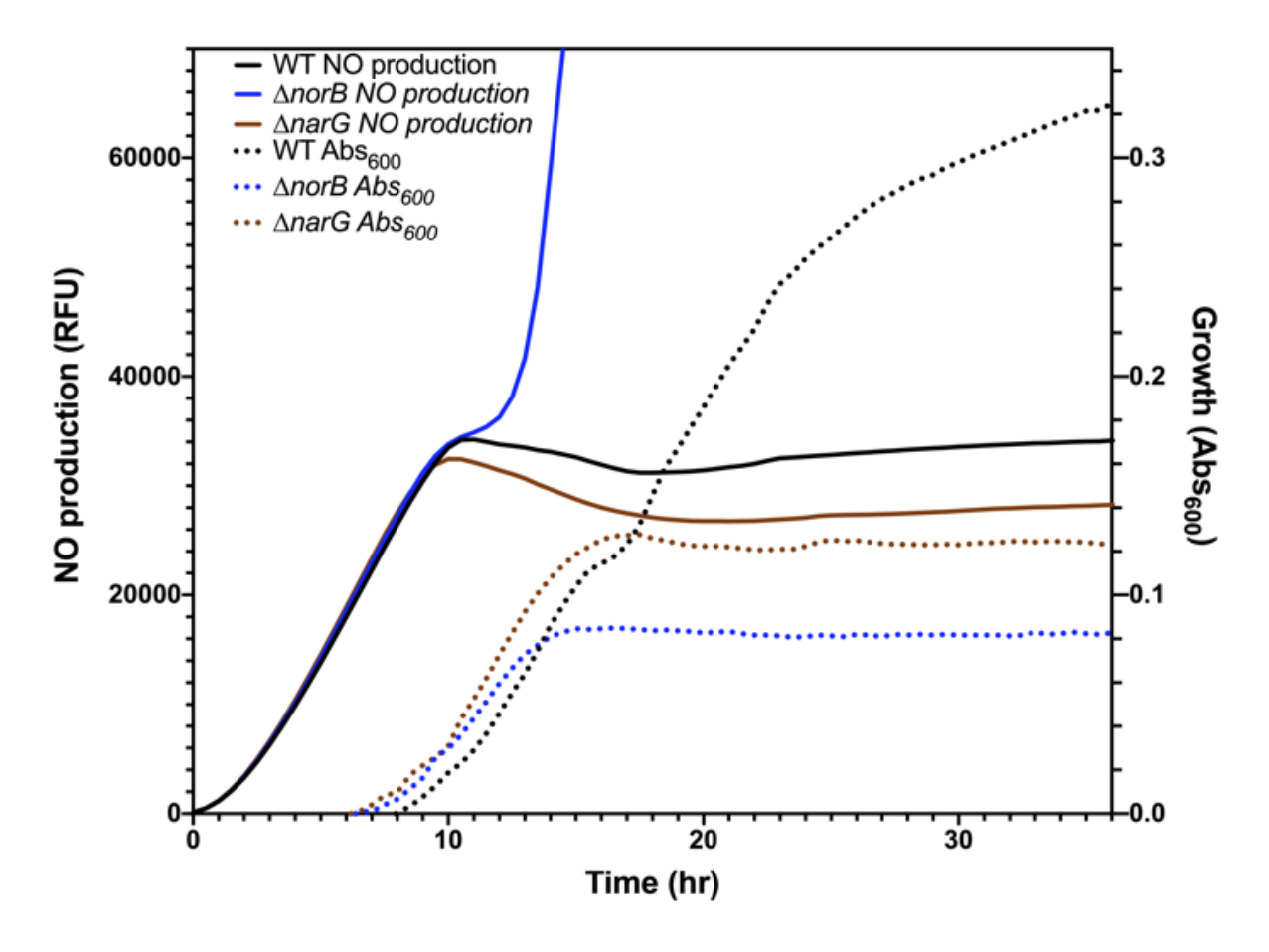
Supplementary Table 1. Bacterial strains, plasmids, and primers

Strains	Relevant characteristics			
R. solanacearum				
GMI1000	Phylotype I seq 18 strain isolated from tomato in French Guyana	(37)		
hrpB::lux	GMI1000 expressing the bacterial <i>lux</i> reporter controlled by the <i>hrpB</i> promoter, Kan ^R	(9)		
ΔnarG	GMI1000 lacking <i>narG</i> , a nitrate reductase. Cannot denitrify and does not produce NO, Gm ^R	(11)		
ΔnorB	GMI1000 lacking <i>norB</i> , a nitric oxide reductase. Can denitrify, but accumulates NO, Gm ^R	(11)		
ΔhrpB	GMI1000 lacking <i>hrpB</i> . Avirulent and does not express a T3SS	This study		
<i>hrpB</i> comp	ΔhrpB complemented.,Kan ^R	This study		
E. coli				
DH5α	dlacZ, Delta M15 Delta(lacZYA-argF) U169 recA1 endA1 hsdR17(rK-mK+) supE44 thi-1 gyrA96 relA1	(80)		
Plasmid	Description	Reference		
pUFR80	Positive sucrose selection vector, Suc ^S , Kan ^R	(75)		
pRCK-GWY	Gateway destination vector that integrates into the GMI1000 genome at the neutral att site; Kan ^R	(78)		
pUFR80-ΔhrpB	Vector used to make unmarked R . solanacearum $\Delta ripB$, Suc ^S , Kan ^R	This study		
pRCK-hrpBcomp	Complementation vector containing WT hrpB and hrcC, Kan ^R	This study		
Cloning Primers				
Primer	Sequence ^a	Reference		
ΔhrpBup_F	5' – cgacggccagtgccaGTTCGATACCAGCGAAAGC target locus: RSp0873	This study		
ΔhrpBup_R	5' – cggagggcGGCAATGCTCCTGAAGCG target locus: RSp0873	This study		
ΔhrpBdwn_F	5' – gcattgccGCCCTCCGGCGGACCGCC target locus: RSp0873	This study		
ΔhrpBdwn_R	5' – acctgcaggcatgcaGCTGTTGCCGACGTATTGACCGGTGC target locus: RSp0873	This study		
hrpBcomp_F	5' – tgcgcgagcaggggaattgcGACAACGTCTCCGGGTTC target locus: RSp0873-RSp0874	This study		
hrpBcomp_R	5' – cgaccctagtctaagatcttCTTCGGCATTCGGCAATG target locus: RSp0873-RSp0874	This study		

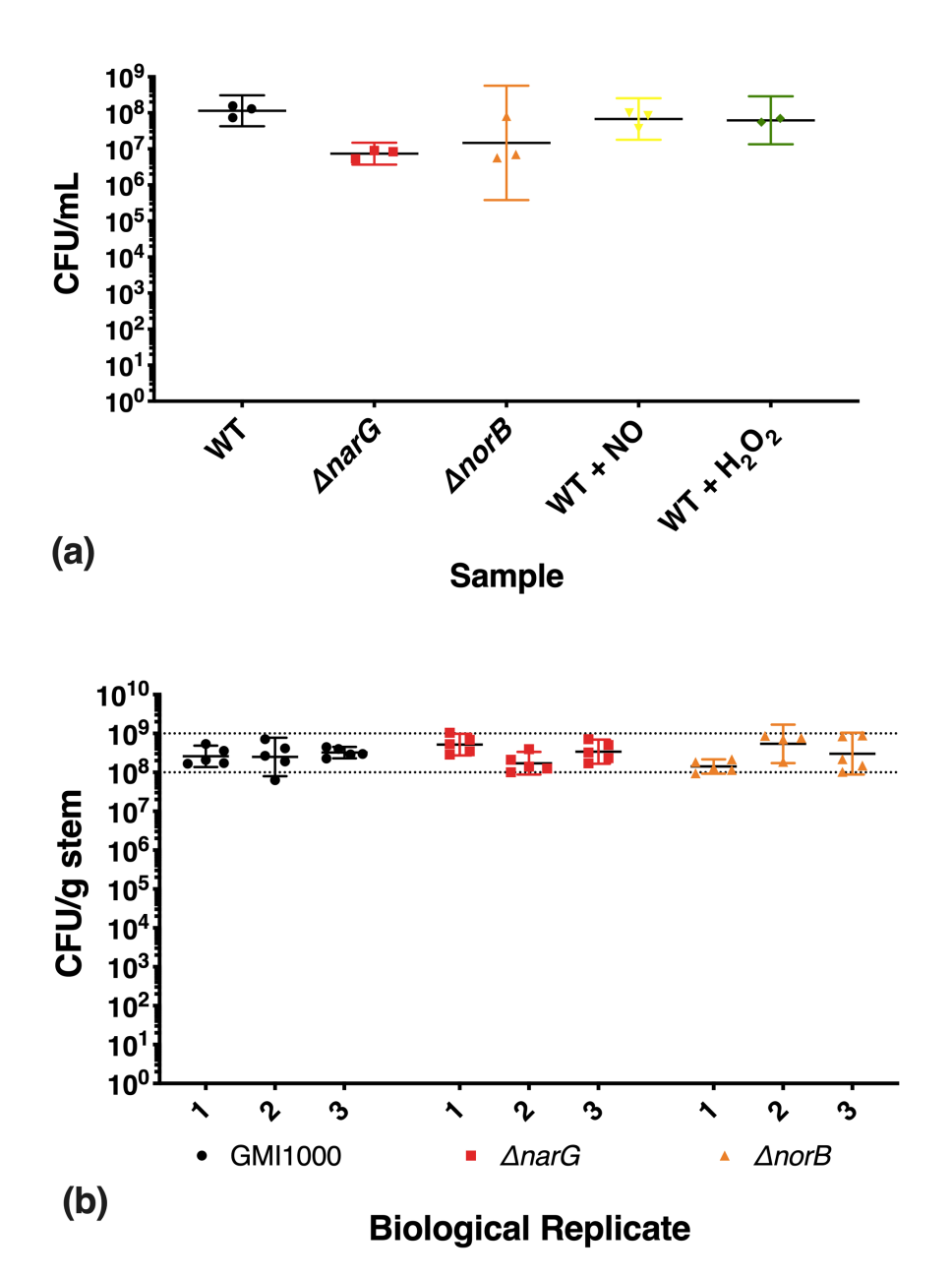
qRT-PCR		
Primers		
Primer	Sequence	Reference
hrpB_F	5' – CCTGCCCGAATACGCAAATG target locus: RSp0873	This study
hrpB_R	5' – CGAATGGCGGATCAGGCGCT target locus: RSp0873	This study
hrpG_F	5' – GCAGAACGTGGAATGTGTCC target locus: R.	This study
	solanacearump0852	
hrpG_R	5' – AGACTGAATGCCTCGGTACG target locus: RSp0852	This study
ripAA_F	5' – GGAATACAGCAACTGCGTGC target locus: RSc0608	This study
ripAA_R	5' – TTGTAGTTGCGGACCCTCAGtarget locus: RSc0608	This study
serC_F	5' – CGCGCAAATACGGTGAAGTG target locus: R. This	
	solanacearumc0903	
serC_R	5' – GTGCACAGATGCACGTAAGC target locus: RSc0903	This study
Actin_F	5' – TCAGCAACTGGGATGATATG target locus: BT013524	(68)
Actin_R	5' – TTAGGGTTGAGAGGTGCTTC target locus: BT013524	(68)

^a Capitalized bp anneal to the target locus, non-capitalized bp anneal to other fragments in a

Gibson assembly reaction

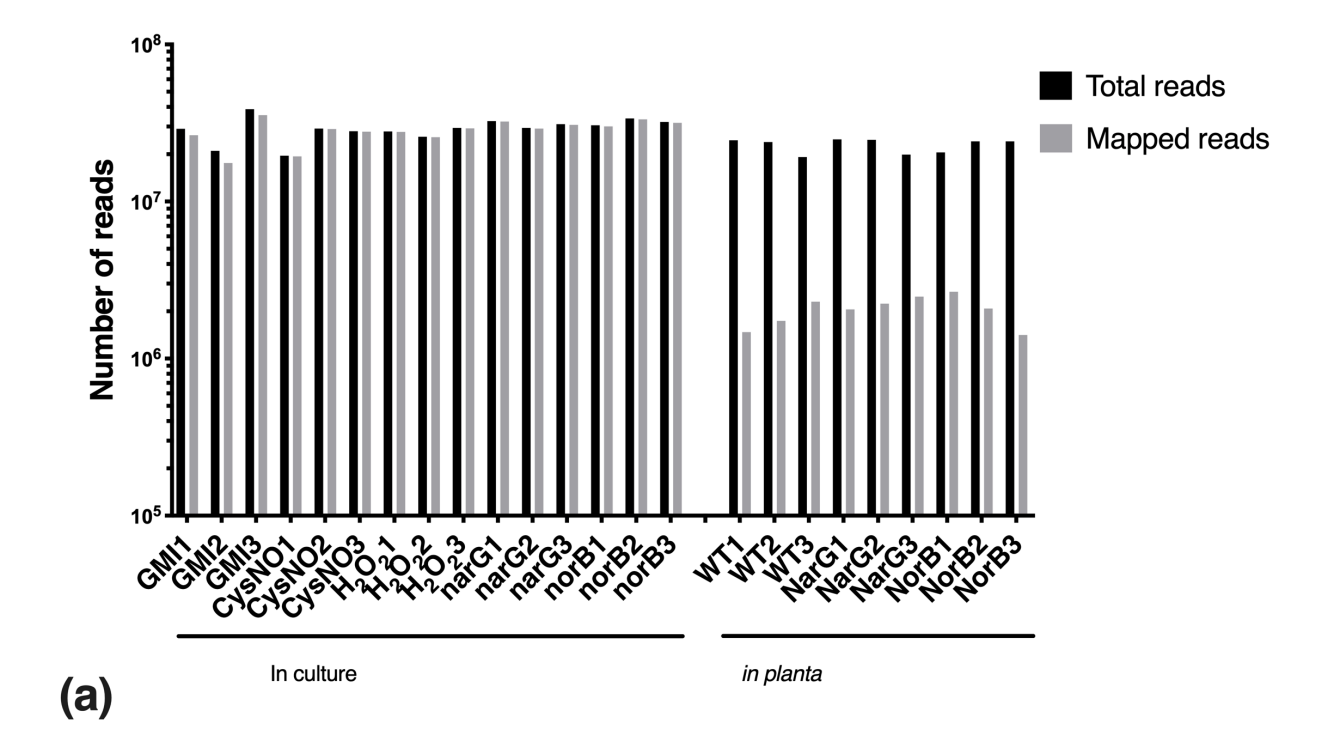


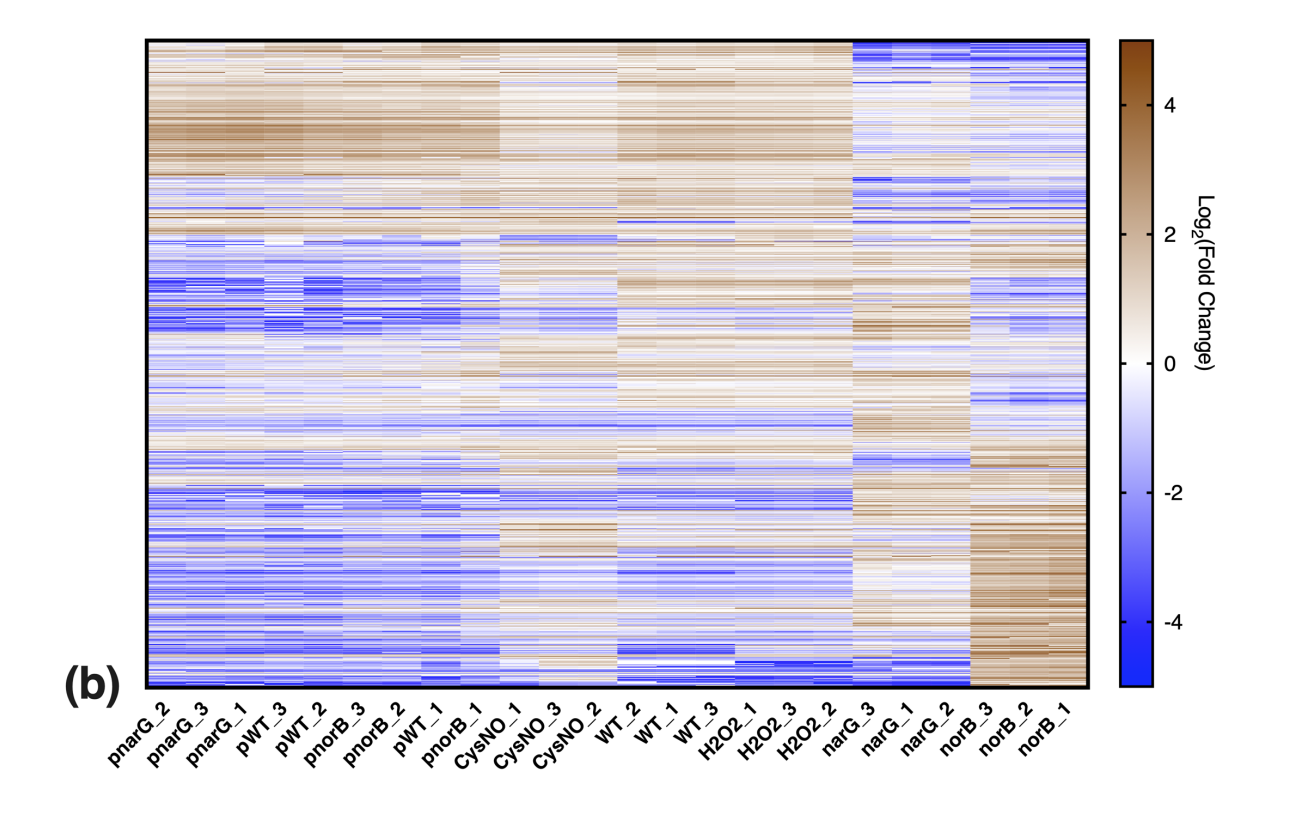
Supplementary Figure 1. Growth and NO levels of *R. solanacearum* strains under denitrifying conditions in culture. Cultures were started at a concentration of 10^6 CFU/mL in VDM containing the NO-detecting fluorescent dye DAF-FM DA at $10 \mu M$. Cultures were incubated in in clear-bottomed, white-walled 96-well plates at 30C for 24 h at $[O_2] = 0.1\%$. Culture growth (dotted lines) is shown as absorbance at 600 nm. NO concentration (solid lines) was measured as DAF-FM fluorescence at 495/515 nm. The $\Delta norB$ mutant strain accumulates NO, which significantly impairs its growth.



Supplementary Figure 2. In vitro cell densities and tomato stem colonization of samples used in RNA-seq. (a) Cell densities of culture samples as measured by dilution plating. One H₂O₂-treated plate was uncountable due to plate contamination. OD₆₀₀ values of each culture were also collected and had comparable values. (b) Colonization of tomato plants used for transcriptome sequencing. Roughly 0.1 g of stem tissue was collected from directly below the

sample used for sequencing. The tissue was ground and dilution plated to enumerate CFU/g stem.





Supplementary Figure 3. General RNA-seq quality (a) Total and mapped reads per RNA-seq sample. The *in planta* samples had lower percentage of mapped reads due to the presence of

host RNA. **(b)** Hierarchical clustering and expression heat map of the 1000 most variable genes in the dataset. Blue indicates higher expression and brown indicates lower expression. All genes were normalized to the mean gene expression across all conditions. Samples collected from *R. solanacearum* grown *in planta* are denoted with the prefix "p". Heatmap created using iDEP.90 (81).

Supplementary Materials including a complete list of gene expression and \log_2 fold change values for all conditions included in this study, KEGG enrichment of genes altered in each condition, and annotations, \log_2 fold change relative to wild-type and adjusted p-values for *R. solanacearum* T3SS related genes can be found online at:

Nitric Oxide Regulates the *Ralstonia solanacearum* Type 3 Secretion System Connor G. Hendrich, Alicia N. Truchon, Beth L. Dalsing, Caitilyn Allen bioRxiv 2020.10.26.355339; doi: https://doi.org/10.1101/2020.10.26.355339

https://www.biorxiv.org/content/10.1101/2020.10.26.355339v1

Chapter 3

A two-way street: the use of the *Ralstonia solanacearum* Type II Secretion System during infection by the phage phiAP1

This chapter will be submitted as the following publication:

Xavier, A. S., de Melo, A. G., Hendrich, C. G., Tremblay, D. M., Rousseau, G. M., Plante, P., de Almeida, J. C. F., Forest, K. T., Zerbini, P. A., Allen, C., & Moineau, S. Driving the wrong way: the use of *Ralstonia solanacearum* Type II secretion system during phage infection and the consequences on phage-host arms race

Contributions: ASX, AGM, and CGH all conducted experiments, wrote the text, and created the figures. ASX, DMT, GMR, and PP sequenced and assembled the BIM4 and BIM30 genomes. CGH sequenced and assembled the T2SS/Tfp positive BIM genomes. JCFA wrote text and contributed to experimental design. KTF provided experimental ideas regarding T2SS structure and mutations. PAZ, CA, and SM all contributed to the design and analysis of experiments.

Abstract

Microbial populations have evolved a wide variety of mechanisms to resist viruses.

These mechanisms provide adaptive advantages in the presence of viral pressure and promote the survival and evolution of the host species. Here, we studied the resistance mechanism of the bacterial wilt pathogen *Ralstonia solanacearum* (*Rs*) to the lytic phage phiAP1 using a library of 28 *Rs* spontaneous <u>Bacteriophage Insensitive Mutants</u> (BIMs). Phenotypic and genetic evidence suggest that phiAP1 requires the Type II Secretion System (T2SS) to infect *Rs*, as most BIMs no longer had Type II secretion activity. Because *Rs* uses its T2SS to secrete several key virulence factors, giving up T2SS to gain resistance to phiAP1 imposed a significant fitness penalty on this pathogen. Using a mutation that inactivates the *Rs* T2SS GspE ATPase but allowed the T2SS complex to assemble normally, we found that phiAP1 requires a functional T2SS to enter *Rs*. However, 6 BIMs retained T2SS function and full virulence on tomato plants, indicating other pathways to phiAP1 resistance are possible. Our results provide insight into phage biology, the function of the *Rs* T2SS, and show how pathogen virulence factors can be exploited to develop effective and durable phage biocontrol therapies.

Introduction

In the dynamic arms race between viruses and bacteria, virus-mediated selection plays a central role in the maintenance of bacterial diversity (1, 2). This selective pressure drives rapid molecular evolution due to natural cycles of adaptation and counter adaptation (3–5). Faced with these pressures, the prevalence of particular bacterial genotypes depends on the balance between adaptive advantages and biological sacrifice of cognate functions (6).

Many bacterial innate mechanisms contribute to their survival, including CRISPR-Cas systems (7), Restriction-Modification systems (8), and abortive infection (9). Additionally, viral resistance phenotypes arise from specific mutations that alter critical host factors required for steps in the viral life cycle like adsorption and DNA injection (10–12).

Ralstonia solanaccearum (Rs) are Gram-negative plant pathogenic bacteria that belong to a heterogeneous group with global distribution and an unusually wide host range. They cause bacterial wilt disease on more than 200 species, including economically important crops such as potato, eggplant, banana, and tomato (13–17). The diverse array of Rs strains have been classified into four phylotypes, each with a distinct geographic origin (18). Although Rs have been targeted by phage therapy approaches, they often have antiphage resistance (19–21), apparently using multiple strategies to escape infection (22, 23). Although some Rs isolates carry canonical CRISPR loci, the locus has not been observed to acquire new targets (24). However, phage insensitive Rs mutants arise with high frequency, indicating the existence of other evasion strategies (24).

To expand our knowledge of *Rs* defense viral strategies, we studied a spontaneous library of <u>Bacteriophage Insensitive Mutants</u> (BIMs) generated by exposing the phylotype II *Rs* strain CFBP2957 to the virulent podophage phiAP1. Two of these BIMs, BIM4 and BIM30, were previously characterized with respect to viral adsorption, phage DNA replication and CRISPR spacer acquisition. The CRISPR-Cas system of *Rs* is not responsible for the resistance phenotype of these variants (24).

Here we determine the molecular basis of antiviral resistance in a larger set of *Rs*CFBP2957 BIMs. We identify the genetic determinants of phage insensitivity by sequencing

genomes of several BIMs. We show that the activity of the *Rs* T2SS is used by phiAP1 during infection. We additionally showed that phage resistance imposes a fitness cost on *Rs* by reducing its virulence on tomato. Finally, we demonstrated that the *Rs* prepilin peptidase is required for both Type IV pili and in the T2SS. To the best of our knowledge, this is the first study in the literature showing the utilization of the T2SS in phage infection.

Results

Identification of genetic determinants involved in phage resistance.

To understand the mechanism of *Rs* resistance to phiAP1, we performed whole genome sequencing of two resistant BIMs and their WT parent strain, CFBP2957. Several polymorphisms were identified in the BIMs that were absent in the parental WT CFBP2957. To map candidate mutations potentially involved in phage resistance, we focused on non-synonymous SNPs and INDELS because most synonymous SNPs were shared among the BIMs (Supplementary Table 4). Supplementary Table 3 presents a summary of the non-synonymous mutations or INDELS unique to the BIMs. Both BIM4 and BIM30 had unique insertions in membrane proteins. In BIM4, a mutation occurred in the membrane protein GspL, which is a part of the Type II secretion system (T2SS) inner membrane complex and participates in the formation of the pseudopilus (Figure 1a, Figure 1b) (25). The INDEL of BIM30 occurred in the prepilin peptidase (PiID) that processes prepilins prior to their addition to the Type IV pilus (Tfp). These INDELs caused frameshift mutations near the beginning of the ORFs of both genes, significantly truncating the primary sequence of the resulting protein.

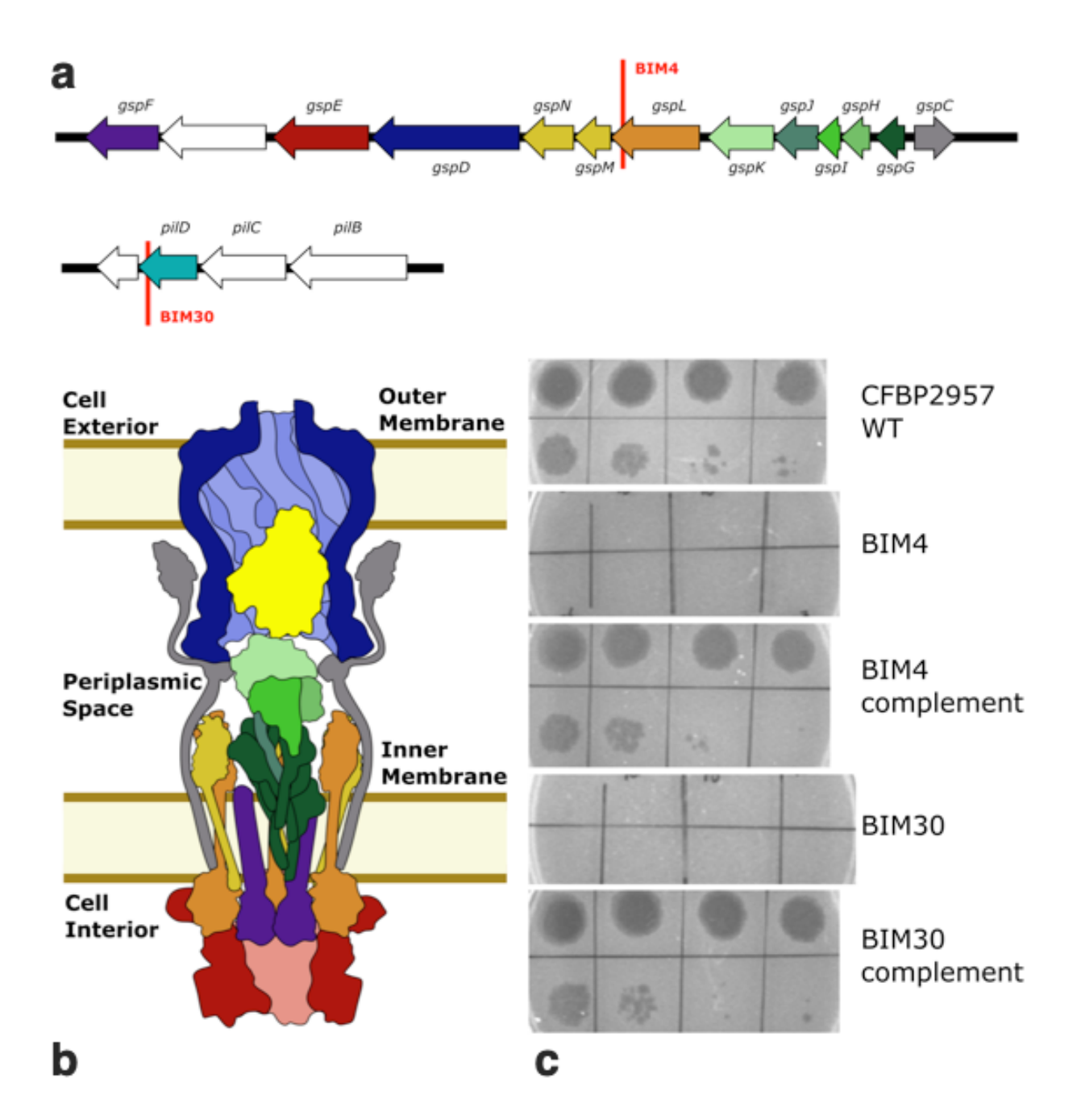


Figure 1. Mutations in *gspL* and *pilD* confer resistance to phiAP1. (a) Genomic location of the unique mutations of *Rs* mutants BIM4 and BIM30. BIM4 contains a mutation in *gspL*, an inner membrane protein of the T2SS. BIM30 contains a mutation in *pilD*, a prepilin peptidase. (b) The structure of the T2SS. The inner membrane complex is composed of the cytoplasmic ATPase GspE (shown in red) and the inner membrane proteins GspC, GspL, GspM, and GspN. GspC

(shown in grey) links the inner membrane complex to the outer membrane complex, which is composed of the outer membrane secretin GspD (shown in blue). GspE uses the energy from ATP hydrolysis to assemble the pseudopilus, which is a polymer of the major pseudopilin GspG (shown in dark green) capped with the minor pseudopilins GspH, GspI, GspJ, and GspK (shown in shades of light green). The growth of the pseudopilus pushes T2SS cargo (shown in yellow) out of the cell. (c) Both BIM4 and BIM30 are resistant to phiAP1 infection and complementing the mutants with *gspL* and *pilD* restores their susceptibility. Ten-fold dilutions of a phiAP1 suspension were spotted onto a lawn of each strain.

Complementation of BIM4 and BIM30 restored phage susceptibility.

To test the hypothesis that the mutations in *gspL* and *pilD* were responsible for phage resistance, we complemented *Rs* CFBP2957 BIM4 and BIM30 with a wildtype copy of *gspL* and *pilD*, respectively. To do so, we used Gibson assembly (26) to introduce each gene to the low-copy plasmid pUFJ10 to be expressed under the control of the kanamycin resistance gene promoter (27). When we transformed this construct into *E. coli* DH5α, the only positive clone in *E. coli* containing *gspL* had the 3′-region past codon 220 deleted, suggesting that this full-length gene might be toxic in *E. coli*. The plasmids p*gspL* and p*pilD* containing 5′ region partial gene (*gspL*) or the complete gene (*pilD*) were transformed in *R. solanacearum* BIM4 and BIM30, respectively. Spot tests were used to verify the ability of phage phiAP1 to infect the BIM4::p*gspL* and BIM30::p*pilD* (Figure 1c). Genetic complementation restored phiAP1 sensitivity, indicating that the loss of GspL or PilD is responsible for phiAP1 resistance in these two mutants.

BIM4 and BIM30 are defective for Type II Secretion, Type 4 pili, or both.

Because the proteins encoded by *gspL* and *pilD* are involved in the T2SS and in the Tfp, we tested the function of these systems in BIM4 and BIM30. We assessed twitching motility by spotting each *Rs* strain on low percentage agar plates and observing the colony margins microscopically after 24 hours (28). The colony edges of BIM4 and WT displayed the diffuse, reticulate margins typical of *Rs* strains with functional twitching motility Tfp (Figure 2a) (28). In contrast, BIM30 coalesced into thick, defined colony edges more rapidly, `. These results indicated that the loss of *pilD* in BIM30 impairs *Rs* twitching motility.

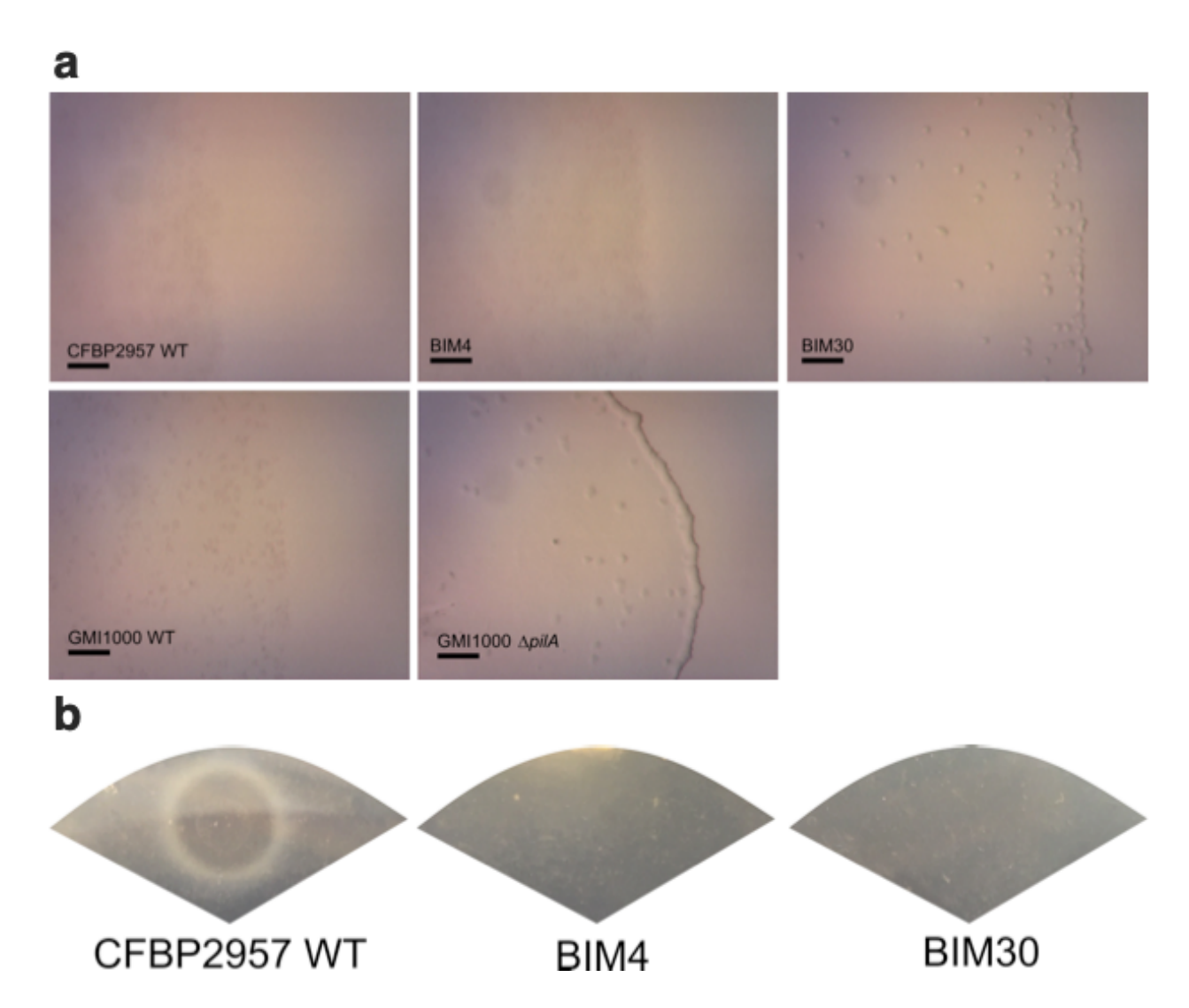


Figure 2. Rs mutants BIM4 and BIM30 are both deficient in T2SS, but only BIM30 is deficient in Tfp-mediated twitching motility. (a) Colony margins of CFBP2957 WT, BIM4, and BIM30 grown on low percentage agar plates. A Tfp deficient mutant, $\Delta pilA$, made in the phylotype I strain GMI1000 is included as a control. The colony margins of WT and BIM4 at low cell densities were diffuse and undefined. In contrast, microcolonies of BIM30 and $\Delta pilA$ coalesced earlier, forming compact, defined masses even at low densities. BIM30 was deficient in twitching motility but BIM4 was not. Scale bars represent 0.1 mm. (b) Secretion of the T2SS exported polygalacturonase enzymes by WT Rs CFBP2957, BIM4, and BIM30. Strains were

plated on minimal media plates containing polygalacturonic acid. After 24 hours of growth, the colonies were rinsed away, and the plates were flooded with HCl to reveal zones of clearing made by polygalacturonase activity. Both BIM4 and BIM30 were unable to export polygalacturonase, indicating they have defects in the T2SS.

As an indicator of T2SS functionality, we tested BIM4 and BIM30 for extracellular activity of polygalacturonase, a Type II secreted enzyme. When grown on agar plates containing polygalacturonic acid, T2SS-positive *Rs* produce a zone of clearing due to the excretion of this enzyme (29). Neither BIM4 nor BIM30 produced a zone of clearing when grown on polygalacturonic acid plates, indicating that neither mutant has a functional T2SS (Figure 2b). In *P. aeruginosa*, PilD not only processes pilins for the Type IV Pilus, but also processes pseudopilins for the T2SS, and loss of PilD abolishes both twitching motility and the T2SS (30). The loss of both systems in BIM30 indicates that PilD plays a similar role in *Rs*.

phiAP1 does not require Rs Tfp during infection.

The phage resistance of BIM4 and BIM30 suggests that the T2SS and Tfp may be required for phiAP1 infection. However, while both BIMs are defective in Type II secretion and fully resistant to phage phiAP1, only BIM30 had impaired twitching motility. These results suggest that the loss of the Tfp might be irrelevant for phiAP1 infection. We tested this hypothesis by asking if phiAP1 could lyse a previously-constructed $\Delta pilA$ mutant of the phiAP1-sensitive phylotype I strain GMI1000. Despite lacking the major pilin subunit of the T4p and

consequently twitching motility, the GMI1000 $\Delta pilA$ mutant retained its sensitivity to phiAP1, indicating that the Tfp is not required for phiAP1 infection (Figure 3a).

We measured the twitching motility and T2SS phenotypes of 26 additional BIMs. Of the tested BIMs, only six displayed T2SS activity (Table 1). Of the 22 T2SS-deficient BIMs, three more were also deficient in twitching motility. Sequencing the *pilD* genes from these three double-phenotype BIMs, revealed that all had either a frameshift near the 5' end of the *pilD* sequence or premature stop codons predicted to result in truncated PilD proteins. Taken together, these results indicate that the T2SS, but not the Tfp, is required for phiAP1 infection.

Table 1. Strain phenotypes

Strain	PhiAP1 infection	Twitching motility ⁽¹⁾	Type II Secretion ⁽²⁾	Virulence (3)	Mutation site
WT CFBP2957	+	+	+	+	N/A
WT GMI1000	+	+	+	+	N/A
ΔpilA (GMI1000)	+	-	+	-	pilA (RSc0558) (Pilin)
GspG OE (GMI1000)	-	Untested	+ (4)	Untested	CFBP2957 gspG expressed with rplM promoter at the Rs GMI1000 att site (31)
GspE mutant	-	Untested	-	-	gspE (RCFBP_10322) (T2SS ATPase)
BIM6	-	-	-	-	pilD (RCFBP_10633) (prepilin peptidase) ⁽⁵⁾
BIM14	-	-	-	-	pilD (RCFBP_10633) (prepilin peptidase) ⁽⁵⁾

(prepili	RCFBP_10633) in peptidase) ⁽⁵⁾
GENIA	m peptidase;
·	RCFBP_10633) ilin peptidase)
(T2SS in	RCFBP_10320) nner membrane protein)
extracellu	10793 (putative ular subtilisin-like ase precursor)
BIM9 - + + No mut	tation detected
membi	.0792 (conserved rane protein of own function)
	FBP_10323) (T2SS nembrane pore)
glutam	21001 (predicted nate/aspartate ansporter)
BIM2 - + L	Untested
	FBP_10326) (T2SS tructural)
BIM5 - + L	Untested
BIM7 - + L	Jntested
BIM11 - + L	Untested
BIM12 - + L	Jntested
BIM13 - + L	Jntested
BIM15 - + U	Jntested
BIM16 - + U	Jntested
BIM18 - + U	Jntested

BIM20	-	+	-	-	Untested
BIM21	-	+	-	-	Untested
BIM22	-	+	-	-	Untested
BIM23	-	+	-	-	Untested
BIM24	-	+	-	-	Untested
BIM26	-	+	-	•	Untested
BIM27	-	+	-	-	Untested
BIM28	-	+	-	-	Untested

- Twitching motility was assessed by observing the colony margins of Rs colonies grown on low-percentage agar plates
- 2. T2SS was assessed by growing each strain on minimal media plates containing polygalacturonic acid, a polymer that is broken down by a T2SS exported enzyme. T2SS positive colonies produce a zone of clearing when plates are flooded with HCl.
- 3. Virulence on tomato of *Rs* BIM strains was assayed by inoculating ~200 CFU of bacteria through a cut leaf petiole and visually rating bacterial wilt disease for 7 days. Five plants were inoculated per strain.
- 4. Rs BIM1 and GspG overexpression strains had reduced, but not completely abolished T2SS activity. In each case, T2SS activity was reduced ~ ten-fold (Figure 3c, Supplementary Figure 1)
- 5. Only the *pilD* gene was sequenced for BIM6, BIM14, and BIM19, all other mutations were identified by whole genome sequencing

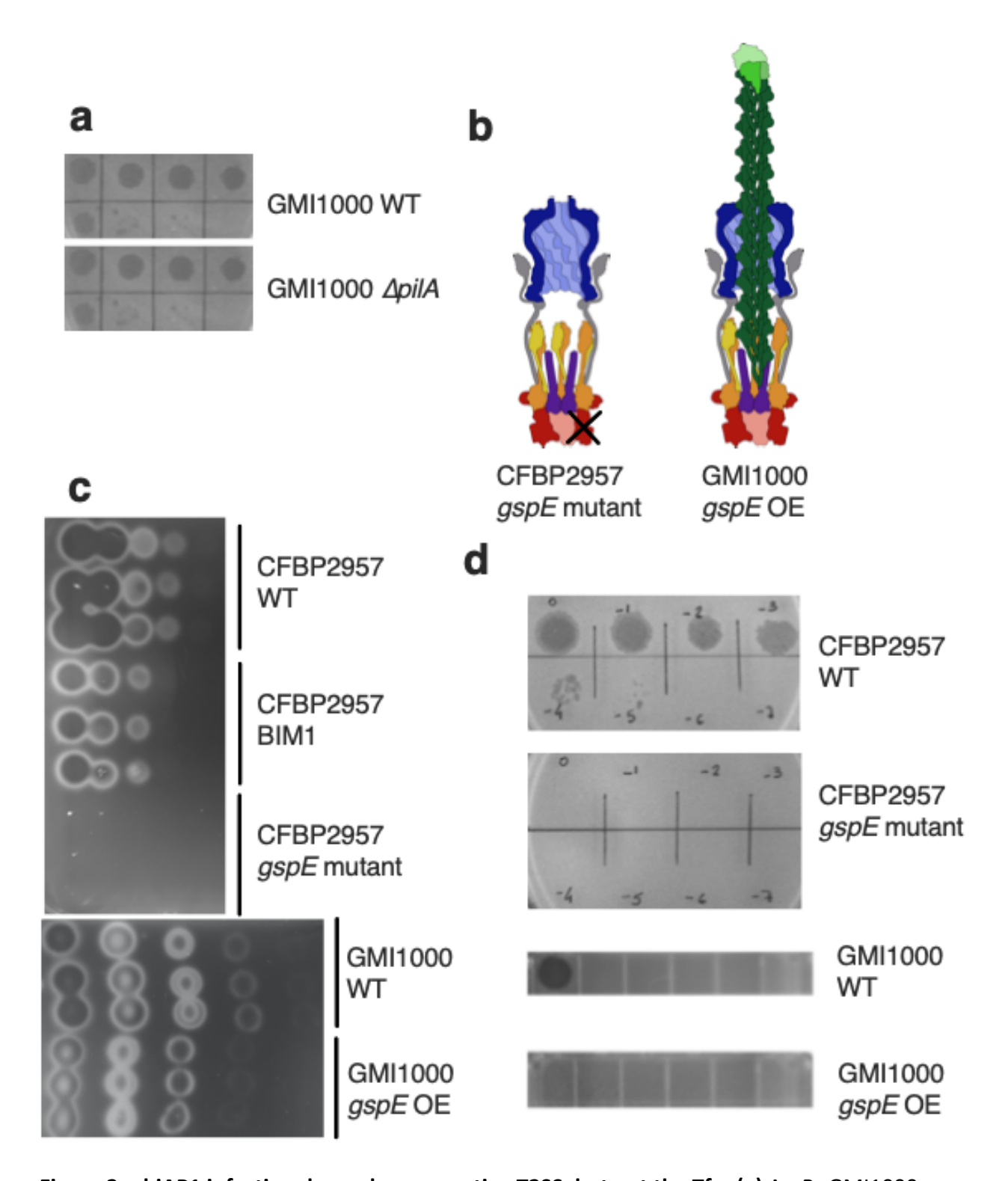


Figure 3. phiAP1 infection depends on an active T2SS, but not the Tfp. (a) An Rs GMI1000 $\Delta pilA$ mutant is susceptible to phiAP1. Ten-fold serial dilutions of phiAP1 suspension were spotted onto a lawn of either GMI1000 WT or GMI1000 $\Delta pilA$. The $\Delta pilA$ mutant was as

susceptible to phiAP1 as WT, indicating that the Tfp is not required for phiAP1 infection. (b) Predicted effects of two T2SS deficient mutants. The Rs strain CFBP2957 gspE mutant contains a single point mutation in the ATP binding domain of the inner membrane ATPase GspE, shown in red. When GspE is unable to bind and hydrolyze ATP, it cannot add pseudopilins to the pseudopilus, and the system cannot export any cargo. The GMI1000 gspE OE mutant contains an additional copy of the major pseudopilin gene qspG (dark green) under the control of an active promoter. This strain expresses qspG roughly ten-fold more than WT (Supplementary Figure 2) and produces an overextended pseudopilus that is predicted to reduce cargo export. In both mutants, the T2SS complex is still predicted to form. (c) Polygalacturonase export by T2SS mutants. Ten-fold serial dilutions of a suspension of each Rs strain were spotted onto minimal media containing polygalacturonic acid. Rs strain CFBP2957 BIM1 and the Rs GMI1000 gspE OE mutant both had roughly ten-fold lower secretion of polygalacturonase compared to WT. The Rs CFBP2957 gspE mutant did not export detectable polygalacturonase. (d) Both the Rs CFBP2957 gspE mutant and Rs GMI1000 gspG OE mutants are resistant to phiAP1. Phage suspensions were spotted onto a lawn of each mutant.

phiAP1 requires a functional T2SS for infection.

The T2SS exports protein complexes by using a dynamic pseudopilus, whose growth and retraction pushes cargo from the periplasm out of the external pore complex into the extracellular space (25). To test if phiAP1 requires a functional T2SS for infection, we made two mutants predicted to interfere with the secretion process while still allowing the T2SS complex to form. In the first, we made a point mutation in the ATP-binding domain of GspE, the inner

membrane ATPase that adds pseudopilins to the T2SS pseudopilus (25). Without ATP binding and cleavage, GspE is unable to grow a functional pseudopilus (Figure 3b) (32, 33). As predicted, this mutant was deficient in the export of both polygalacturonase and pectin methylesterase, two Type II secreted enzymes (Figure 3c, Supplementary Figure 1). Second, we constructed an Rs strain GMI1000 mutant that overexpresses gspG, the main pseudopilin, under the control of a highly active ribosomal peptide promoter (34). Because the formation of the T2SS complex is dependent on the stoichiometry of gene expression (35, 36), increasing the number of available GspG subunits is predicted to increase the length of the pseudopilus, potentially interfering with normal T2SS function (Figure 3b). Semi-quantitative RT-PCR confirmed that expression of gspG in this mutant was roughly ten-fold higher than in wild type (Supplementary Figure 2). While this mutant retained some T2SS activity, its secretion of polygalacturonase and pectin methylesterase was decreased about ten-fold (Figure 3c, Supplementary Figure 1). Both these targeted mutants were resistant to phiAP1 infection (Figure 3d). These results suggest that to infect Rs, phiAP1 requires not just an assembled T2SS complex, but the system must be functional as well.

Phage-resistance imposes a fitness cost by reducing Rs virulence.

Because twitching motility and the T2SS contribute to virulence, we hypothesized that the BIMs may have to give up fitness *in planta* to escape phiAP1. To determine if the BIM4 and BIM30 mutations reduce *Rs* fitness *in planta*, we quantified the virulence of each BIM on bacterial wilt-susceptible tomato plants using a naturalistic soil soak inoculation that mimics the pathogen's infection process. BIM4 and BIM30 caused little or no disease compared to the WT

parent strain CFBP2957 (Figure 4). Adding back *gspL* and *pilD* on the low-copy number plasmid pUFJ10 partially complemented the mutations, leading to intermediate virulence phenotypes that were lower than wild-type (37). However, the complemented BIMs were more virulent than the BIMs.

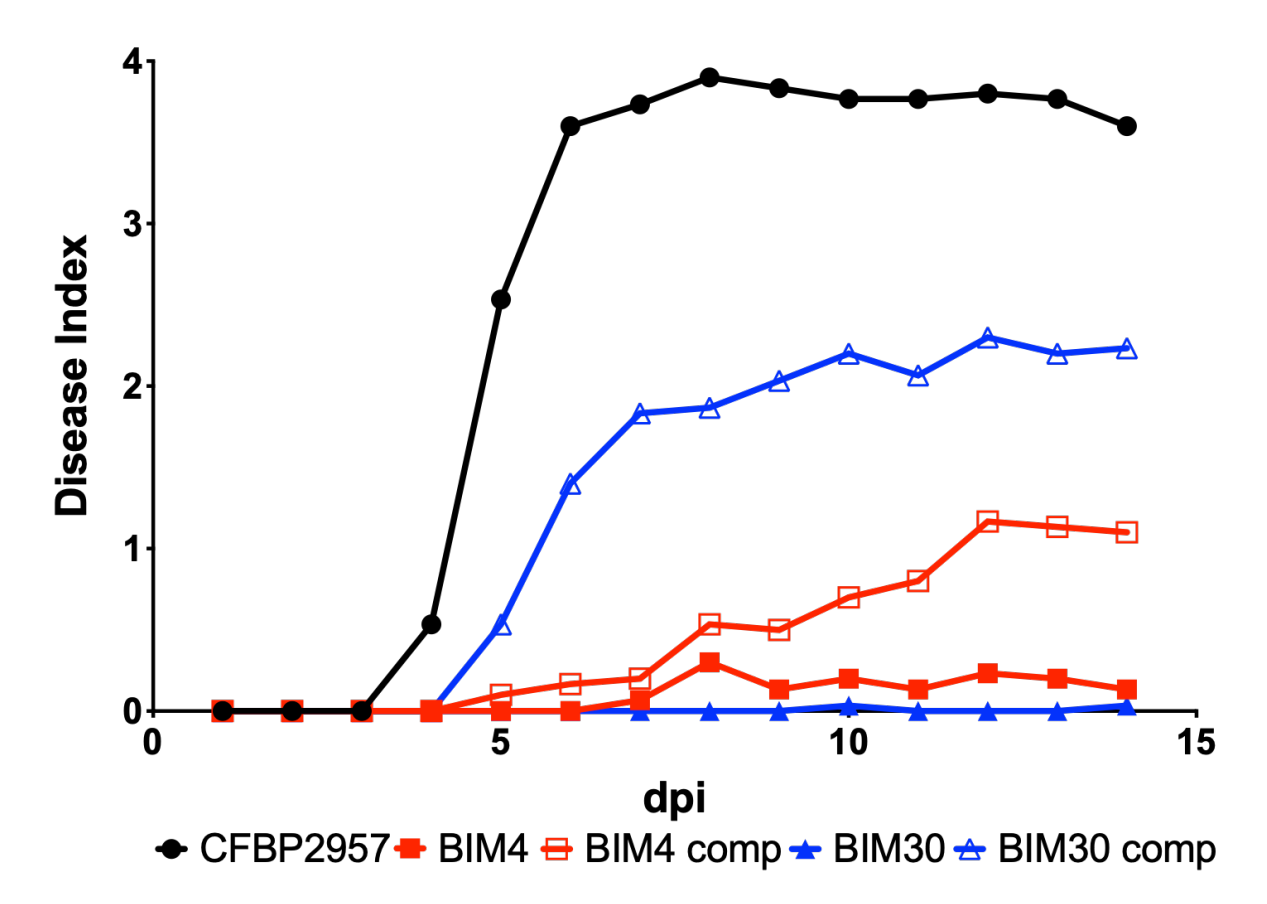


Figure 4. BIM4 and BIM 30 have reduced virulence on tomato. Unwounded 17-day old Bonny Best tomato plants were inoculated by pouring 50 mL of a 10⁸ CFU/mL solution of each *Rs* strain onto the soil. Both BIM mutants caused very little disease compared to *Rs* CFBP2957 WT. This virulence defect could be partially complemented by adding back a copy of *gspL* or *pilD* on the low-copy number plasmid pUFJ10. Each disease curve represents an average of three assays with ten plants per assay and results were analyzed using repeated measures ANOVA. *Rs* WT strain CFBP2957 was more virulent than BIM4 or BIM30 (P< 0.0005). BIM4 comp was more

virulent than BIM4 (P=0.024) and BIM30 comp was more virulent than BIM30 (P=0.0016). The wildtype strain was more virulent than either complemented BIM strain (P<0.001).

The virulence of the remaining 22 BIMs on tomato was measured in a rapid assay that places ~200 CFU of each strain ton a cut leaf petiole. This inoculation method introduces the bacteria directly into the xylem of the plant, leading to quicker, more consistent disease. After a week of growth in planta, the amount of disease correlated directly with the T2SS capability of the BIM (Table 1, Supplementary Figure 3). The only BIMs that were able to cause disease on tomato were the five of the phage-resistant strains that still had a functional T2SS (BIM3, BIM9, BIM17, BIM25, BIM29). BIM1, which did have a functional T2SS, had substantially reduced virulence on tomato. We sequenced the genome of BIM1 and found it contained a 15 bp insertion in the T2SS inner membrane protein, GspF. This insertion added a set of five hydrophobic amino acids (VLAAI) near the midpoint of the protein. In order to test how this mutation might affect T2SS function, we tested the secretion of two Type II secreted products by BIM1. For both polygalacturonase and pectin methylesterase, BIM1 had a level of secretion roughly ten-fold lower than WT (Figure 3c, Supplementary Figure 1). This indicated that while BIM1 retained some T2SS activity, the mutation in GspF both reduced its virulence and provided resistance to phiAP1.

Type II Secretion-positive BIMs had mutations in diverse Rs genes.

We sequenced the genomes of the other five T2SS positive BIMs. After aligning the assembled reads to the WT parent CFBP2957 genome, we found at least one unique variant for

each T2SS positive BIM (Supplementary Table 3). Mutations shared among multiple BIMs are listed in Supplementary Table 4. Among these BIMs, BIM25 had two unique mutations. The first mutation was a four base pair deletion in the cell-wall remodeling protein AmiC (RCFBP_10858). A previously constructed *Rs* strain GMI1000 ΔamiC mutant was still sensitive to phiAP1 (data not shown), indicating that this mutation cannot explain the phiAP1 resistance of BIM25. The second mutation was a G to T mutation at codon 130 of GspD, an outer membrane protein in the T2SS complex. This mutation converts an alanine to aspartate near the N-terminal end of the protein. This mutation is likely in the periplasmic region of the protein, near where it interacts with the inner membrane machinery. Although BIM25 appears to have a functional T2SS and corresponding wild-type virulence, the phage-resistant phenotype of this GspD mutant is consistent with an important role of the *Rs* T2SS for phiAP1 infection.

The other four T2SS positive BIMs had mutations that were difficult to interpret and in non-T2SS genes. BIM3 had a single base deletion roughly midway through RCFBP_10793, which is predicted to encode an extracellular subtilisin-like protease precursor. BIM9 had only one unique predicted variant, an A to G mutation in a predicted transposon that did not change the amino acid sequence. BIM17 contained a C to T mutation in RCFBP_10792, leading to a premature stop codon near the end of this gene encoding a conserved membrane protein of unknown function. BIM29 encoded a G to A mutation in RCFBP_21001, a predicted glutamate/aspartate transporter, which created a premature stop codon early in the protein.

Discussion

The T2SS is a complex, highly dynamic molecular machine that bacteria use to transport folded protein cargo from the periplasm to the exterior of the cell. This system is composed of an outer secretin complex made of fifteen GspD subunits and a hexameric inner membrane complex formed by the transmembrane proteins GspL, GspM, and GspF and the cytoplasmic ATPase GspE (25, 38). ATP hydrolysis by GspE provides energy that drives assembly of the pseudopilus, a structure homologous to the Type IV pilus. It is composed of a polymer of the major pseudopilin GspG with a terminal cap composed of four minor pseudopilins (25). The growth of the pseudopilus forces cargo through the outer membrane pore and out of the cell. The inner and outer complexes are anchored together by the periplasmic transmembrane protein GspC, which also may also bind to specific cargo and load them into the T2SS complex (39, 40). Pseudopilins are transported across the inner membrane by the sec secretion system, and prior to their addition to the growing pseudopilus, charged leader peptides must be removed from prepseudopilins by a prepilin peptidase (41). In P. aeruginosa, this prepilin peptidase is PilD, which also processes prepilins for the Type IV pilus (30). The Rs homolog of PilD was mutated in phage-resistant strain BIM30. This mutant was deficient in both T2SS and in Tfp, indicating PilD process Rs pseudopilins like it does in P. aeruginosa.

The whole genome sequences of two phiAP1 resistant BIMs gave the first hint that phiAP1 may exploit the *Rs* T2SS for its infection cycle. BIM4 and BIM30 had acquired mutations in *gspL* and *pilD*, which are both key components of the T2SS. As expected, these mutations were sufficient to abolish the secretion of known T2SS-dependent enzymes and also to render the mutants nearly avirulent on tomato plants. Screening a larger library of BIMs largely

supported the correlation between phage sensitivity and a functional T2SS. Of the twenty-five BIMs screened, only six retained the ability to secrete the T2SS enzyme polygalacturonase. Three BIMs were also deficient in twitching motility, but they all had mutations in pilD, a peptidase required for both Type II secretion and T4p function. This suggests that twitching motility is unrelated to phiAP1 infection. This conclusion is supported by the phenotypes of a Rs strain GMI1000 $\Delta pilA$ mutant, which remains susceptible to phiAP1 despite lacking twitching motility.

To test if the T2SS complex is a passive receptor for phiAP1 attachment or if its activity is required for phage entry, we designed T2SS mutants that would have reduced secretion activity but still assembled the T2SS complex. First, we mutated a conserved lysine to alanine in the Walker A motif ATP binding motif of GspE. An analogous mutation in EspE of *Vibrio cholerae* was shown *in vitro* to have reduced ATPase activity both alone and when copurified with other T2SS inner membrane subunits (32, 33). This mutant was unable to export key T2SS enzymes.

Interfering with the stoichiometry of T2SS subunits can also alter the structure and function of the T2SS complex. Overexpressing the entire *gsp* operon can lead to the production of extended pseudopili in *E. coli* (42). This effect can also be achieved by overexpressing just the major pseudopilin (35, 36). We predicted that the formation of these extended pseudopili in *Rs* would interfere with the proper export of T2SS enzymes, despite the presence of a fully assembled T2SS structure. We created a *Rs* construct expressing *gspG* under the control of the promoter of the ribosomal protein *rplM*, which has previously been shown to be highly expressed in culture conditions like those found in our T2SS and phiAP1 infection assays (34). In this construct, *gspG* expression was increased roughly tenfold, which corresponded to about a

ten-fold decrease in secretion of certain T2SS substrates. This was similar to the secretion decrease in BIM1, which had reduced, but not completely abolished, secretion of polygalacturonase. In both strains, a decrease in T2SS activity was associated with resistance to phiAP1. Taken together, the phenotypes of these three mutants demonstrate that the T2SS is not a passive binding site for phiAP1, and that some aspect of T2SS activity, whether it be the conformational changes that occur during secretion or the export of particular T2SS targets, is required for successful phiAP1 infection.

While our results indicate that a functional T2SS is necessary for phiAP1 infection, they also demonstrate that *Rs* resistance to phiAP1 is not entirely dependent on a functional T2SS. The majority of tested BIMs were deficient in T2SS, but six BIMs retained both T2SS activity and virulence. Two of these, BIM1 and BIM25 had mutations in known T2SS components. The BIM1 mutation was an in-frame 15 bp insertion in the T2SS inner membrane protein GspF, adding five hydrophobic amino acids after leucine 230. GspF, along with GspE, forms the inner membrane complex of the T2SS (25). The protein is composed of an N-terminal cytoplasmic domain followed by two transmembrane regions, a second cytoplasmic domain, and a third transmembrane domain (43). The two cytoplasmic domains interact with GspF and GspL to form the inner membrane complex. Aligning the *Rs* GspF protein with its homologs in *P. aeruginosa* and *V. cholerae* suggest that the BIM1 insertion occurs in the second transmembrane region (43, 44). Given that the BIM1 mutation is probably buried in the inner membrane, it seems unlikely that the mutated region interacts directly with phiAP1. The mutation more likely affects phiAP1 invasion through its detrimental effects on the T2SS.

The BIM25 mutation maps to the T2SS protein GspD, an outer membrane secretin whose structure creates the exit pore for T2SS cargo (25). In addition to the secretin domain, GspD has four periplasmic domains, N0 to N3, which interact with the inner membrane complex component GspC as well as with secreted products (38, 39). The interaction between GspD and GspC is likely required for proper T2SS formation and function and is thought to involve the N0, N1, and N3 domains of GspD (40, 45). In BIM25, alanine 130 of GspD is mutated to an aspartate. Aligning the Rs GspD sequence with its P. aeruginosa homologue, XpcQ, suggests that this residue is near the C terminal end of the N0 domain (46). Unfortunately, the structure of the NO domain is difficult to determine, perhaps because it forms the linkage points between the pentadecameric outer membrane pore and the hexameric inner membrane complex (47). In 2011, Korotkov et al. identified the specific residues of the V. cholerae N0 that interact directly with GspC, but all of these residues are upstream of the BIM25 mutation in Rs (40). In P. aeruginosa, both XcpC (GspC) and the NON1 subdomains of XcpQ (GspD) interact with the T2SS substrate LasB (39). However, they do not interact with LapA, which is exported by a separate T2SS, suggesting that GspC and GspD help determine substrate specificity of the T2SS. As of now, it is difficult to predict if the BIM25 mutation affects GspD binding to the inner membrane complex, to the profile secreted protein substrates, or if it directly interacts with viral factors. If phiAP1 needs a secreted factor to modify either a Rs extracellular cell wall component or a viral protein prior to invasion, altering the secreted protein profile could promote resistance. Further experiments could test for the interaction of the NO domain of GspD with viral factors in vitro or to examine the secreted protein profile of BIM25. Additional experiments could also test the phiAP1 sensitivity of mutants in the Tat secretion system, which delivers a subset of T2SS substrates into the periplasm prior to export (48). These experiments would not only provide insight into phiAP1 biology but would also allow us to learn more about the structure and function of GspD both in *Rs* and other Gram-negative bacteria.

Three BIMs did not have mutations in genes known to be directly involved in T2SS. BIM3 and BIM17 had mutations in two neighboring genes, RCFBP_10792 and RCFBP_10793, suggesting that these two genes could be necessary for the phiAP1 life cycle. RCFBP_10792 is predicted to encode a membrane protein of unknown function and RCFBP_10793 is predicted to encode an extracellular subtilisin-like precursor protein. RCFBP_10792 is found directly downstream of *glnE*, a predicted Glutamate-ammonia-ligase adenylyltransferase which in *E. coli* is involved in the regulation of glutamate synthesis (49). RCFBP_10793 is located downstream of this pair on the opposite strand of the genome. BIM29 contains a mutation in RCFBP_21001, a predicted glutamate-aspartate transporter. Our data do not indicate which stage of the phiAP1 life cycle these mutations impact. A *Bordetella pertussis* subtilisin-like protein, SphB1, was found to process secreted proteins prior to their export, suggesting the testable hypothesis that RCFBP_10793 acts on T2SS cargo to prepare it for export (50).

Disrupting the T2SS or twitching motility of *Rs* caused significant defects in bacterial wilt virulence (28, 29). By secreting substrates like plant cell wall degrading enzymes, the T2SS contributes to bacterial movement between xylem vessels and the disruption of water flow through the host plant xylem vessels (29). These contributions to virulence and the fact that the T2SS and *pilD* are a hotspot for mutations conferring phage resistance explain why most phiAP1 BIMs have significant virulence defects. The tradeoff between phiAP1 resistance and virulence could improve the durability of phiAP1 as a *Rs* biocontrol agent. However, while the T2SS is an

important component in successful phiAP1 infections, a few BIMs had mutations which either permitted some degree of T2SS function (BIM1 and BIM25) or that may be completely unrelated to the T2SS (BIMs 3, 9, 17, and 29). These BIMs also retained their virulence on tomato. However, we do not currently know if they would produce any fitness defects in the rhizosphere or early in infection. A durable control regime would have to account for these less-detrimental pathways to resistance. Recent reports indicate the importance of studying the evolution of parasite resistance in ecologically relevant environments (51). Virus-mediated biocontrol of bacterial wilt disease might be most durable if based on a cocktail of different phages with distinct targets that reduced the probability of resistance, especially when considering the phenotypic segregation of virulence in the progeny of *Rs* BIMs.

Methods

Bacterial isolates, virus and growth conditions.

Rs CFBP2957 WT and its virus-resistant derivative lines (BIMs) were cultured in CPG containing casein (g/l), peptone (10g/l) and glucose (5g/l) (52) at 28°C with shaking at 250 rpm. *Ralstonia* virus phiAP1, a recently characterized phikmvvirus (23), was propagated on *Rs* strain GMI1000 as described elsewhere (20) with modifications (23).

BIM4, BIM30 and CFBP2957 WT whole genome sequencing.

Genomic DNA of the Rs BIM strains and of the virus sensitive parental CFBP2957 WT was extracted as described (53), with exception of the lysozyme step. Libraries were prepared using the Nextera XT kit, Nextera XT Index kit, and a MiSeq Reagent kit v2 (Illumina, San Diego,

CA) according to the manufacturer's instructions. The whole genome sequencing (2×250 nt) was performed on an Illumina MiSeq system at the Plateforme de Séquençage et de Génotypage des Génomes at the CHUL/CHUQ Research Center for sequencing (Quebec, QC, Canada). The CFBP2957 WT genome was assembled with Ray Assembler (54) version 2.3.1 using a k-mer size of 31 and compared to CFBP2957 reference sequence (GenBank accession PRJEA50685). The BIM genome sequence reads were aligned to the CFBP2957 reference sequence updated using Burrows-Wheeler Alignment tool (BWA) version 0.7.10 (55). The SNPs and INDELs were found using a pipeline consisting of BAM file manipulation (merging, adding header) with Picard (version 1.123) (56), indexing with Samtools (version 1.1) (57) and SNPs/INDELs searching with GATK (version 3.3-0) (58). The resulting vcf files were compared manually.

Creation of Rs BIM4 and BIM3 complemented strains

All primers and strains used in this study are listed in Supplementary Tables 1 and 2. To complement phiAP1 resistance and restore phage sensitivity, the CFBP2957 WT GspL and PilD genes were introduced into BIM4 and BIM30 using the low-copy replicative plasmid, pUFJ10 (37). The empty vector was linearized using *Bsr*GI, which cuts downstream of Kan^R. Terminators were searched using ARNold to verify if the cloned genes would be expressed under the control of the promoter of the Kan^R gene (59). *pilD* was amplified using PilDF/R and GspL amplified using GspLF/R. The genes were placed under the control of the promoter of the Kan^R gene using Gibson assembly (26). The final constructs were transformed into *Rs* using electroporation and confirmed using PCR.

Creation of *gspE* mutant and *gspG* overexpression.

gspE was replaced in its native locus with an ATPase mutant using the positive selection suicide vector pUFR80 (60). The WT version of the gene was amplified from CFBP2957 gDNA using gspE region_F/R and inserted into pUFR80 digested with Xbal and EcoRI using Gibson assembly (26). A mutated version of pUFR80-gspE was made using a QuickChange mutagenesis protocol with the primers gspEmutation_F/R (Agilent, Santa Clara, CA, USA). pUFR80-gspEmutant was then transformed into WT CFBP2957 using a natural transformation.

Transformants were first screened on CPG + kanamycin and then counter selected on CPG + 5% w/v sucrose. Sucrose resistant colonies were screened for T2SS on Pgl plates and then confirmed by sequencing gspE.

To create an *Rs* strain overexpressing *gspG*, *gspG* and the *rplM* promoter were amplified from WT CFBP2957 gDNA using gspG_F/R and rplM_F/R, respectively. Resulting fragments were added to pRCK-GWY digested with AvrII and XbaI using Gibson Assembly (31). The correct construction of the resulting plasmid was confirmed with sequencing, and then transformed into GMI1000 and selected on CPG + kanamycin. *gspG* overexpression was confirmed using semi-quantitative RT-PCR. RNA was extracted from roughly 10^9 CFU of cells from an overnight CPG culture. The cells were pelleted and resuspended in 400 μ L ice cold TE pH 8 with 1 mg/mL Lysozyme, 80 μ L of 10% SDS, and 0.25 μ L of SUPERase IN RNAse Inhibitor (Invitrogen, Carlsbad, CA, USA) and incubated room temperature with shaking for two minutes. RNA was extracted from this lysate using the Zymo Quick-RNA Miniprep Kit (Zymo Research, Irvine, CA, USA). DNA was removed using the DNA-Free DNA removal kit (Invitrogen, Carlsbad, CA, USA).

Phage-sensitivity assays.

The sensitivity assay to phiAP1 was performed using the BIMs, complemented BIMs, and the WT sensitive Rs strains CFBP2957 or GMI1000. Serial dilutions of phiAP1 crude lysate were performed up to 10^{-7} . 250 μ L of an overnight Rs bacterial culture was added to 3 mL of CPG soft agar (CPG 0.75% agar) and poured over solid CPG agar plates to create a bacterial lawn. 5 μ L of phage dilutions were spotted onto the soft agar layer. The plates were then incubated at 30°C for 24 hours. Phage sensitivity of two other mutants with deletions of other components of the T2SS (CFBP2957 $\Delta gspE$) or in the Tfp (GMI1000 $\Delta pilA$::tetA^R) was performed as described above.

Tomato disease assays.

The virulence of BIM mutants was measured on wilt-susceptible tomato plants (cv. Bonny Best) as described previously (61). For soil soak inoculations, overnight cultures of each *Rs* strain were resuspended in water to a final concentration of 10⁸ CFU/mL. Fifty mL of this suspension was poured directly onto soil of each pot containing one unwounded 17-day old plant in a 28°C growth chamber with a 12-hour photoperiod. Disease was rated daily for two weeks on a 0-4 Disease Index scale where 0 = no leaflets wilted, 1 = 1-25% wilted, 2 = 26-50% wilted, 3 = 51-75% wilted, and 4 = 76-100% wilted (62). Soil soak assays were replicated in 3 independent experiments containing 10 plants per strain (total N=30 plants per strain). For petiole inoculations, roughly 200 CFU of each strain suspended in water were introduced to 21-day old plants through a cut petiole. Disease was rated daily for one week. Five plants were inoculated per strain.

Twitching motility test.

Twitching motility assays were conducted as described previously (28). Briefly, ten-fold serial dilution of bacterial suspensions in water were spotted onto CPG plates with 0.75% agar. Colonies were allowed to grow for 24 hours, after which the colony margins were imaged under a light microscope.

Type II Secretion system assays.

Activity of the Type II Secretion System was tested as described in Liu, 2005 (29).

Bacterial cultures suspended in water to 10⁵ CFU/mL were spotted on modified BMM plates with 0.1% yeast extract, 0.5% glycerol, and 1.6% agar. Polygalacturonic acid was added to Pgl media to a final concentration of 0.5% (w/v), and to Pme media was added 0.1 mM CaCl₂ 1 mM MgSO₄, and 0.5% pectin. After 24 hours of growth at 28C, the plates were flooded with 2N HCl.

Whole genome sequencing of Type II Secretion positive BIMs.

Genomic DNA was extracted from BIM1, BIM3, BIM9, BIM17, BIM25, and BIM29 using the Epicentre MasterPure gDNA extraction kit (Epicentre Technologies, Madison, WI). Whole genome sequencing was conducted by the Microbial Genome Sequencing Center (MIGS, Pittsburgh, PA) using an Illumina NextSeq 550 platform. Reads were cleaned using Trimmomatic version 0.39 using a sliding window of 4 and trimming bases with a phred score below 20 (63). Trimmed reads were then assembled to the CFBP2957 genome using BWA version 0.7.17 (55). The assemblies were then indexed using Samtools version 1.9 and variants were detected and

vcf file produced using bcftools version 1.9. Afterwards, variants were compared manually, as described above.

Acknowledgements

This research was supported by grant APQ-01926-14 (FAPEMIG) to PAZ and Canadian Research Chairs. ASX was the recipient of a FAPEMIG graduate fellowship. AGM earned a scholarship from the National Council for Scientific and Technological Development (CNPq-Brazil) in partnership with CALDO (Canada). SM holds a Tier 1 Canada Research Chair in Bacteriophages. This material is based upon work supported by the National Science Foundation Graduate Research Fellowship Program under Grant No. DGE-1747503. Any opinions, findings, and conclusions or recommendations expressed in this material are those of the author(s) and do not necessarily reflect the views of the National Science Foundation. The authors would like to thank Dr. Tiffany Lowe-Power for the creation of the GMI1000 Δ*pilA* mutant.

References

- 1. Buckling A, Rainey PB. 2002. Antagonistic coevolution between a bacterium and a bacteriophage. Proc R Soc B Biol Sci 269:931–936.
- 2. Banfield And JF, Young M. 2009. Variety-the splice of life-in microbial communities. Science (80-) 326:1198–1199.
- 3. Paterson S, Vogwill T, Buckling A, Benmayor R, Spiers AJ, Thomson NR, Quail M, Smith F, Walker D, Libberton B, Fenton A, Hall N, Brockhurst MA. 2010. Antagonistic coevolution accelerates molecular evolution. Nature 464:275–278.
- 4. Dy RL, Przybilski R, Semeijn K, Salmond GPC, Fineran PC. 2014. A widespread bacteriophage abortive infection system functions through a Type IV toxin-antitoxin

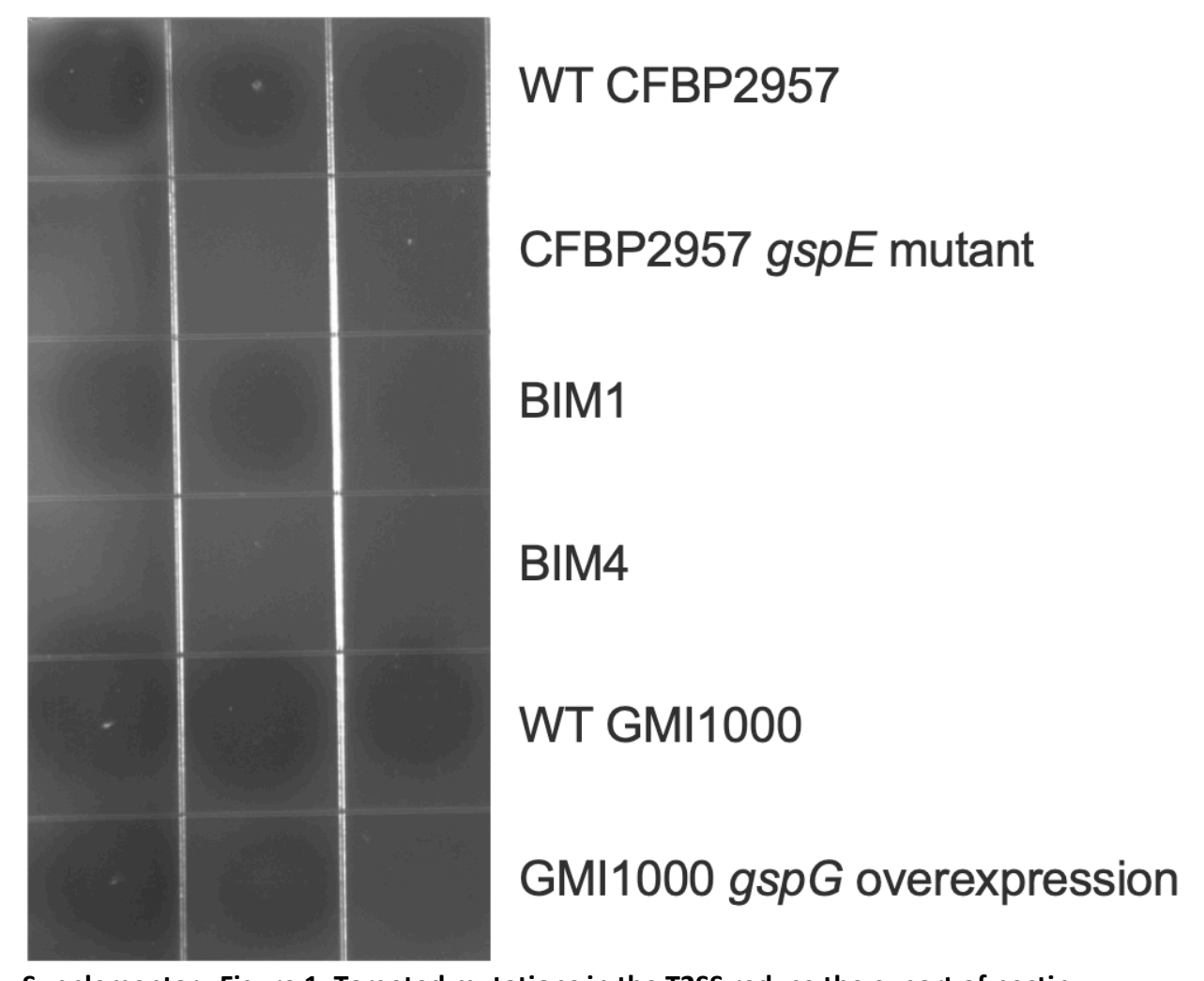
- mechanism. Nucleic Acids Res 42:4590–4605.
- 5. Van Valen L. 1974. Molecular evolution as predicted by natural selection. J Mol Evol 3:89–101.
- 6. Meaden S, Paszkiewicz K, Koskella B. 2015. The cost of phage resistance in a plant pathogenic bacterium is context-dependent. Evolution (N Y) 69:1321–1328.
- 7. Marraffini LA. 2015. CRISPR-Cas immunity in prokaryotes. Nature 526:55–61.
- 8. Tock MR, Dryden DTF. 2005. The biology of restriction and anti-restriction. Curr Opin Microbiol 8:466–472.
- 9. Chopin MC, Chopin A, Bidnenko E. 2005. Phage abortive infection in lactococci: Variations on a theme. Curr Opin Microbiol 8:473–479.
- 10. Nordström K, Forsgren A. 1974. Effect of Protein A on Adsorption of Bacteriophages to *Staphylococcus aureus*. J Virol 14:198–202.
- 11. Lu MJ, Stierhof YD, Henning U. 1993. Location and unusual membrane topology of the immunity protein of the *Escherichia coli* phage T4. J Virol 67:4905–4913.
- 12. Leprohon P, Gingras H, Ouennane S, Moineau S, Ouellette M. 2015. A genomic approach to understand interactions between *Streptococcus pneumoniae* and its bacteriophages. BMC Genomics 16:1–13.
- 13. Fegan M, Prior P. 2005. How complex is the "Ralstonia solanacearum species complex"?, p. 449–461. In Allen, C, Prior, P, Hayward, AC (eds.), Bacterial wilt disease and the Ralstonia solanacearum species complex, 1st ed. APS Press, St Paul, MN.
- 14. Safni I, Cleenwerck I, De Vos P, Fegan M, Sly L, Kappler U. 2014. Polyphasic taxonomic revision of the *Ralstonia solanacearum* species complex: proposal to emend the descriptions of *Ralstonia solanacearum* and *Ralstonia syzygii*... Int J Syst Evol Microbiol 64:3087–3103.
- 15. Denny TP. 2006. Plant pathogenic Ralstonia species, p. 573–644. *In* Gnanamanickam, SS (ed.), Plant Associated Bacteria. Springer, Dordrecht, the Netherlands.
- 16. Hayward AC. 1991. Biology and epidemiology of bacterial wilt caused by *Pseudomonas solanacearum*. Annu rev Phytopathol 29:65–87.
- 17. Hayward AC. 2000. *Ralstonia solanacearum*, p. 32–42. *In* Encyclopedia of Microbiology, 2nd ed. Academic Presss, San Diego, CA.
- 18. Genin S, Denny TP. 2012. Pathogenomics of the *Ralstonia solanacearum* species complex. Annu Rev Phytopathol 50:67–89.

- 19. Yamada T. 2012. Bacteriophages of *Ralstonia solanacearum*: Their Diversity and Utilization as Biocontrol Agents in Agriculture. Bacteriophages.
- 20. Yamada T, Kawasaki T, Nagata S, Fujiwara A, Usami S, Fujie M. 2007. New bacteriophages that infect the phytopathogen *Ralstonia solanacearum*. Microbiology 153:2630–2639.
- 21. Wang X, Wei Z, Yang K, Wang J, Jousset A, Xu Y, Shen Q, Friman VP. 2019. Phage combination therapies for bacterial wilt disease in tomato. Nat Biotechnol 37:1513–1520.
- 22. Kawasaki T, Shimizu M, Satsuma H, Fujiwara A, Fujie M, Usami S, Yamada T. 2009. Genomic characterization of *Ralstonia solanacearum* phage φRSB1, a T7-like wide-host-range phage. J Bacteriol.
- da Silva Xavier A, da Silva FP, Vidigal PMP, Lima TTM, de Souza FO, Alfenas-Zerbini P.
 2018. Genomic and biological characterization of a new member of the genus
 Phikmvvirus infecting phytopathogenic *Ralstonia* bacteria. Arch Virol.
- 24. da Silva Xavier A, de Almeida JCF, de Melo AG, Rousseau GM, Tremblay DM, de Rezende RR, Moineau S, Alfenas-Zerbini P. 2019. Characterization of CRISPR-Cas systems in the *Ralstonia solanacearum* species complex. Mol Plant Pathol 0:223–239.
- 25. McLaughlin LS, Haft RJF, Forest KT. 2012. Structural insights into the Type II secretion nanomachine. Curr Opin Struct Biol 22:208–216.
- 26. Gibson DG, Young L, Chuang RY, Venter JC, Hutchison CA, Smith HO. 2009. Enzymatic assembly of DNA molecules up to several hundred kilobases. Nat Methods 6:343–345.
- 27. Gabriel DW, Allen C, Schell M, Denny TP, Greenberg JT, Duan YP, Flores-Cruz Z, Huang Q, Clifford JM, Presting G, González ET, Reddy J, Elphinstone J, Swanson J, Yao J, Mulholland V, Liu L, Farmerie W, Patnaikuni M, Balogh B, Norman D, Alvarez A, Castillo JA, Jones J, Saddler G, Walunas T, Zhukov A, Mikhailova N. 2006. Identification of open reading frames unique to a select agent: *Ralstonia solanacearum* race 3 biovar 2. Mol Plant Microbe Interact 19:69–79.
- 28. Liu H, Kang Y, Genin S, Schell MA, Denny TP. 2001. Twitching motility of *Ralstonia* solanacearum requires a type IV pilus system. Microbiology 147:3215–3229.
- 29. Liu H, Zhang S, Schell M a, Denny TP. 2005. Pyramiding unmarked deletions in *Ralstonia solanacearum* shows that secreted proteins in addition to plant cell-wall-degrading enzymes contribute to virulence. Mol Plant Microbe Interact 18:1296–1305.
- 30. Filloux A. 2004. The underlying mechanisms of type II protein secretion. Biochim Biophys Acta Mol Cell Res 1694:163–179.
- 31. Monteiro F, Solé M, van Dijk I, Valls M. 2012. A chromosomal insertion toolbox for

- promoter probing, mutant complementation, and pathogenicity studies in *Ralstonia* solanacearum. Mol Plant Microbe Interact 25:557–68.
- 32. Camberg JL, Sandkvist M. 2005. Molecular analysis of the *Vibrio cholerae* type II secretion ATPase EpsE. J Bacteriol 187:249–256.
- 33. Camberg JL, Johnson TL, Patrick M, Abendroth J, Hol WGJ, Sandkvist M. 2007. Synergistic stimulation of EpsE ATP hydrolysis by EpsL and acidic phospholipids. EMBO J 26:19–27.
- 34. Jacobs JM, Babujee L, Meng F, Milling AS, Allen C. 2012. The *in planta* transcriptome of *Ralstonia solanacearum*: conserved physiological and virulence strategies during bacterial wilt of tomato. MBio 3:e00114-12.
- 35. Durand É, Michel G, Voulhoux R, Kürner J, Bernadac A, Filloux A. 2005. XcpX controls biogenesis of the *Pseudomonas aeruginosa* XcpT-containing pseudopilus. J Biol Chem 280:31378–31389.
- 36. Vignon G, Köhler R, Larquet E, Giroux S, Prévost MC, Roux P, Pugsley AP. 2003. Type IV-like pili formed by the type II secreton: Specificity, composition, bundling, polar localization, and surface presentation of peptides. J Bacteriol 185:3416–3428.
- 37. Gabriel DW, Allen C, Schell M, Denny TP, Greenberg JT, Duan YP, Flores-Cruz Z, Huang Q, Clifford JM, Presting G, González ET, Reddy J, Elphinstone J, Swanson J, Yao J, Mulholland V, Liu L, Farmerie W, Patnaikuni M, Balogh B, Norman D, Alvarez A, Castillo JA, Jones J, Saddler G, Walunas T, Zhukov A, Mikhailova N. 2006. Identification of Open Reading Frames Unique to a Select Agent: *Ralstonia solanacearum* Race 3 Biovar 2. Mol Plant-Microbe Interact 19:69–79.
- 38. Yan Z, Yin M, Xu D, Zhu Y, Li X. 2017. Structural insights into the secretin translocation channel in the type II secretion system. Nat Struct Mol Biol 24:177–183.
- 39. Douzi B, Ball G, Cambillau C, Tegoni M, Voulhoux R. 2011. Deciphering the Xcp *Pseudomonas aeruginosa* Type II Secretion machinery through multiple interactions with substrates. J Biol Chem 286:40792–40801.
- 40. Korotkov K V., Johnson TL, Jobling MG, Pruneda J, Pardon E, Héroux A, Turley S, Steyaert J, Holmes RK, Sandkvist M, Hol WGJ. 2011. Structural and functional studies on the interaction of GspC and GspD in the Type II Secretion System. PLoS Pathog 7.
- 41. Campos M, Cisneros DA, Nivaskumar M, Francetic O. 2013. The type II secretion system a dynamic fiber assembly nanomachine. Res Microbiol 164:545–555.
- 42. Sauvonnet N, Vignon G, Pugsley AP, Gounon P. 2000. Pilus formation and protein secretion by the same machinery in *Escherichia coli*. EMBO J 19:2221–2228.
- 43. Arts J, de Groot A, Ball G, Durand E, El Khattabi M, Filloux AF, Tommassen J, Koster MC.

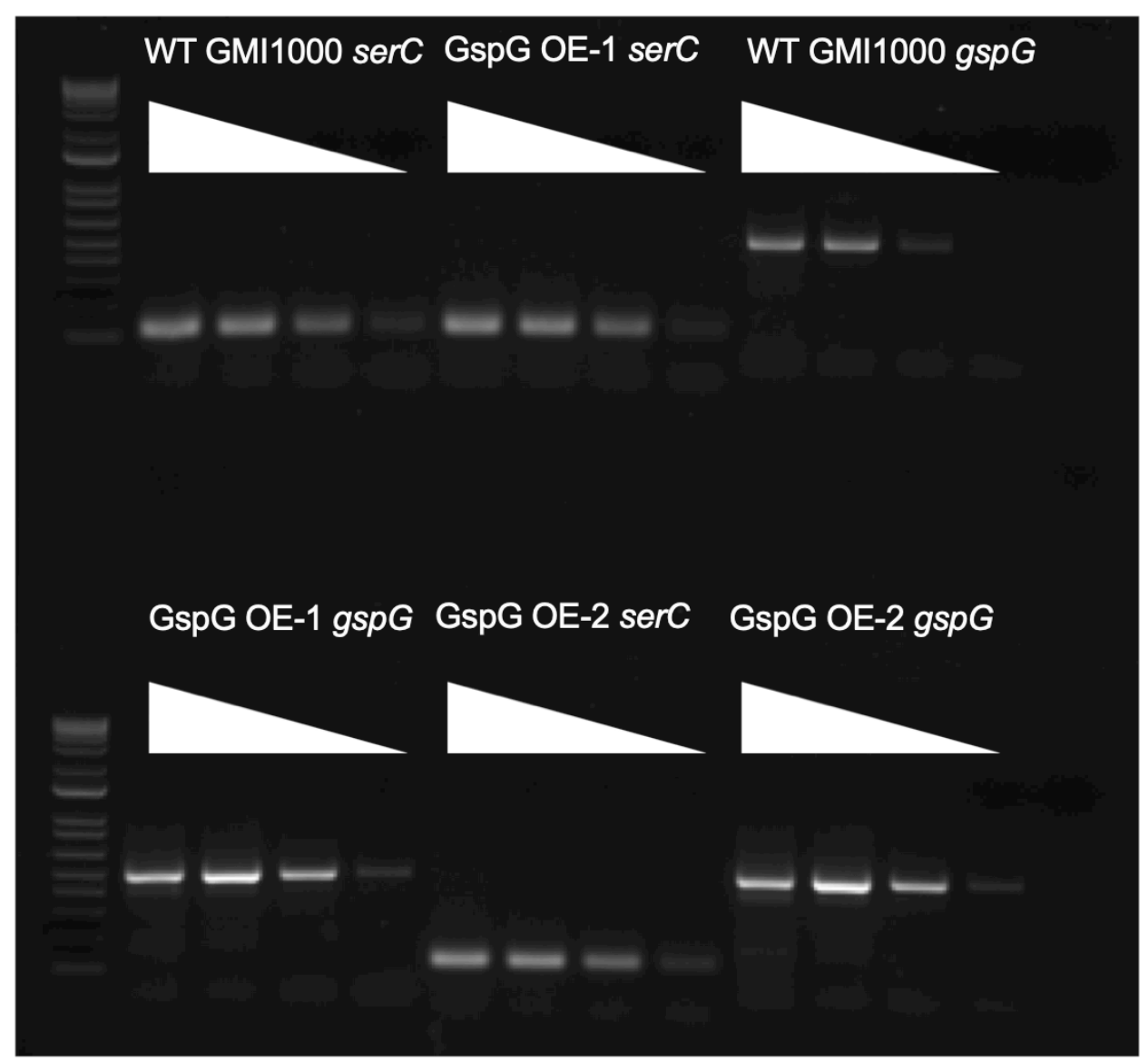
- 2007. Interaction domains in the *Pseudomonas aeruginosa* type II secretory apparatus component XcpS (GspF). Microbiology 153:1582–1592.
- 44. Abendroth J, Mitchell DD, Korotkov K V., Johnson TL, Kreger A, Hol WGJ. 2009. The three-dimensional structure of the cytoplasmic domains of EpsF from the type 2 secretion system of *Vibrio cholerae*. J Struct Biol 166:303–315.
- 45. Lybarger SR, Johnson TL, Gray MD, Sikora AE, Sandkvist M. 2009. Docking and assembly of the type II secretion complex of *Vibrio cholerae*. J Bacteriol 191:3149–3161.
- 46. Van Der Meeren R, Wen Y, Van Gelder P, Tommassen J, Devreese B, Savvides SN. 2013. New insights into the assembly of bacterial secretins: Structural studies of the periplasmic domain of XcpQ from *Pseudomonas aeruginosa*. J Biol Chem 288:1214–1225.
- 47. Hay ID, Belousoff MJ, Lithgow T. 2017. Structural basis of type 2 secretion system engagement between the inner and outer bacterial membranes. MBio 8:1–6.
- 48. González ET, Brown DG, Swanson JK, Allen C. 2007. Using the *Ralstonia solanacearum* tat secretome to identify bacterial wilt virulence factors. Appl Environ Microbiol 73:3779–3786.
- 49. Reitzer L. 2003. Nitrogen Assimilation and Global Regulation in *Escherichia coli*. Annu Rev Microbiol 57:155–176.
- 50. Coutte L, Antoine R, Drobecq H, Locht C, Jacob-Dubuisson F. 2001. Subtilisin-like autotransporter serves as maturation protease in a bacterial secretion pathway. EMBO J 20:5040–5048.
- 51. Hernandez CA, Koskella B. 2019. Phage resistance evolution in vitro is not reflective of in vivo outcome in a plant-bacteria-phage system. Evolution (N Y) 73:2461–2475.
- 52. Horita M. TK. 2002. Causal agent of bacterial wilt disease *Ralstonia solanacearum*. Natl Inst Agric Sci 12.
- 53. Garneau JE, Dupuis MÈ, Villion M, Romero DA, Barrangou R, Boyaval P, Fremaux C, Horvath P, Magadán AH, Moineau S. 2010. The CRISPR/cas bacterial immune system cleaves bacteriophage and plasmid DNA. Nature 468:67–71.
- 54. Boisvert S, Laviolette F, Corbeil J. 2010. Ray: Simultaneous assembly of reads from a mix of high-throughput sequencing technologies. J Comput Biol 17:1401–1415.
- 55. Li H, Durbin R. 2009. Fast and accurate short read alignment with Burrows-Wheeler transform. Bioinformatics 25:1754–1760.
- 56. 2018. Picard Toolkit. 1.123. Broad Institute, GitHub Repos. Broad Institute.

- 57. Li H, Handsaker B, Wysoker A, Fennell T, Ruan J, Homer N, Marth G, Abecasis G, Durbin R. 2009. The Sequence Alignment/Map format and SAMtools. Bioinformatics 25:2078–2079.
- 58. McKenna A, Hanna M, Banks E, Sivachenko A, Cibulskis K, Kernytsky A, Garimella K, Altshuler D, Gabriel S, Daly M, DePristo MA. 2010. The Genome Analysis Toolkit: A MapReduce framework for analyzing next-generation DNA sequencing data. Genome Res 20:1297–1303.
- 59. Naville M, Ghuillot-Gaudeffroy A, Marchais A, Gautheret D. 2011. ARNold: A web tool for the prediction of rho-independent transcription terminators. RNA Biol.
- 60. Castañeda A, Reddy J, El-Yacoubi B, Gabriel D. 2005. Mutagenesis of all eight *avr* genes in *Xanthomonas campestris* pv. *campestris* had no detected effect on pathogenicity, but one *avr* gene affected race specificity. Mol Plant-Microbe Interact 18:1306–1317.
- 61. Dalsing BL, Truchon AN, Gonzalez-Orta ET, Milling AS, Allen C. 2015. *Ralstonia solanacearum* uses inorganic nitrogen metabolism for virulence, ATP production, and detoxification in the oxygen-limited host xylem environment. MBio 6:1–13.
- 62. Tans-kersten J, Huang H, Allen C. 2001. *Ralstonia solanacearum* needs motility for invasive virulence on tomato. J Bacteriol 183:3597–3605.
- 63. Bolger AM, Lohse M, Usadel B. 2014. Trimmomatic: A flexible trimmer for Illumina sequence data. Bioinformatics 30:2114–2120.
- 64. Prior P, Steva H. 1990. Characteristics of Strains of *Pseudomonas solanacearum* from the French West Indies. Plant Dis.
- 65. Boucher CA, Barberis PA, Trigalet AP, Demery DA. 1985. Transposon mutagenesis of *Pseudomonas solanacearum*: Isolation of Tn5-induced avirulent mutants. J Gen Microbiol 131:2449–2457.
- 66. Milling AS, Babujee L, Allen C. 2011. *Ralstonia solanacearum* extracellular polysaccharide is a specific elicitor of defense responses in wilt-resistant tomato plants. PLoS One 6.

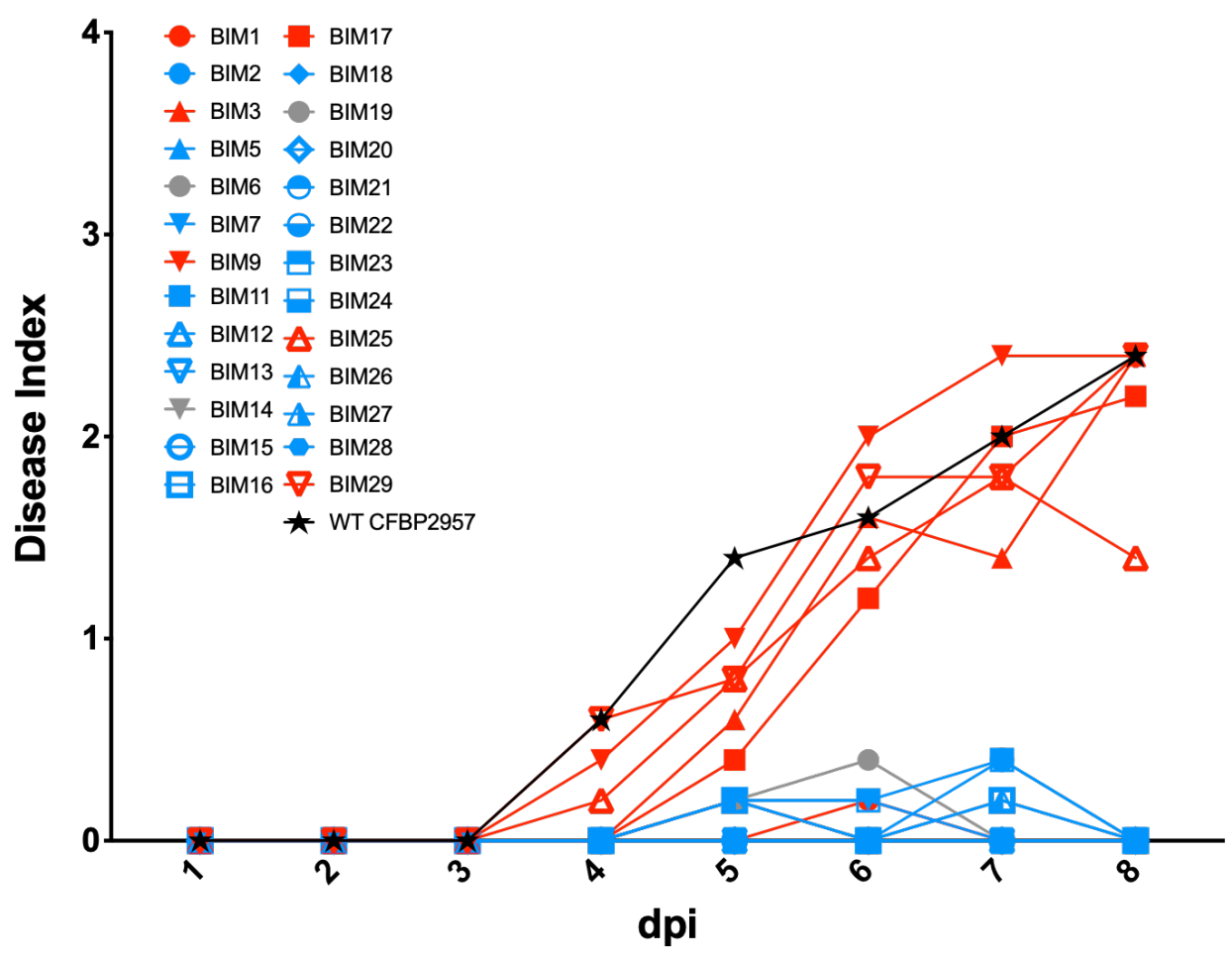


Supplementary Figure 1. Targeted mutations in the T2SS reduce the export of pectin methylesterase. Ten-fold serial dilutions of each strain were spotted on minimal media plates containing pectin. After 24 hours of growth, the colonies were rinsed off and the plates were washed with HCl. BIM1 and a GspG overexpression strain produced a zone of clearing at tenfold higher dilution than WT. A point mutation in GspE led to a loss of pectin methylesterase

excretion.



Supplementary Figure 2. Introducing *gspG* under the control of the *rplM* promoter increases *gspG* expression roughly ten-fold. Semi-quantitative RT-PCR was used to measure expression of two independent clones of GspG OE. The stably-expressed *serC* transcript is used as an endogenous control.



Supplementary Figure 3. Only T2SS-positive BIMs retain virulence. 21 day-old Bonny Best tomato plants were inoculated through a cut leaf petiole with 200 CFU of each BIM. Five plants were included per treatment. BIMs that have both functional T2SS and twitching motility are shown in red, those that are deficient in both T2SS and twitching motility are shown in grey, and BIMs that are deficient in T2SS but have WT levels of twitching motility are shown in blue.

Plasmid	Description	Citation
pUFJ10	GM ^R , Kan ^R , stable cosmid in <i>R. solanacearum</i>	(27)
pGspLG1	pUFJ10 carrying CFBP2957 <i>gspL</i> under the control of the <i>Kan^R</i> promoter	This study
pGspLRG1	pUFJ10 carrying CFBP2957 <i>gspL</i> under the control of the native <i>gsp</i> promoter	This study
pPilDG1	pUFJ10 carrying CFBP2957 <i>pilD</i> under the control of the <i>Kan^R</i> promoter	This study
pPilDRG1	pUFJ10 carrying CFBP2957 <i>pilD</i> under the control of the native <i>pil</i> promoter	This study
pUFR80	Suc ^s , Kan ^R , positive selection suicide vector	(60)
pUFR80-gspE	pUFR80 carrying WT <i>gspE</i>	This study
pUFR80-gspE mutant	pUFR80 carrying gspE with k274 replaced with alanine	This study
pRCK-GWY	Kan ^R , contains recombination regions matching a neutral region in the GMI1000 chromosome	(31)
pRCK-gspG overexpression	pRCK-GWY carrying CFBP2957 <i>gspG</i> under the control of the <i>rplM</i> promoter	This study
Strain	Description	Reference
CFBP2957	WT, Phylotype IIA, isolated from tomato in Martanique	(64)
GMI1000	WT, Phylotype I, isolated from tomato in French Guyana	(65)
BIM4	Spontaneous CFBP2957 mutant resistant to PhiAP1, frameshift in <i>gspL</i>	(24)

BIM30	Spontaneous CFBP2957 mutant resistant to PhiAP1, frameshift in <i>pilD</i>	(24)
BIM4 comp	BIM4 complemented with pGspLG1, Kan ^R	This study
BIM4+pUFJ10	BIM4 carrying pUFJ10, Kan ^R	This study
BIM30 comp	BIM30 complemented with pPilDG1, Kan ^R	This study
BIM30+pUFJ10	BIM30 carrying pUFJ10, Kan ^R	This study
CFBP2957 gspE mutant	CFBP2957 with <i>gpsE</i> replaced in its native locus with <i>gspE K274A</i>	This study
ΔpilA	GMI1000 lacking <i>pilA</i> , Tet ^R	This study
GMI1000 gspG overexpression	GMI1000 expressing CFBP2957 <i>gspG</i> under the control of the <i>rplM</i> promoter, Kan ^R	This study
E. coli DH5alpha	F— Φ 80/acZΔM15 Δ (/acZYA-argF) U169 recA1 endA1 hsdR17 (rK—, mK+) phoA supE44 λ — thi-1 gyrA96 relA1	Invitrogen

Supplementary Table 1. Strains and plasmids

Primer	Sequence	Reference
pilD_F	5'- gttttcatggcttgttatgactgtttttttCGATCATCATCGTGATCCTGGGCGTG	This study
pilD_R	5'-cttgctgcttggatgcccgaggcatagactGCCGTTCCTTACCGCGCCAGC	This study
gspL_F	5'-gttttcatggcttgttatgactgtttttttGCCTTCGCCGTATTGTCATC	This study
gspL_R	5'cttgctgcttggatgcccgaggcatagactCGATCGTTATTGCGCGATGG	This study
gspEregion_F	5'-tgcatgcctgcaggtcgactCCTGGGCGATATTCCCATC	This study
gspEregion_F	5'-cagctatgaccatgattacgCGCATTGATGAAGAGCACGG	This study
gspEmutation_F	5'-GACCGGGTCGGGCGCGACCACCGCTG	This study
gspEmutation_R	5'-CAGCGTGGTCGCCCCGACCCGGTC	This study
rplM_F	5'-tgcgcgagcaggggaattgcATTCTTTTCCTTGTGTCAAG	This study
rpIM_R	5'-cttgcatcatGATTTTCCAAATTTGAGTCAG	This study
gspG_F	5'-tggaaaaatcATGATGCAAGGCCAACTTC	This study
gspG_R	5'-cgaccctagtctaagatcttTCAATTGTCCCAGTTGCC	This study

serC_F	5'-CGCGCAAATACGGTGAAGTG	(66)
serC_R	5'-GTGCACAGATGCACGTAAGC	(66)

Supplementary Figure 2. Primers

Function/Protein ID	Locus	CFBP2957 genome position
Histone, WP_042548866.1		???
GspL protein, T2SS - WP_013204870.1	RCFBP_RS01505	349506*
Prepilin peptidase (PilD), Tfp - WP_043892401.1	RCFBP_RS03025	662145*
General secretion pathway protein F, T2SS - WP_043908127.1	RCFBP_RS01475	340184*
Putative extracellular subtilisin-like protease precursor, WP_013205222.1	RCFBP_RS03800	834259*
Conserved membrane protein of unknown function - WP_013205221.1	RCFBP_RS03795	833270
General Secretory Pathway protein D, T2SS - WP_013204867.1	RCFBP_RS01490	346357*
N-acetylmuramoyl-L-alanine amidase (amiC) - WP_013205274.1	RCFBP_RS04110	894374
Glutamate/aspartate transport protein (gltJ) - WP_013206970.1	RCFBP_RS13830	2943934*
Prepilin peptidase (PilD), Tfp - WP_043892401.1	RCFBP_RS03025	661880*
Prepilin peptidase (PilD), Tfp - WP_043892401.1	RCFBP_RS03025	661709*
Prepilin peptidase (PilD), Tfp - WP_043892401.1	RCFBP_RS03025	661880*

Mutant	Change	Position in protein	Mutation (nt)
BIM4	Frameshift		T > ?
BIM4	Frameshift	Codon 55/481	GGCA > G
BIM30	Frameshift	Codon 42/289	AACGC > C
BIM1	Insertion	Codon 231/403	ACCAGCACGATCGCCGCCAGC > ACCAGCACGATCGCCGCCAGC
BIM3	Frameshift	Codon 387/681	2225 < 22225
BIM17	Premature stop codon	Codon 192/206	G > A
BIM25	A > D substitution	Codon 130/809	G>T
BIM25	Frameshift	Codon 10/510	GCCGACCGACCG > GCCGACCGACCG
BIM29	Premature stop codon	Codon 39/242	G > A
BIM6	Premature stop codon	Codon 130/290	G > A
BIM14	Frameshift	Codon 105/290	ACCCGGCC > ACCCGGC
BIM19	Premature stop codon	Codon 130/290	G > A

Supplementary Table 3. Unique BIM mutations. * indicates gene in the antiparallel strand

Function/Protein ID	Locus	CFBP2957 genome position
	Intergenic	2,167649
putative carbohydrate-selective porin OprB, WP_013207399.1	RCFBP_mp10029	28999
chloride channel protein clcB-like, WP_013207393.1	RCFBP_mp10023	22731
Putative transcription regulator protein, MarR family, WP_003262413.1	RCFBP_RS04715	1030473*
Putative transcription regulator protein, MarR family, WP_003262413.1	RCFBP_RS04715	1030467*
DUF2345 domain-containing protein	RCFBP_mp20178	881950*
	Intergenic	608928
Hypothetical protein, WP_013208141.1	RCFBP_mp20203	915,919
Conserved exported protein of unknown function, Formate dehydrogenase region TAT target,	RCFBP_RS04970	1083771
	Intergenic	952467
putative transcriptional regulator, WP_013208267.1	RCFBP_mp20336	1074056
DNA translocase FtsK, WP_013208262.1	RCFBP_mp20331	1065969
	Intergenic	69410
Transposase of insertion sequence ISRta2, IS256 family, WP_013205860.1	RCFBP_RS07505	1635319
Putative Fe-S electron transport protein, WP_042590583.1	RCFBP_RS04100	893137*

Mutant	Change	Position in the protein	Mutation (nt)
BIM1, 3, 5, 9, 17, 25, 29			C > A**
BIM1, 3, 5, 9, 17, 25, 29	P > H	Codon 224/476	A > C**
BIM1, 3, 5, 9, 17, 25, 29	P > T	Codon 189/461	C > A**
BIM1, 3, 9, 17, 25, 29	P > R	Codon 8/139	* * 0 < 9
BIM9, 25, 29	P > L	Codon 10/139	G > A**
BIM1, 3, 9, 25, 29	E > G	Codon 194/370	T > C**
BIM1, 3, 5, 9, 17, 25, 29			G > T**
BIM1, 3, 5, 9, 17, 25, 29	R > S	Codon 356/367	**) < 9
BIM3, 17, 25, 29	A > S	Codon 48/80	**L<5
BIM1, 3, 9, 17, 25, 29			G > T**
BIM1, 3, 5, 9, 17, 25, 29	T > P	Codon 7/201	A > C**
BIM3, 5, 9, 17, 25	V > A		T > C
BIM1, 3, 5, 9, 17, 25, 29		Codon 530/1126	G > A**
BIM1, 3, 5, 17, 25	D > G	Codon 163/417	A > G
BIM3, 5, 9, 17, 25, 29	A > D	Codon 207/379	G > T**

Supplementary Table 4. Shared BIM mutations. * indicates gene in the antiparallel strand. **

indicates that the mutation matches the published CFBP2957 genome

Chapter 4

Conclusions and future directions

Contributions: Beth Dalsing analyzed the *Rs* proteome for S-nitrosylated proteins. Lucas

Frungillo attempted to purify HrpB *in vitro* and provided technical advice about the biotin

switch technique. Yigeng Tan designed the cloning plan to inactivate the *czcABC* and RSp0528
30 operons in *Rs*. Derrick Grunwald created yeast strains producing RipAX1 and RipAX2,

analyzed the response of those strains to stress, and contributed to writing, experimental

planning, and analysis of the proposed RipAX study. Raka Mitra, Sasha Kyrysyuk, and Nina

Denne transformed RipAX expression vectors into *Agrobacterium* and performed the initial GFP

localization experiments for RipAX in tobacco leaves. Connor Hendrich did the remaining

experimental work, produced the figures, and wrote the text.

In this thesis, I examined two *Ralstonia solanacearum* secretion systems that are required for *Rs* virulence. In Chapter 2, I showed that the Type III Secretion System (T3SS) is activated by a byproduct of denitrifying metabolism, nitric oxide (NO). Because NO is produced by both the host and by *Rs* denitrification during tomato infection, we think that the bacterium uses NO as a signal of the in-host environment (1, 2). In Chapter 3, I examined the role of the Type II Secretion System (T2SS) during *Rs* infection by the lytic phage phiAP1. The T2SS is required for *Rs* virulence, and it is exploited by phiAP1 as an entry point into the bacterial cell (3). Taken together, these studies demonstrate the integral roles that secretion systems play in *Rs* virulence, even to the point that expression of the T3SS is tied to a foundational metabolic pathway. However, these secretion systems can also be significant weaknesses, as demonstrated by the exploitation of the T2SS by phiAP1. The data produced in these two studies suggest a variety of further questions. In this chapter, I will describe several future experiments to answer those questions. In addition, I will summarize findings on several related questions that I have explored during my doctoral studies.

Future directions

What is the mechanism of NO-mediated T3SS induction?

While Chapter 2 demonstrated that NO activates the expression of T3SS-related genes, I was not able to conclusively discover the mechanism of this regulation. Future research could build on my attempts to determine the biochemical details of NO-dependent T3SS gene induction. One likely mechanism is the NO-dependent post-translational modification of a T3SS

gene or regulator. Although these types of modification have not been well studied in bacteria, they are often used in plants and other eukaryotes (4, 5). Three major categories of modification include the nitrosylation of reduced cysteine, the nitration of tyrosine, and the binding of transition metals like iron (6–12). These modifications occur as a natural result of reactive nitrogen species (RNS), and are known to play an important role in many plant developmental and defense signaling pathways (13).

S-nitrosylation occurs in bacteria, although it is not always known if the modifications are adaptive. Under certain conditions, NO will bind to any available reduced thiol (14). Proteomics has been used to describe the full repertoire of S-nitrosylated proteins in some bacterial species. For example, Xue et al. isolated S-nitrosylated proteins from Mycobacterium tuberculosis following treatment with an exogenous source of NO. They identified a total of 29 S-nitrosylated proteins involved in a variety of metabolic and stress response pathways (15). However, because this study focused on finding antimicrobial effects of RNS, it did not determine if S-nitrosylation provides an adaptive function. Seth et al. described the first known example of functional S-nitrosylation in bacteria when they showed that the activity of E. coli oxidative stress response regulator OxyR is changed by S-nitrosylation. This modification shifted the regulatory targets of OxyR to trigger a distinct reactive nitrogen species response (16). Given the diversity and adaptability of bacteria, it is likely that other bacterial species use these types of modification. Even among plant-associated bacteria, there are examples of NO signaling and S-nitrosylation. S-nitrosylated proteins can be detected in the developing root nodules of nitrogen-fixing Rhizobium species, and NO may play a regulatory role in nodule development (17). Given the degree of nitrosative stress experienced by Rs in tomato xylem, it

is plausible that S-nitrosylation or other NO-responsive modifications regulate key virulence pathways like the T3SS.

A program that predicts S-nitrosylated residues based on primary sequence similarity to known S-nitrosylated proteins suggested many potentially modified cysteines in the Rs proteome (18). Among the predicted targets were the T3SS-regulators hrpB and hrpG (19). HrpB contained three predicted S-nitrosylation sites, one of which, cys112, was extremely wellconserved across Rs phylotypes and also in the HrpB-type T3SS transcriptional regulators of other plant pathogens (Figure 1). To test the hypothesis that S-nitrosylation at this conserved site affects HrpB function, I created a mutant version of the protein by replacing the cysteine at position 112 with a serine. This modification is commonly used to disrupt S-nitrosylation without radically altering protein structure (20). I used this C₁₁₂S mutant to indirectly test T3SS activity using two assays. First, I tested the ability of the mutant to cause disease on tomato. T3SS activity is required for virulence, so a decrease in T3SS gene expression leads to a reduction in virulence. The cysteine swap mutant had reduced virulence in a biologically realistic soil-soak assay, although the mutant did still cause some disease (Figure 2a). I also infiltrated the HrpB C₁₁₂S mutant into tobacco leaves. Tobacco is an incompatible host for Rs GMI1000 because it has a resistance (R) protein that recognizes the GMI1000 T3SS effector RipAA (formerly AvrA) (21). If Rs GMI1000 cells have a functional T3SS that injects RipAA into tobacco cells, recognition of RipAA by this R gene product triggers a programmed cell death known as the hypersensitive response (HR) that quickly kills the bacterium. When the cysteine swap mutant was introduced into tobacco, it caused a delayed HR, as measured by the increased survival of the mutant compared to WT in the tobacco leaf over time (Figure 2b).

Together, the tomato virulence and tobacco HR results suggested that the *Rs* HrpB C₁₁₂S mutant, which cannot be S-nitrosylated at position 112, had reduced but not abolished T3SS activity. This result is consistent with, but does not prove, a role for S-nitrosylation in HrpB function.

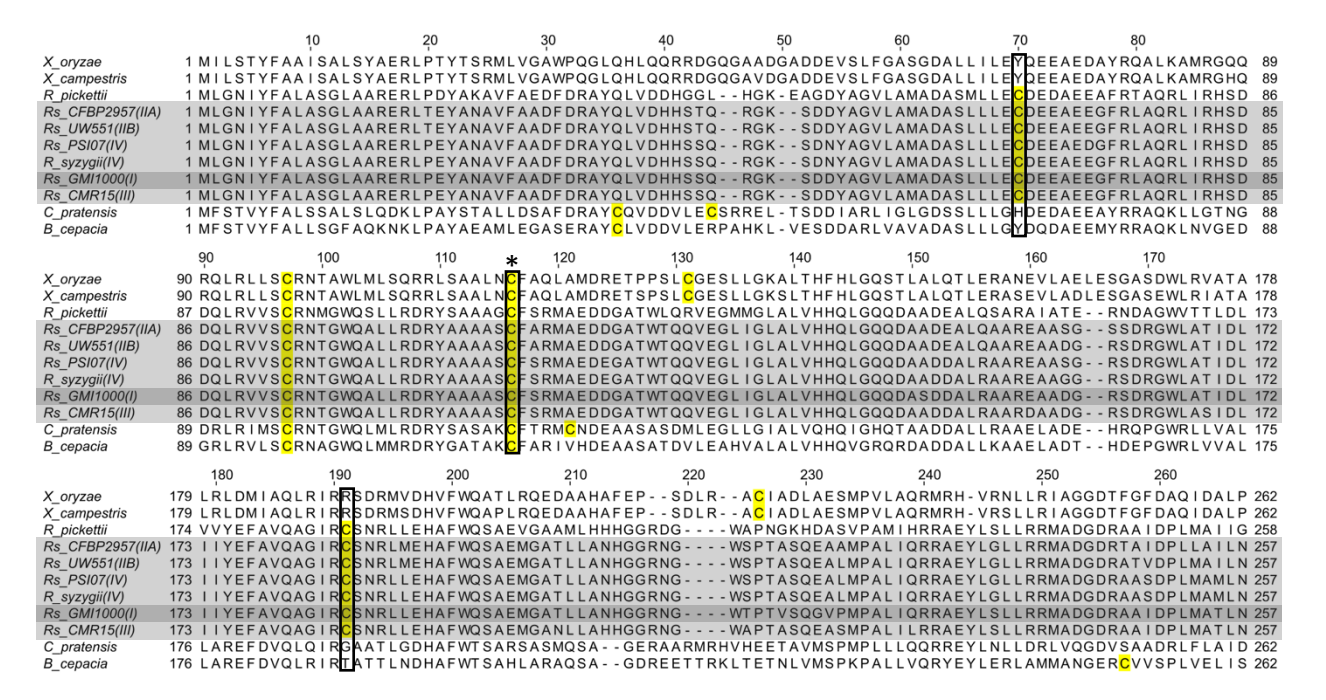


Figure 1. The predicted S-nitrosylation site Cys112 of *Rs* GMI1000 *hrpB* is well conserved among many HrpB homologues. Alignment of *hrpB* and its homologues in *Xanthomonas*, *Collomonas*, and *Burkholderia*. *Rs* phylotypes are denoted in parentheses next to their name. Predicted nitrosylated residues are boxed (18). Cys112 is marked with *. Only the N-terminal half of HrpB is shown. Alignment created with Clustal Omega, and shading created using JalView (22, 23).

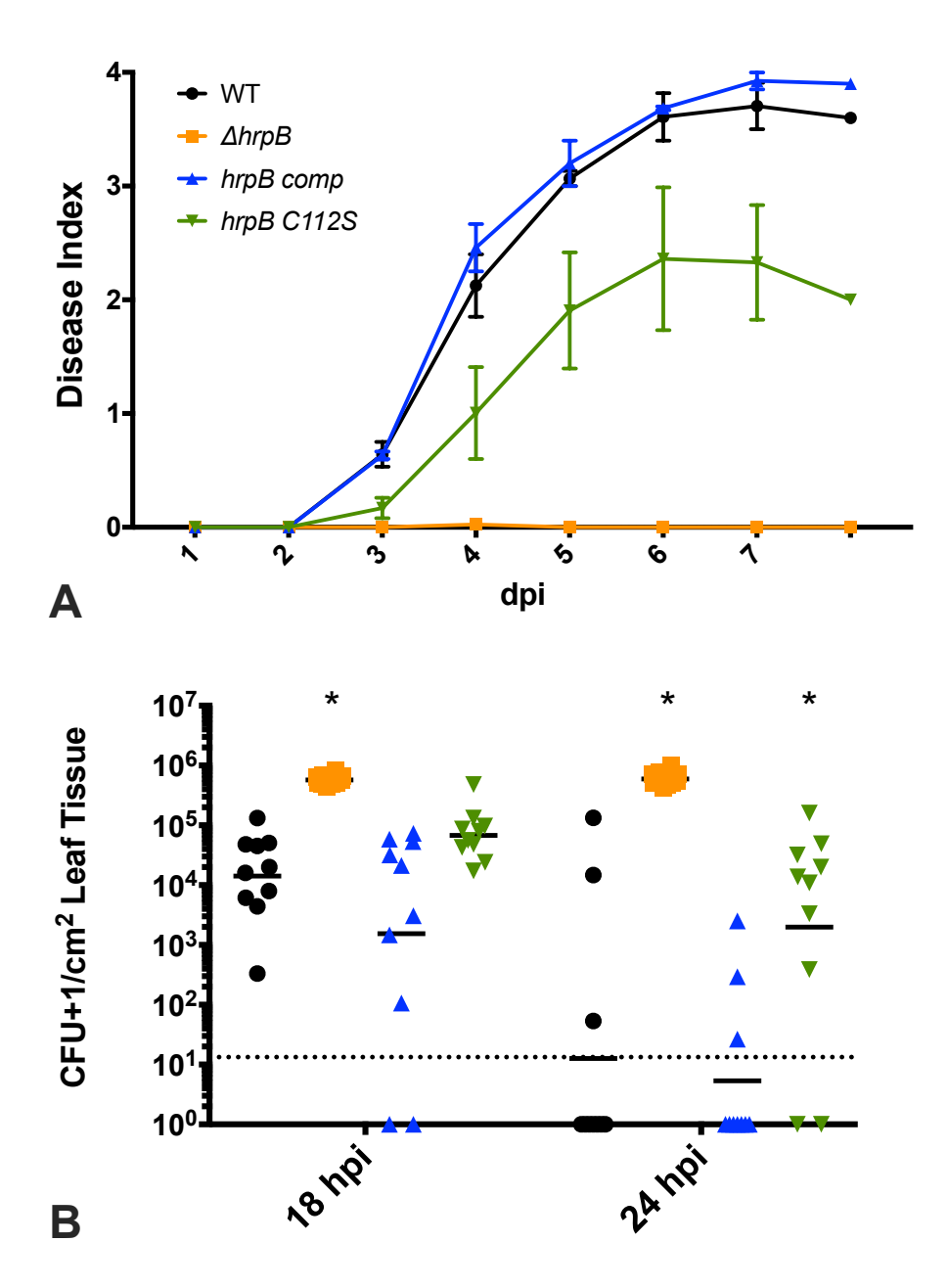


Figure 2. Mutating Cys112, a predicted S-nitrosylation (SNO) site, in hrpB alters Rs behaviors in planta. (A) The C_{112} S mutant had reduced virulence on tomato. 2000 CFU of Rs were introduced through a cut petiole into 21-day old wilt-susceptible Bonny Best tomato plants. Disease was then rated on a 0-4 scale over the course of the next week. Each data point represents the average of three independent replicate experiments per strain, with 10-20

plants in each biorep. Error bars represent the standard error of the mean. The C₁₁₂S mutant had significantly reduced virulence (Friedman test with multiple comparisons, P<0.05). **(B)** The C₁₁₂S mutant survives for longer in leaves of the incompatible host *Nicotiana tabacum*, which responds to *Rs* strain GMI1000 in a T3SS-dependent manner. Tobacco leaves (cv. Bottom Special) were infused with a 10⁸ CFU/mL suspension of bacteria using a blunt syringe. At 18 and 24 hpi, a roughly 1.8 cm² circle of tissue was collected, ground, and dilution plated to measure the surviving bacterial population. Each symbol indicates the bacterial population size in one leaf sample, N= 10 samples per treatment. Bars indicate the geometric mean and the dotted line indicates the limit of detection. * indicates that a population is significantly different from that of WT GMI1000 at the same time point, P<0.05 (One-way ANOVA with multiple comparisons).

These assays could not determine if the reduction of T3SS activity occurred because the modified HrpB could not be S-nitrosylated at position 112 or because the mutation changed HrpB structure in ways that otherwise interfered with its function. Two alternate methods could be used to confirm S-nitrosylation. The first would biochemically determine if HrpB can be modified *in vitro* or *in planta* using the biotin switch technique. This process involves specifically biotinylating nitrosylated cysteine residues (24). This allows multiple downstream applications, such as the purification of S-nitrosylated proteins using streptavidin (25). I created his-tagged versions of both WT and cysteine swap *hrpB*. I introduced these tagged versions of the protein into *Rs* and into an *E. coli* expression vector. Using this vector, we could purify WT HrpB, subject it to an exogenous source of NO, and use the biotin switch method to test if it can

be S-nitrosylated in vitro. If it can, we would also determine if the cysteine swap mutant can be modified. However, an experienced collaborator found in repeated attempts that HrpB is challenging to purify in sufficient quantities for use in the biotin switch assay. Its stability and solubility could be increased by using a different tag, such as GFP. Alternatively, we could infect tomato with the Rs strain encoding his-tagged HrpB. Then, bulk protein from the tomato stem could be subjected to the biotin switch technique, biotinylated proteins could be purified, and the resulting mixture could either be used for proteomics to identify all of the S-nitrosylated proteins, or used for a western blot using an anti-his tag probe to determine if HrpB was Snitrosylated. As before, the cysteine swap mutant would be included to determine if the loss of cys112 prevents the S-nitrosylation of HrpB. If it is shown that HrpB can be nitrosylated at cys112 and that this modification is required for NO regulation, this result could also provide insight into the structure and function of hrpB-type regulators. HrpB is an AraC-type regulator, a family of proteins which share a conserved, DNA-binding C-terminal domain (26). However, the central and N-terminal regions of these proteins are not well conserved and are typically thought to play roles in regulating the activity of the protein. Cys112 is in the HrpB N-terminal domain of unknown function, and understanding its role would add to our knowledge of the function of this region of the protein.

An alternate approach would combine a *hrpB::lux* reporter strain with a cysteine swap mutant. In Chapter 2, I used a *hrpB::lux* reporter to show that the presence of tomato seedlings induced *hrpB* expression in an NO-dependent manner. A similar approach could determine if the loss of T3SS activity seen in the cysteine swap mutant depends on NO. To do this, we could create a strain encoding both the Lux operon under the control of the *hrpB* promoter and the

cysteine swap mutant of HrpB. The strain would be incubated alongside tomato seedlings with and without the NO-scavenger cPTIO (27). Previously, I found the presence of tomato seedlings activated expression of *hrpB::lux* expression in wild type *Rs* cells, but this induction was significantly reduced when NO was removed by cPTIO. If NO contributes to the induction of *hrpB* gene expression via the nitrosylation of HrpB cys112, the cysteine swap mutant will not be affected by cPTIO.

Should cys112 of HrpB not be clearly nitrosylated, we could use untargeted techniques to find potential regulators. For example, we could use SNOSID, which combines the biotin switch technique with mass spectrometry to identify all S-nitrosylated proteins in a sample (25). S-nitrosylated proteins could be isolated from Rs grown in conditions with known NOdependent T3SS gene induction, such as treatment with CysNO or using a $\Delta norB$ mutant. The results of such a screen could be compared with the predictions made by GPS-SNO and a list of known T3SS-regulators to find prospective proteins and residues for further study. A similar approach could identify potential nitrated tyrosine using commercial anti-3-nitrotyrosine antibodies to isolate nitrated targets (28). An even more unbiased approach would be a genetic screen for mutants unable to induce T3SS gene expression in response to NO. This could be accomplished with the use of a positive selection marker like SacB, which produces a toxic product in the presence of sucrose (29). This gene could be placed under the control of a promoter that is extremely responsive to NO, for example the promoter for ripG8, the most highly upregulated T3SS-related gene in our RNA-seq dataset. This construct could be mutagenized using the mariner transposon (30). The mutant library could be grown in liquid rich media, which suppresses Rs T3SS gene expression, and then treated with the exogenous

NO donor CysNO and sucrose. Any cells whose T3SS was induced by NO would be killed by SacB, and the surviving cells would be isolated and their transposon insertion sites determined by sequencing. This approach should identify known T3SS regulators, and it may reveal other putative NO-dependent regulators of T3SS gene expression.

How do T2SS positive BIMs evade phiAP1?

Chapter 3 describes how the bacteriophage phiAP1 infects *Rs* using the activity of the T2SS. While the majority of the spontaneous *Rs* bacteriophage insensitive mutants (BIMs) were deficient in T2SS, we found that six BIMs were still capable of secreting pCWDEs via the T2SS. The mechanism of resistance of these BIMs was outside of the scope of the paper but does provide a good opportunity to study other stages of the phiAP1 life cycle.

Two T2SS positive BIMs had mutations in genes encoding T2SS proteins. One of these, BIM1, had reduced T2SS activity, but the other, BIM25, appeared to have full activity.

Intriguingly, BIM25 contained a single alanine to aspartate mutation in the T2SS outer membrane secretin GspD. If we could understand how this change provides resistance to PhiAP1, we could gain a better understanding of exactly how phiAP1 uses the T2SS activity during infection. Because the mutated region of GspD is periplasmic and may be involved in the selection and loading of T2 secreted cargo, altering this residue could affect the substrate specificity of the T2SS complex (31, 32). If phiAP1 must bind a secreted protein or if a secreted protein modifies an extracellular cell wall component required for phiAP1 binding, altering the profile of T2SS cargo could interfere with phiAP1 infection. One way to test this hypothesis

would be to suspend BIM25 cells in filtered supernatant from a culture of WT *Rs*. If the WT supernatant contains a secreted factor that BIM25 is unable to export but that is required for PhiAP1 infection, it may restore PhiAP1 susceptibility to BIM25. Potential candidate restoration factors could be characterized by using mass spectrometry to identify proteins found in the supernatants of WT *Rs* and BIM25. If a candidate appears in WT supernatant but not in BIM25 supernatant, we could create a mutant deficient in that gene and confirm its resistance to PhiAP1.

Four other T2SS positive BIMs had mutations in unrelated genes or did not have any identifiable mutations, as was the case for BIM9. BIM3 and BIM17 had mutations in two neighboring genes: RCFBP 10792, a membrane protein of unknown function, and RCFBP 10793, a predicted extracellular subtilisin-like precursor protein. BIM29 had a mutation in a predicted glutamate-aspartate transporter. The first step to finding the mechanism of phage resistance for these BIMs would be to determine which step in the phiAP1 life cycle is blocked. BIM4 and BIM30 allow phiAP1 to bind to Rs but prevent it from inserting its DNA (33). We could test the ability of phiAP1 to bind the T2SS positive BIMs by incubating phiAP1 with the mutant, removing the BIM cells with centrifugation, and then measuring the concentration of phage in the resulting supernatant using a plaque assay (33). If the phage is able to bind the bacteria, the phage concentration in the supernatant will be reduced. We can then examine the ability of phiAP1 to inject its DNA into the mutants. To do this, we can treat phiAP1 with a fluorescent DNA-binding dye, challenge BIM cultures with the labeled phiAP1, and then counter-stain the mixture with a fluorescent dye that binds to the outer membrane. If phiAP1 is able to successfully inject its DNA, we will be able to detect the DNA-binding dye inside the

bacterial cell; otherwise, it should be relegated to the exterior (34). If phiAP1 can successfully inject its DNA into the T2SS positive mutants, we can test for formation of phage particles in the mutants. This could be accomplished by raising an antibody to a phage coat protein. Mutant cultures could be infected with phiAP1, and then samples of the culture could be collected over time, their proteins extracted, and the concentration of phage coat protein measured at each time point using a Western blot. If the mutant prevents phiAP1 from replicating its proteins, we will not see an increase in phage protein over time. If we do see an increase, it might indicate that the phages are unable to lyse and exit the mutants.

Do divalent metal cation transports contribute to Rs survival in the xylem?

During the research described in Chapter 2, I profiled transcriptomes of *Rs* grown in anaerobic denitrifying conditions in culture and of *Rs* growing in tomato stems. Comparing this dataset to other published transcriptomes of *Rs* grown *in planta* vs. *Rs* grown in culture revealed that some of the most highly upregulated genes *in planta* are predicted to encode two RND-type heavy metal efflux pumps (HME-RND), *czcABC* and an unnamed operon spanning RSp0528 to RSp0530 (35). This was striking because the other genes that consistently shared a similar pattern of expression were mostly involved in the T3SS or sugar utilization, two traits that have been conclusively shown to be important during infection (36, 37). I hypothesize that these transporters contribute to *Rs* success in the host plant xylem. Further, they are well-conserved across the RSSC, with both transporter gene clusters being found in strains from all four phylotypes.

inner membrane component, an outer membrane component, and a periplasmic linker protein (38). Based on their homology to well characterized transporters in the soil-dwelling bacterium *Cupravidus necator* (formerly *Ralstonia eutrophus*), it is predicted that CzcABC and RSp0528-30 export divalent cations such as zinc, copper, cobalt, or cadmium (39). Equivalent systems in other species have varying substrate specificity, with some being generalists, like those found in *C. necator* and in *Caulobacter crescentus*; and others having a more limited substrate range, like the CzcABC system of *Marinobacter adhaerens*, which can only export zinc (39–41). While these systems have mainly been studied in soil and environmental microbes, the Czc system of the xylem-dwelling plant pathogen *Xylella fastidiosa* has been characterized. Interfering with the regulation of zinc export in *X. fastidiosa* not only reduced this pathogen's zinc tolerance but also reduced the mutant's ability to form biofilm and cause disease (42). This observation, along with the fact that minerals like zinc and copper are transported in plant xylem, suggests that *Rs* may require heavy metal resistance to survive and cause disease in plant xylem (43).

To test this hypothesis, mutants lacking either CzcABC, RSp0528-30, or both could be created in *Rs* GMI1000. These mutants would be subjected to a panel of serially diluted metal stressors to determine the minimum inhibitory concentrations (MIC) of each metal. By examining potential changes in MIC between the mutants and WT, we could determine the substrates for each transporter. We could then measure the concentrations of these metals in both healthy and *Rs*-infected tomato xylem using inductively coupled plasma with optical spectroscopy (ICP-OES), as has been done previously with *X. fastidiosa* (44). This experiment would require finding a collaborator with access to and experience with this equipment. Finally,

we could test the ability of the metal transport mutants to cause disease on tomato plants. If our hypothesis is correct, the transport mutants will be reduced in virulence. The importance of this trait can be further examined by using two inoculation methods, a naturalistic soil soak or the direct inoculation of bacteria into the xylem through a cut petiole. As petiole inoculation bypasses the soil and root stages of infection, comparing these two methods could help us determine if metal resistance is required those parts of the *Rs* life cycle.

What are the in planta targets of the Rs Type III effectors RipAX1 and RipAX2?

A recent large-scale genomic survey for genes with sequence similarity to the Clostridium botulinum neurotoxin (BoNT) found a family of homologs in plant pathogenic Proteobacteria (45). These included predicted proteins in Xanthomonas and Acidovorax species, the Type III effector HopH1 in Pseudomonas syringae, and the Type III effectors RipAX1 and RipAX2 in Rs. None of these effectors are well studied, although RipAX2 has been shown to induce HR in the wild eggplant relative Solanum torvum and a cognate resistance gene has been found in cultivated eggplant, Solanum melongena (46–48). Like BoNTs, RipAX1 and RipAX2 have a predicted zinc-dependent protease motif and mutating the active site of this domain in RipAX2 prevents HR induction in S. torvum, although, puzzlingly, not in S. melongena. BoNTs in Clostridium species act by cleaving soluble N-ethylmaleimide-sensitive factor attachment protein receptors (SNAREs), which are membrane-bound proteins involved in vesicle fusion in eukaryotic cells (49). SNAREs located in the membranes of both the vesicle and the target membrane bind tightly together, bringing the two membranes close enough to fuse. BoNTs act

on SNAREs in the synapses of animal neurons, preventing the release of neurotransmitters, and stopping the synapse from firing (49).

Plant cells also use SNAREs for vesicular trafficking and they play a role in pathogen defense (50). For example, a screen for Arabidopsis mutants lacking resistance to the fungal pathogen Blumeria graminis discovered the SNARE PEN1 (51). Although the cargo that PEN1 helps secrete is unknown, PEN1 mutants induce delayed deposition of callose, a polysaccharide that helps strengthen plant cell walls in response to pathogen attack (50). Similarly, the defense protein PR1a did not accumulate in the cell wall of tobacco plants when the SNARE SYP132 was silenced (52). Some pathogen effectors may also interact with host vesicular trafficking. A SNARE-like protein secreted from the esophageal gland of the soybean cyst nematode (SCN) Heterodera glycines physically interacts with an aberrant α -SNAP encoded by the soybean SCN resistance locus rhg1 (53). α-SNAPs normally facilitate the dissociation and re-use of SNARE complexes, and the atypical α -SNAP encoded in multi-copy *Rhg1* contributes to SCN resistance in soybean (54, 55). Mutating two soybean SNARE proteins that were identified as binding partners to the atypical α -SNAP increased the SCN susceptibility of a resistant soy variety, suggesting that the nematode needs to control an aspect of vesicular trafficking for successful infection (56). Plant vesicular trafficking may also be an attractive target for Rs, and the similarity of RipAX1 and RipAX2 to BoNT suggests a potential mechanism for Rs to interfere with host vesicular trafficking.

Working collaboratively with Derrick Grunwald, I created expression vectors encoding Myc-tagged RipAX1 or RipAX2 and His-tagged versions of two tomato SNAREs, SNAP30 and VAMP7b, which have high conservation to known BoNT cut sites in mammalian SNAREs (57).

Future work would express the two tagged constructs both individually and together in *E. coli*. After induction of expression, the *E. coli* could by lysed and their proteins could be run on an SDS-PAGE gel. A Western blot using anti-his antibodies could be used to probe for the presence and size of the tomato SNARE. If the SNARE is cleaved by the *Rs* effector, its band will be shifted or reduced in intensity. Similar experiments are used to study *Clostridium* BoNTs (58). As a control, the tomato SNAREs could be co-expressed with a tagged version of RipAX containing a point mutation in the predicted zinc binding motif that should prevent protease activity. If the SNARE cleavage is dependent on RipAX protease activity, the protease negative mutant will not affect the SNARE's integrity *in vitro*.

We found that expressing *ripAX1* in yeast increases their sensitivity to both sorbitol and caffeine. Yeast, as unicellular eukaryotes that are easy to experimentally and genetically manipulate, have provided an excellent platform to study the function of plant pathogen effectors (59). Effectors that target conserved eukaryotic pathways can inhibit yeast growth either alone or when combined with stressors that force the yeast cell to rely on pathways targeted by the effector (60–62). Sorbitol and caffeine cause osmotic and cell wall stresses, respectively, and responses to these stressors involve many pathways (63–65). Targeted deletions in key pathways could be combined with effector expression to narrow down how RipAX1 counteracts yeast stress responses. First, however, a control experiment using the protease negative RipAX1 mutant will confirm if this increased sensitivity is due to the enzymatic activity of the effector. Further, we can use invertase export assays to examine if the expression of RipAX1 causes defects in vesicle-mediated protein export (66).

Should we find a promising result in either *E. coli* or *S. cerevisiae*, we can examine the activity of RipAX1 and RipAX2 *in planta*. We examined the localization of GFP-tagged versions of each effector when expressed in tobacco leaves using *Agrobacterium*. We found that RipAX1 and RipAX2 are primarily cytoplasmic proteins, but they form discrete foci scattered around the cell (Figure 3). We could use fluorescently tagged organelle markers to determine if RipAX1 and RipAX2 colocalize with any known cellular compartments (67). Of particular interest might be ER markers, which could provide a good benchmark for involvement with vesicular trafficking. Finally, we can delete RipAX1 and RipAX2 both individually and dually from *Rs* strain GMI1000 and determine if their loss causes any virulence defects.

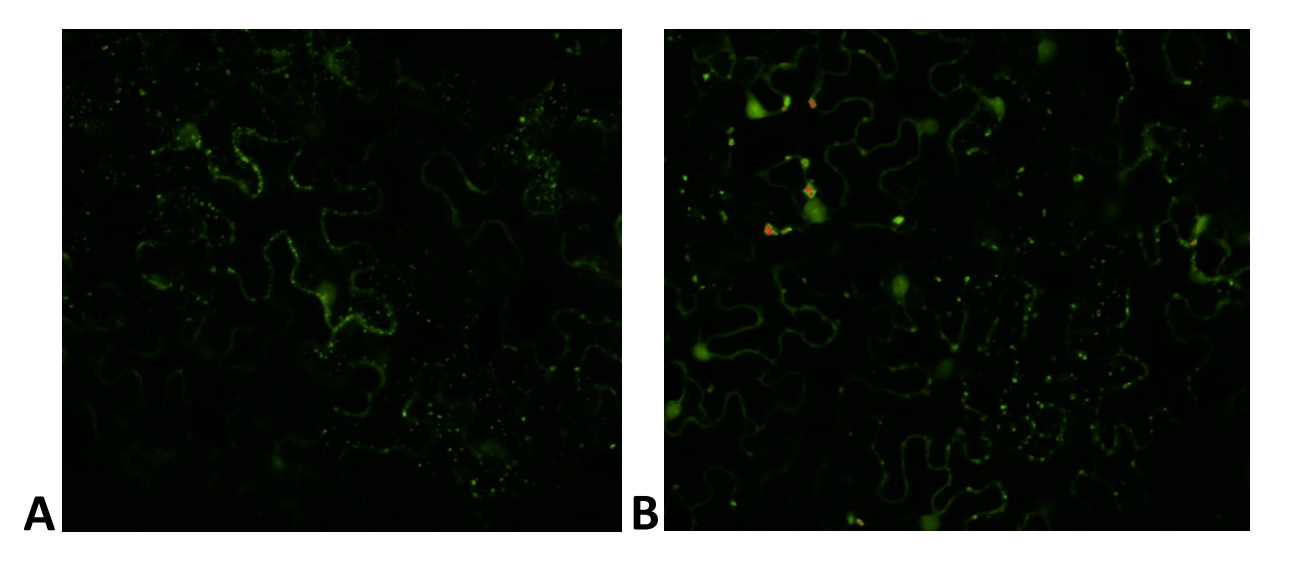


Figure 3. RipAX1 and RipAX2 form discrete foci when expressed in tobacco leaves.

Fluorescence microscopy showing localization of GFP-tagged RipAX1 (a) and RipAX2 (b) when transiently expressed in tobacco leaves using *Agrobacterum*. Images were taken 48 hours after *Agrobacterium* infiltration.

Do Rs dehydrogenases contribute to anaerobic growth?

Rs can growing anaerobically using the denitrification pathway with nitrate as an alternate electron acceptor (2). This ability is widely (but not universally) distributed throughout Rs phylotypes. In tomato, xylem oxygen levels are depleted late in BWD but xylem sap is rich in nitrate, so it is unsurprising that denitrification contributes to tomato infection (2). However, mutants unable to use the denitrification pathway retain some virulence, suggesting that Rs is not wholly reliant on denitrifying respiration for energy inside the plant. Further, a mutant lacking $\Delta narG$, the first enzyme in the pathway, can grow in anaerobic conditions, albeit to a lesser extent than WT (19). These results indicate that Rs has one or more alternate energy-generating metabolic strategies that allow it to persist and survive in low oxygen conditions when it cannot use nitrate for denitrification. However, the identity of any such alternate pathways is unknown.

The Rs in planta transcriptome study described in Chapter 2 provides a way to address this question. We compared transcriptomes of Rs $\Delta narG$ to wildtype grown in tomato stems and in low oxygen denitrifying conditions in culture. In planta, only 187 genes were differentially expressed in $\Delta narG$ compared to WT. Among these were two predicted dehydrogenases: a lactate dehydrogenase encoded by IdhA and an alcohol dehydrogenase encoded by IdhA and an alcohol dehydrogenase encoded by IdhA. The activity of these two enzymes, which respectively reduce pyruvate to lactate or acetaldehyde to ethanol, could allow anaerobically growing IdhA cells to ferment as an alternative to respiration (68, 69). As such, these genes are candidates for non-denitrifying anaerobic metabolism in IdhA so IdhA and an alcohol dehydrogenase

While both genes are upregulated in ΔnarG in planta, in denitrifying conditions in culture IdhA has slightly lower and adhA has unchanged expression in $\Delta narG$ relative to WT. However, the absolute expression of both genes is much higher in anaerobic denitrifying conditions in culture compared with in Rs growing in tomato. In another transcriptomic study comparing Rs growing in aerobic rich medium and in tomato, both genes were highly upregulated in planta (36). This pattern of expression, with the lowest level of expression seen in rich medium, the highest in anaerobic conditions in culture, and tomato xylem between the two, matches the expression of most genes involved in denitrification. This pattern suggests that the IdhA lactate dehydrogenase and the adhA alcohol are similarly involved in anaerobic growth. Another interesting comparison can be seen in a study examining the transcriptome of two closely related Rs strains grown in rich media, in their preferred host (either banana or melon), or in tomato (35). While adhA is upregulated in both strains in tomato and in the melon adapted strain in melon, it is significantly downregulated in the banana-adapted strain grown in banana. The authors found that the banana-adapted strain had higher expression of genes involved in low-oxygen metabolism in tomato compared to in banana; this included denitrification genes and a high-affinity oxidase involved in microaerobic metabolism. Based on this, the authors predicted that banana xylem contains higher oxygen levels than tomato during Rs pathogenesis. All of these gene expression studies point to AdhA and LdhA as important for low-oxygen growth.

To test if AdhA or LdhA allow for anerobic growth in the absence of denitrification, we could delete them singly, together, and in combination. These mutations could be made in both WT and a $\Delta narG$ background. These mutants could then be grown in aerobic rich media and in

anaerobic denitrifying conditions. If they do provide a backup to denitrification, the mutants lacking the dehydrogenases and narG will be unaffected in aerobic rich media but will grow poorly or not at all in denitrifying conditions without oxygen. We could then infect tomato with the mutants to determine if they have additional virulence defects compared to a $\Delta narG$ single mutant. Additionally, we could test the virulence of $\Delta narG$ and the $\Delta narG$ dehydrogenase double mutants on banana. If banana xylem does contain higher levels of oxygen than tomato xylem, any virulence defects seen in the mutants will be lower in banana than compared with tomato. Further, we could use an oxygen sensitive microsensor to measure the oxygen levels of banana xylem both with and without Rs infection to directly compare its oxygen levels to tomato.

Conclusions

The work presented in this thesis demonstrate the complex roles that virulence factors like secretion systems play in the biology of an important agricultural pathogen. These virulence factors are inexorably tied to basic biology and metabolism. Investigating these virulence factors leads to better understanding both of how the pathogen adapts to its *in planta* environment and also can provide clear routes to combatting bacterial diseases.

References

- 1. Baudouin E, Hancock JT. 2014. Nitric oxide signaling in plants. Front Plant Sci 4:1–3.
- 2. Dalsing BL, Truchon AN, Gonzalez-Orta ET, Milling AS, Allen C. 2015. Ralstonia

- solanacearum uses inorganic nitrogen metabolism for virulence, ATP production, and detoxification in the oxygen-limited host xylem environment. MBio 6:1–13.
- 3. Liu H, Zhang S, Schell MA, Denny TP. 2005. Pyramiding unmarked deletions in *Ralstonia solanacearum* shows that secreted proteins in addition to plant cell-wall-degrading enzymes contribute to virulence. Mol Plant Microbe Interact 18:1296–1305.
- 4. Asgher M, Per TS, Masood A, Fatma M, Freschi L, Corpas FJ, Khan NA. 2017. Nitric oxide signaling and its crosstalk with other plant growth regulators in plant responses to abiotic stress. Environ Sci Pollut Res 24:2273–2285.
- 5. Lindermayr C, Durner J. 2009. S-Nitrosylation in plants: Pattern and function. J Proteomics 73:1–9.
- 6. Cooper CE. 1999. Nitric oxide and iron proteins. Biochim Biophys Acta Bioenerg 1411:290–309.
- 7. Russwurm M, Koesling D. 2004. NO activation of guanylyl cyclase. EMBO J 23:4443–4450.
- 8. Leitner M, Vandelle E, Gaupels F, Bellin D, Delledonne M. 2009. NO signals in the haze. Nitric oxide signalling in plant defence. Curr Opin Plant Biol 12:451–458.
- 9. Wünsche H, Baldwin IT, Wu J. 2011. S-Nitrosoglutathione reductase (GSNOR) mediates the biosynthesis of jasmonic acid and ethylene induced by feeding of the insect herbivore *Manduca sexta* and is important for jasmonate-elicited responses in *Nicotiana attenuata*. J Exp Bot 62:4605–4616.
- 10. Simmonds MJ, Detterich JA, Connes P. 2014. Nitric oxide, vasodilation and the red blood cell. Biorheology 51:121–134.
- Zhang R, Hess DT, Qian Z, Hausladen A, Fonseca F, Chaube R, Reynolds JD, Stamler JS.
 2015. Hemoglobin βCys93 is essential for cardiovascular function and integrated response to hypoxia. Proc Natl Acad Sci U S A 112:6425–6430.
- 12. Kolbert Z, Feigl G, Bordé Á, Molnár Á, Erdei L. 2017. Protein tyrosine nitration in plants: Present knowledge, computational prediction and future perspectives. Plant Physiol Biochem 113:56–63.
- 13. Zaffagnini M, De Mia M, Morisse S, Di Giacinto N, Marchand CH, Maes A, Lemaire SD, Trost P. 2016. Protein S-nitrosylation in photosynthetic organisms: A comprehensive overview with future perspectives. Biochim Biophys Acta Proteins Proteomics.
- 14. Van Faassen E, Vanin AF. 2007. Nitric oxide radicals and their reactionsRadicals for Life: The Various Forms of Nitric Oxide. Elsevier B.V.
- 15. Rhee KY, Erdjument-Bromage H, Tempst P, Nathan CF. 2005. S-nitroso proteome of

- Mycobacterium tuberculosis: Enzymes of intermediary metabolism and antioxidant defense. Proc Natl Acad Sci U S A 102:467–72.
- 16. Seth D, Hausladen A, Wang Y-J, Stamler JS. 2012. Endogenous Protein S-Nitrosylation in *E. coli*: Regulation by OxyR. Science (80-) 336:470–3.
- 17. Signorelli S, Sainz M, Tabares-da Rosa S, Monza J. 2020. The Role of Nitric Oxide in Nitrogen Fixation by Legumes. Front Plant Sci 11:1–14.
- 18. Xue Y, Liu Z, Gao X, Jin C, Wen L, Yao X, Ren J. 2010. GPS-SNO: Computational prediction of protein s-nitrosylation sites with a modified GPS algorithm. PLoS One 5:1–7.
- 19. Dalsing BL. 2015. Virulence-related functions of inorganic nitrogen metabolism and signaling in *Ralstonia solanacearum*. University of Wisconsin-Madison.
- 20. Hess DT, Matsumoto A, Kim S-O, Marshall HE, Stamler JS. 2005. Protein S-nitrosylation: purview and parameters. Nat Rev Mol Cell Biol 6:150–166.
- 21. Poueymiro M, Cunnac S, Barberis P, Deslandes L, Peeters N, Boucher C, Genin S. 2009. Two Type III Secretion System Effectors from *Ralstonia solanacearum* GMI1000 Determine Host-Range Specificity on Tobacco 22:538–550.
- 22. Waterhouse AM, Procter JB, Martin DMA, Clamp M, Barton GJ. 2009. Jalview Version 2-A multiple sequence alignment editor and analysis workbench. Bioinformatics 25:1189–1191.
- 23. Sievers F, Wilm A, Dineen D, Gibson TJ, Karplus K, Li W, Lopez R, McWilliam H, Remmert M, Soding J, Thompson JD, Higgins DG. 2011. Fast, scalable generation of high-quality protein multiple sequence alignments using Clustal Omega. Mol Syst Biol 7:539–545.
- 24. Forrester MT, Foster MW, Benhar M, Stamler JS. 2009. Detection of Protein S-Nitrosylation with the Biotin Switch Technique. Free Radic Biol Med 46:119–126.
- 25. Derakhshan B, Wille PC, Gross SS. 2007. Unbiased identification of cysteine snitrosylation sites on proteins. Nat Protoc 2:1685–1691.
- 26. Gallegos MT, Schleif R, Bairoch A, Hofmann K, Ramos JL. 1997. Arac/XylS family of transcriptional regulators. Microbiol Mol Biol Rev 61:393–410.
- 27. Pfeiffer S, Leopold E, Hemmens B, Schmidt K, Werner ER, Mayer B. 1997. Interference of carboxy-PTIO with nitric oxide-and peroxynitrite- mediated reactions. Free Radic Biol Med 22:787–794.
- 28. Liu Z, Cao J, Ma Q, Gao X, Ren J, Xue Y. 2011. GPS-YNO2: computational prediction of tyrosine nitration sites in proteins. Mol Biosyst 7:1197.

- 29. Castañeda A, Reddy J, El-Yacoubi B, Gabriel D. 2005. Mutagenesis of all eight *avr* genes in *Xanthomonas campestris* pv. *campestris* had no detected effect on pathogenicity, but one *avr* gene affected race specificity. Mol Plant-Microbe Interact 18:1306–1317.
- 30. Georgoulis S, Shalvarjian KE, Helmann TC, Hamilton CD, Carlson HK, Deutschbauer AM, Lowe-Power TM. 2020. Genome-wide identification of tomato xylem sap fitness factors for *Ralstonia pseudosolanacearum* and *Ralstonia syzygii*. bioRxiv.
- 31. Douzi B, Ball G, Cambillau C, Tegoni M, Voulhoux R. 2011. Deciphering the Xcp *Pseudomonas aeruginosa* Type II Secretion machinery through multiple interactions with substrates. J Biol Chem 286:40792–40801.
- 32. Yan Z, Yin M, Xu D, Zhu Y, Li X. 2017. Structural insights into the secretin translocation channel in the type II secretion system. Nat Struct Mol Biol 24:177–183.
- 33. da Silva Xavier A, de Almeida JCF, de Melo AG, Rousseau GM, Tremblay DM, de Rezende RR, Moineau S, Alfenas-Zerbini P. 2019. Characterization of CRISPR-Cas systems in the *Ralstonia solanacearum* species complex. Mol Plant Pathol 0:223–239.
- 34. Baldvinsson SB, Holst Sørensen MC, Vegge CS, Clokie MRJ, Brøndsted L. 2014. *Campylobacter jejuni* motility is required for infection of the flagellotropic bacteriophage F341. Appl Environ Microbiol 80:7096–7106.
- 35. Ailloud F, Lowe TM, Robène I, Cruveiller S, Allen C, Prior P. 2016. In planta comparative transcriptomics of host-adapted strains of *Ralstonia solanacearum*. PeerJ 2016.
- 36. Jacobs JM, Babujee L, Meng F, Milling AS, Allen C. 2012. The *in planta* transcriptome of *Ralstonia solanacearum*: conserved physiological and virulence strategies during bacterial wilt of tomato. MBio 3:e00114-12.
- 37. Hamilton CD, Steidl OR, Macintyre AM, Hendrich CG, Allen C. 2020. *Ralstonia solanacearum* depends on catabolism of myo-inositol, sucrose, and trehalose for virulence in an infection stage-dependent manner. MPMI.
- 38. Costa TRD, Felisberto-Rodrigues C, Meir A, Prevost MS, Redzej A, Trokter M, Waksman G. 2015. Secretion systems in Gram-negative bacteria: structural and mechanistic insights. Nat Rev Microbiol 13:343–59.
- 39. Nies DH, Nies A, Chu L, Silver S. 1989. Expression and nucleotide sequence of a plasmid-determined divalent cation efflux system from Alcaligenes eutrophus. Proc Natl Acad Sci U S A 86:7351–7355.
- 40. Valencia EY, Braz VS, Guzzo C, Marques M V. 2013. Two RND proteins involved in heavy metal efflux in *Caulobacter crescentus* belong to separate clusters within proteobacteria. BMC Microbiol 13.

- 41. Stahl A, Pletzer D, Mehmood A, Ullrich MS. 2015. *Marinobacter adhaerens* HP15 harbors two CzcCBA efflux pumps involved in zinc detoxification. Antonie van Leeuwenhoek, Int J Gen Mol Microbiol 108:649–658.
- 42. Navarrete F, De La Fuente L. 2015. Zinc detoxification is required for full virulence and modification of the host leaf ionome by *Xylella fastidiosa*. Mol Plant-Microbe Interact 28:497–507.
- 43. White MC, Chaney RL, Decker AM. 1981. Metal Complexation in Xylem Fluid. Plant Physiol 67:311–315.
- 44. de la Fuente L, Parker JK, Oliver JE, Granger S, Brannen PM, van Santen E, Cobine PA. 2013. The Bacterial Pathogen *Xylella fastidiosa* Affects the Leaf Ionome of Plant Hosts during Infection. PLoS One 8:1–9.
- 45. Mansfield MJ, Wentz TG, Zhang S, Lee EJ, Dong M, Sharma SK, Doxey AC. 2019. Bioinformatic discovery of a toxin family in *Chryseobacterium piperi* with sequence similarity to botulinum neurotoxins. Sci Rep 9:1–11.
- 46. Morel A, Guinard J, Lonjon F, Sujeen L, Barberis P, Genin S, Vailleau F, Daunay MC, Ditinger J, Poussier S, Peeters N, Wicker E. 2018. The Type III effector RipAX2 enables the control of the *Ralstonia solanacearum* species complex (RSSC) by eggplant AG91-25 carrying the resistance locus EBWR9. Mol Plant Pathol 19:2459–2472.
- 47. Morel A, Guinard J, Lonjon F, Sujeeun L, Barberis P, Genin S, Vailleau F, Daunay MC, Dintinger J, Poussier S, Peeters N, Wicker E. 2018. The eggplant AG91-25 recognizes the Type III-secreted effector RipAX2 to trigger resistance to bacterial wilt (*Ralstonia solanacearum* species complex). Mol Plant Pathol 19:2459–2472.
- 48. Nahar K, Matsumoto I, Taguchi F, Inagaki Y, Yamamoto M, Toyoda K, Shiraishi T, Ichinose Y, Mukaihara T. 2014. *Ralstonia solanacearum* type III secretion system effector Rip36 induces a hypersensitive response in the nonhost wild eggplant *Solanum torvum*. Mol Plant Pathol 15:297–303.
- 49. Rossetto O, Pirazzini M, Montecucco C. 2014. Botulinum neurotoxins: Genetic, structural and mechanistic insights. Nat Rev Microbiol 12:535–549.
- 50. Kwon C, Yun HS. 2014. Plant exocytic secretion of toxic compounds for defense. Toxicol Res 30:77–81.
- 51. Collins NC, Thordal-Christensen H, Lipka V, Bau S, Kombrink E, Qiu J-L, Hückelhoven R, Stein M, Freialdenhoven A, Somerville SC, Schulze-Lefert P. 2003. SNARE-protein-mediated disease resistance at the plant cell wall. Nature 425:973–977.
- 52. Kalde M, Nühse TS, Findlay K, Peck SC. 2007. The syntaxin SYP132 contributes to plant resistance against bacteria and secretion of pathogenesis-related protein 1. Proc Natl

- Acad Sci U S A 104:11850–11855.
- 53. Bekal S, Domier LL, Gonfa B, Lakhssassi N, Meksem K, Lambert KN. 2015. A SNARE-Like Protein and Biotin Are Implicated in Soybean Cyst Nematode Virulence. PLoS One 10:e0145601.
- 54. Bayless AM, Zapotocny RW, Grunwald DJ, Amundson KK, Diers BW. 2018. An atypical Nethylmaleimide sensitive factor enables the viability of nematode-resistant Rhg1 soybeans. Proc Natl Acad Sci USA 1–10.
- 55. Bayless AM, Smith JM, Song J, McMinn PH, Teillet A, August BK, Bent AF. 2016. Disease resistance through impairment of α -SNAP-NSF interaction and vesicular trafficking by soybean Rhg1. Proc Natl Acad Sci U S A 113:E7375–E7382.
- 56. Dong J, Zielinski RE, Hudson ME. 2020. t-SNAREs bind the *Rhg1* α -SNAP and mediate soybean cyst nematode resistance. Plant J 104:318–331.
- 57. Zhang S, Lebreton F, Mansfield MJ, Miyashita S-I, Zhang J, Schwatrzman JA, Tao L, Masuyer G, Carranza MM, Stenmark P, Gilmore MS, Doxey AC, Dong M. 2018. Identification of a botulinum neurotoxin-like toxin in a commensal strain of *Enterococcus faecium*. Cell Host Microbe 23:169–176.
- 58. Jin R, Sikorra S, Stegmann CM, Pich A, Binz T, Brunger AT. 2007. Structural and biochemical studies of botulinum neurotoxin serotype C1 light chain protease: Implications for dual substrate specificity. Biochemistry 46:10685–10693.
- 59. Munkvold KR, Martin ME, Bronstein PA, Collmer A. 2008. A survey of the *Pseudomonas syringae* pv. *tomato* DC3000 type III secretion system effector repertoire reveals several effectors that are deleterious when expressed in *Saccharomyces cerevisiae*. Mol Plant-Microbe Interact 21:490–502.
- 60. Salomon D, Dar D, Sreeramulu S, Sessa G. 2011. Expression of *Xanthomonas campestris* pv. *vesicatoria* Type III effectors in yeast affects cell growth and viability. Mol Plant-Microbe Interact 24:305–314.
- 61. Salomon D, Bosis E, Dar D, Nachman I, Sessa G. 2012. Expression of *Pseudomonas syringae* type III effectors in yeast under stress conditions reveals that HopX1 attenuates activation of the high osmolarity glycerol MAP kinase pathway. Microbiol (United Kingdom) 158:2859–2869.
- 62. Valdivia RH. 2004. Modeling the function of bacterial virulence factors in *Saccharomyces cerevisiae*. Eukaryot Cell 3:827–834.
- 63. Miermont A, Waharte F, Hu S, McClean MN, Bottani S, Léon S, Hersen P. 2013. Severe osmotic compression triggers a slowdown of intracellular signaling, which can be explained by molecular crowding. Proc Natl Acad Sci U S A 110:5725–5730.

- 64. Calvo IA, Gabrielli N, Iglesias-Baena I, García-Santamarina S, Hoe KL, Kim DU, Sansó M, Zuin A, Pérez P, Ayté J, Hidalgo E. 2009. Genome-wide screen of genes required for caffeine tolerance in fission yeast. PLoS One 4.
- 65. Auesukaree C, Damnernsawad A, Kruatrachue M, Pokethitiyook P, Boonchird C, Kaneko Y, Harashima S. 2009. Genome-wide identification of genes involved in tolerance to various environmental stresses in *Saccharomyces cerevisiae*. J Appl Genet 50:301–310.
- 66. Troy AA H. 2014. A Simplified Method for Measuring Secreted Invertase Activity in *Saccharomyces cerevisiae*. Biochem Pharmacol Open Access 03.
- 67. Dangol S, Singh R, Chen Y, Jwa NS. 2017. Visualization of multicolored in vivo organelle markers for co-localization studies in Oryza sativa. Mol Cells 40:828–836.
- 68. Nissen LS, Basen M. 2019. The emerging role of aldehyde:ferredoxin oxidoreductases in microbially-catalyzed alcohol production. J Biotechnol 306:105–117.
- 69. Juturu V, Wu JC. 2016. Microbial production of lactic acid: the latest development. Crit Rev Biotechnol 36:967–977.

Appendix 1

Decoding tomato resistance to bacterial wilt disease using metatranscriptomics

The material presented in this appendix will be included in the following manuscript in preparation:

Meline, V., Hendrich, C. G., Truchon, A. N., Rivera-Zuluaga, K., MacIntyre, A. M., K., Mitra, R., Iyer-Pascuzzi, A. S., Allen, C. Defining the core tomato response bacterial wilt disease through the synthesis of multiple transcriptome studies. *Planned submission in early 2021*

Contributions: All authors designed experiments and analyzed data. VM conducted metaanalysis of RNA-seq data, created the figures and wrote figure legends. CGH, ANT, and RM all extracted and prepared RNA for sequencing. ANT, VM, and KR are performing further wet-lab experiments to validate predictions from the bioinformatic analysis. CGH wrote the text.

Abstract

Tomato is one of the most important vegetable crops in the world. Bacterial wilt disease caused by *Ralstonia solanacearum* (*Rs*) can be devastating for tomato production. The breeding line Hawaii 7996 is a source of genetic resistance to *Rs*. However, the mechanism of resistance in Hawaii 7996 is not completely understood, in part because it is governed by multiple loci scattered throughout the genome. Transcriptomics provides a useful tool for studying complex phenotypes like Hawaii 7996-mediated resistance by allowing us to view broad gene expression changes in resistant compared to susceptible plant host lines. Unfortunately, the breadth provided by RNA-seq comes with the drawback of reduced clarity. Sifting through the resulting large datasets can be challenging. Further, RNA-seq studies usually reveal gene expression in specific tissue types at one or a few time points, limiting their interpretation. We tried to more broadly understand tomato resistance to BWD by simultaneously analyzing three independent transcriptome studies of tomato during *Rs* infection. This meta-analysis allows us to make novel predictions about the biology of tomato resistance to *Rs* and distinguish consistent, broadly meaningful signals from the experimental noise of individual experiments.

Introduction

Genetic resistance produced through conventional breeding or biotechnology is one of the most important tools for combating plant diseases and improving crop yields (1, 2). Plants have two layers of immunity. The first, pattern triggered immunity (PTI), relies on the recognition of conserved molecular patterns found in microbes and provides a general defense against invaders (3). The second immunity layer, which is much more rapid and intense than

PTI, relies on recognition of individual pathogen effectors by resistance genes (R genes), and is called effector triggered immunity (ETI) (4). Both systems can be manipulated to create resistant crop varieties, although R genes have received more attention because of their ability to target and completely exclude specific pathogens (5, 6).

In many plant-pathogen interactions, gene-for-gene immunity mediated by R genes plays a only minor role. One example is bacterial wilt disease (BWD) caused by the Ralstonia solanacearum (Rs) species complex on tomato and other hosts. Rs is a soil-borne pathogen that infects hosts through their roots and spreads through the xylem, eventually clogging xylem vessels and preventing water transport (7–9). There is considerable diversity in the Rs species complex, which is divided into four phylotypes with distinct geographic origins (10). Although this pathogen is known for its extremely wide host range, tomato is one of the most important Rs hosts, and is often used as a model organism in the study of BWD (9, 11). Tomato has only one known R gene against Rs, Ptr1, which was found in the tomato relative Solanum lycopersicoides and recognizes RipBN, a Type III-secreted effector found in the phylotype III strain CMR15 (12, 13). Although transferring R genes from other plant families like tobacco or Arabidopsis can confer Rs resistance to tomato, most naturally occurring Rs resistance in tomato is dependent on multiple loci, all with small contributions to resistance (2, 5, 14). One source for such quantitative (QTL-mediated) resistance is the breeding line Hawaii 7996 (HA) (15). The bacterial wilt resistance provided by HA is broad but complex, delaying colonization or restricting movement of Rs in both roots and stems and involving multiple physiological and enzymatic barriers (8, 16). Deciphering the multitude of loci and mechanisms underlying HA defenses has proved challenging (2).

In the past two decades, transcriptomic analysis using RNA-seq has emerged as a powerful tool to study such complex biological processes (17). By allowing researchers to measure the expression of almost every gene in a sample simultaneously, RNA-seq greatly expands the number of biological process that can be examined in a single experiment compared to older gene expression methods like qRT-PCR. Further, as RNA-seq is untargeted, it can be used to generate hypothesis where the exact gene targets underlying a biological process are not known. This technique has been employed in various ways to understand host gene expression during BWD (18-25). However, this breadth of RNA-seq studies comes with drawbacks. Hundreds or thousands of genes might be differentially regulated in a given study, and sifting through the data to find relevant observations is challenging, and requires further analyses like GO enrichment (17). Yet even the extraordinarily wide perspective provided by RNA-seq does not cover the full complexity of biology. Most RNA-seq studies can only capture a snapshot of gene expression at a few time points in a few conditions. Comparing transcriptomes from multiple published datasets can help expand our view, but the comparisons come with their own set of challenges. Different studies have found completely different results, such as divergent changes in expression of salicylic acid and jasmonic acidrelated genes in different experiments (19–21, 23, 24, 26–29). Weighing the evidence provided by different studies is challenging. Additionally, direct comparisons of differentially expressed genes found by two experiments, even in the same system, often reveal little overlap (30).

To better understand resistance to BWD in tomato we used meta-analysis, a powerful computational tool that combines results of multiple independent studies to increase statistical power and identify consistent results (30). Using the metaRNASeq R package, we analyzed

three RNA-seq datasets from tomato plants responding to *Rs* infection. These derived from a range of experimental conditions, included a previously published comparison of gene expression in the roots of susceptible and HA tomato plants and two new RNA-seq experiments. This analysis identified new potential components of HA resistance, including novel pattern recognition receptors involved in PTI. The data provides a foundation for further targeted studies of HA resistance in tomato.

Results

We analyzed RNA-seq data from a total of twelve experimental conditions described in Table 1. Experiments by French et al. (26), examined responses to the phylotype IIA *Rs* strain K60 in the roots of resistant HA and susceptible West Virginia 700 (WV) tomato plants at two time points. A new transcriptional analyses of tomato challenged with *Rs* compared root responses of resistant HA seedlings to the susceptible variety Bonny Best (BB). Sterilized seeds were germinated on water agar plates and then grown on 0.5x Murashige-Skoog (MS) agar plates for four days. The seedlings were inoculated with the phylotype I *Rs* strain GMI1000 by dripping a bacterial suspension onto the roots. Root tissue was harvested 24 hpi. Based on comparable studies, seedlings inoculated at this stage would have a colonization level of roughly 10⁵ CFU/mL (31). RNA was extracted using Trizol, and library creation and sequencing was conducted at the UW Biotechnology Center (UWBC, Madison, USA). A second experiment, extracted from the same samples as used in Chapter 2, we collected RNA from the stem tissue of susceptible adult BB plants petiole-inoculated with either *Rs* strain GMI1000 or with water. After 72 hours, we extracted RNA using a hot-phenol chloroform method from stems that were

colonized with between 10^8 and 10^9 CFU/g of tissue (32). cDNA library construction and sequencing were conducted by Novogene (Beijing, China). Reads were trimmed for quality control and mapped to the S. lycopersicum genome, followed by differential expression analysis compared to uninoculated WT using DESeq2 (33). The expression and P-values produced by DESeq2 were then used in the meta-analysis using metaRNASeq.

Table 1. Experiment metadata

M4

S3

This study

Trizol

(Invitrogen)

Experiment & Reference	Sample ¹	Tomato host ²	Rs Strain		Strain Inoculation method ³		Tissue type		nt Age at culation	popu sar	eximate <i>Rs</i> ulation at mpling CFU/g)	
	M1		N/A K60 (Phylotype IIA) N/A K60 (Phylotype IIA)			0 hpi	Root			1	N/A	
	R1	Hawaii 7996				24 hpi		ļ		1x10 ⁶		
Group A French et	R2	(Resistant)				48 hpi		1.1	17 days	1x10 ⁷		
al., 2018 ²	M3	West				0 hpi		-17 days	N/A			
ai., 2010	S1	Virginia 700				24 hpi			1x10 ⁶			
	S2	(Susceptible)			Soll soak	48 hpi			1x10 ⁷			
	M2	Hawaii 7996	N/A GMI1000 (Phylotype I) N/A GMI1000 (Phylotype I)			24 hpi		Seedlings		N/A		
Group B This study	R3	(Resistant)								~5x10 ^{5 4}		
	M4	Danny Doot								N/A		
	S3	Bonny Best (Susceptible)								~5x10 ^{5 4}		
Group C	M5	Danny Bost	N/A GMI1000 (Phylotype I)		Petiole			tem 21 days			N/A	
This study	S4	Bonny Best (Susceptible)			inoculation	72 hpi	Stem			1x10 ⁸		
Experiment & Reference	Sample ¹	RNA extraction method	Minimum RIN value	RNA clean- up		cDNA synthesis	Sequencing Sequentype facil			Platform		
Group A French et al., 2018	M1 R1 R2 M3 S1	Trizol (Invitrogen) with Nortek Column (Norgen BioTek Corp)	7.8	d	Ribo- lepletion	Illumina TruSeq stranded mRNA preparation kit	Purdu Paired end Genom Cente		nics	Illumina HiSeq 2500		
Group B	M2 R3	Trizol		PolyA		Illumina TruSeg	UW		V	Illumina		

PolyA

enrichment

nd

TruSeq

stranded

mRNA

Paired end

Biotechnology

Center

HiSeq

2000

					preparation kit			
					NEBNext			Illumina
	M5				Ultra			NovaSeq
Group C		Phenol-	7.4	Ribo-	Directional	Paired end	Novagene	
This study	S4	Chloroform ⁵	7.4	depletion	RNA Library	i airea eria	ivovagene	
					Prep Kit for			
					Illumina			

- 1 Blue samples are uninoculated controls, red samples are inoculated
- 2 Green cultivars are resistant, yellow are susceptible
- 3 Reference: Khokhani, D. *et al.* (2018) 'Plant Assays for Quantifying Ralstonia solanacearum Virulence', *Bio-Protocol*, 8(18).
- 4 Reference: Hamilton, C.D., Steidl, O.R., Macintyre, A.M., Hendrich, C.G. and Allen, C. (2020) *Ralstonia solanacearum* depends on catabolism of myo-inositol, sucrose, and trehalose for virulence in an infection stage-dependent manner. *MPMI*.
- 5 Reference: Jacobs, J. M. *et al.* (2012) 'The *in planta* transcriptome of *Ralstonia* solanacearum: conserved physiological and virulence strategies during bacterial wilt of tomato', *mBio*, 3(4)

MetaRNASeg reveals more differentially expressed genes than DESeg2

We first examined the number of differentially expressed genes (DEGs) to see if metaRNASeq could make predictions that were not found in comparing DEG lists directly.

Overall, DESeq2 found a similar number of DEGs in each condition (Figure 1a). The wilt-resistant HA tomato genotype had between 645 and 1720 upregulated genes compared to between 438 and 1837 in the susceptible tomato genotypes. Slightly fewer genes were downregulated, with between 600 and 1207 found in the resistant HA genotype and between 571 and 1777 found in

the susceptible genotypes. Comparing the overlap in DEGs found by DESeq2 between conditions identified a small number of shared genes within resistant and susceptible genotypes (Figure 1b). A total of 98 up- and downregulated DEGs were found in the resistant genotype, and only 32 were found in the susceptible genotypes. The meta-analysis using metaRNASeq increased this number substantially. metaRNASeq predicted a total of 629 shared DEGs in the resistant genotypes and 383 DEGs in the susceptible genotypes. This suggested that the meta-analysis increases sensitivity to identify signals and make predictions that would otherwise be lost by examining only DEGs shared between individual analyses of separate experiments.

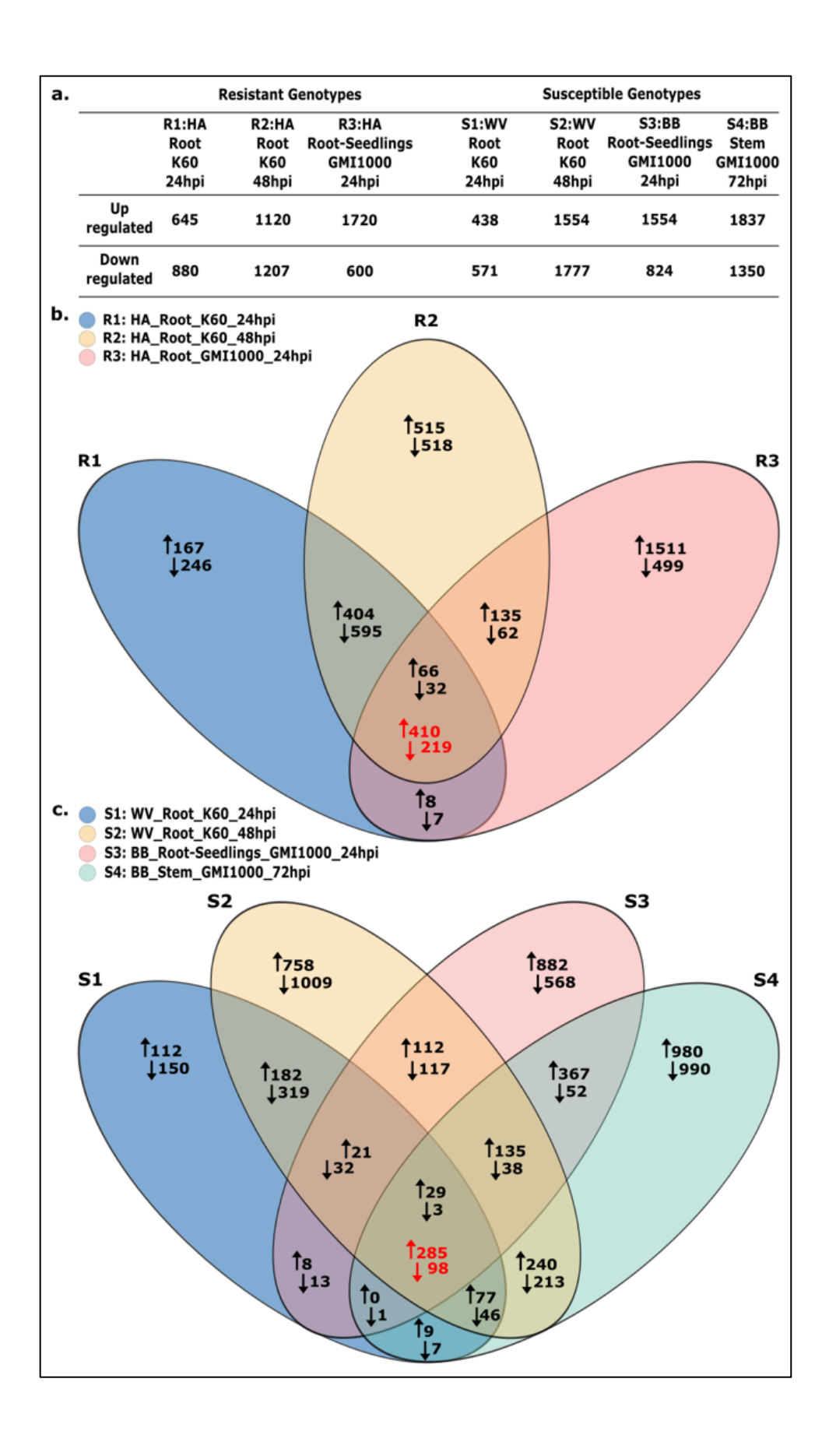


Figure 1. Individual experiments identified similar numbers of DEGs, and the meta-analysis revealed more DEGs than comparing individual analyses. (a) Number of up and downregulated DEGs within each resistant and susceptible tomato genotype. There were no large differences between experiments in the number of DEGs. (b & c) Venn diagrams of up- and downregulated DEGs showing overlap from pairwise comparisons between plant tissues, *Rs* strains and timepoint after inoculation within the responses of resistant and susceptible genotypes respectively. Up and down arrows indicate the up and down regulated DEGs, respectively. Black and red numbers show the overlap of DEGs identified with DESeq2 and metaRNASeq packages respectively. MetaRNASeq revealed more shared DEGs than comparing individual DESeq2 analyses. DEGs were filtered with a fold change cutoff of |1.5|. Abbreviations: HA, wilt-resistant tomato breeding line Hawaii7996; WV, wilt-susceptible tomato line West Virginia 700; BB, wilt-susceptible tomato cultivar 'Bonny Best'.

The largest effect on gene expression was the individual experimental conditions

To determine the effect on overall gene expression of experimental differences such as plant age, genotype, inoculation method, etc., we compared numbers of common DEGs between experimental conditions. As expected, there was a great deal of variation between samples (Figure 2). Indeed, comparing the overlap in DESeq2-predicted DEG's between samples revealed that the experimental conditions were the greatest predictor of the pattern of expression (Table 2). For example, when comparing the DEGs upregulated in resistant HA tomato, sample R1 (resistant roots 24 hours after inoculation with K60) shared the greatest number of DE genes with other datasets from the same experiment, R2, S1, and S2 (41.96%,

57.99%, and 23.49% respectively) but it shared only 4.30% of DEGs with R3 (resistant seedling roots 24 hours after inoculation with GMI1000) (Table 2a). Similarly, susceptible seedling roots shared many more DEGs with resistant seedling roots (70.99% of DEGs) than with susceptible adult roots (13.24% and 19.11% of DEGs) or susceptible adult stem tissue (28.91% of DEGs). This effect was also observed for the downregulated genes (Table 2b). This finding underscores the importance of experimental variables like age, tissue type, inoculation method, or growth conditions for gene expression. However, it also suggests that the DEGs that our meta-analysis identified as shared in resistant and susceptible genotypes are more likely to be important for the tomato response to BWD, as they rise above the large amount of noise between experimental conditions.

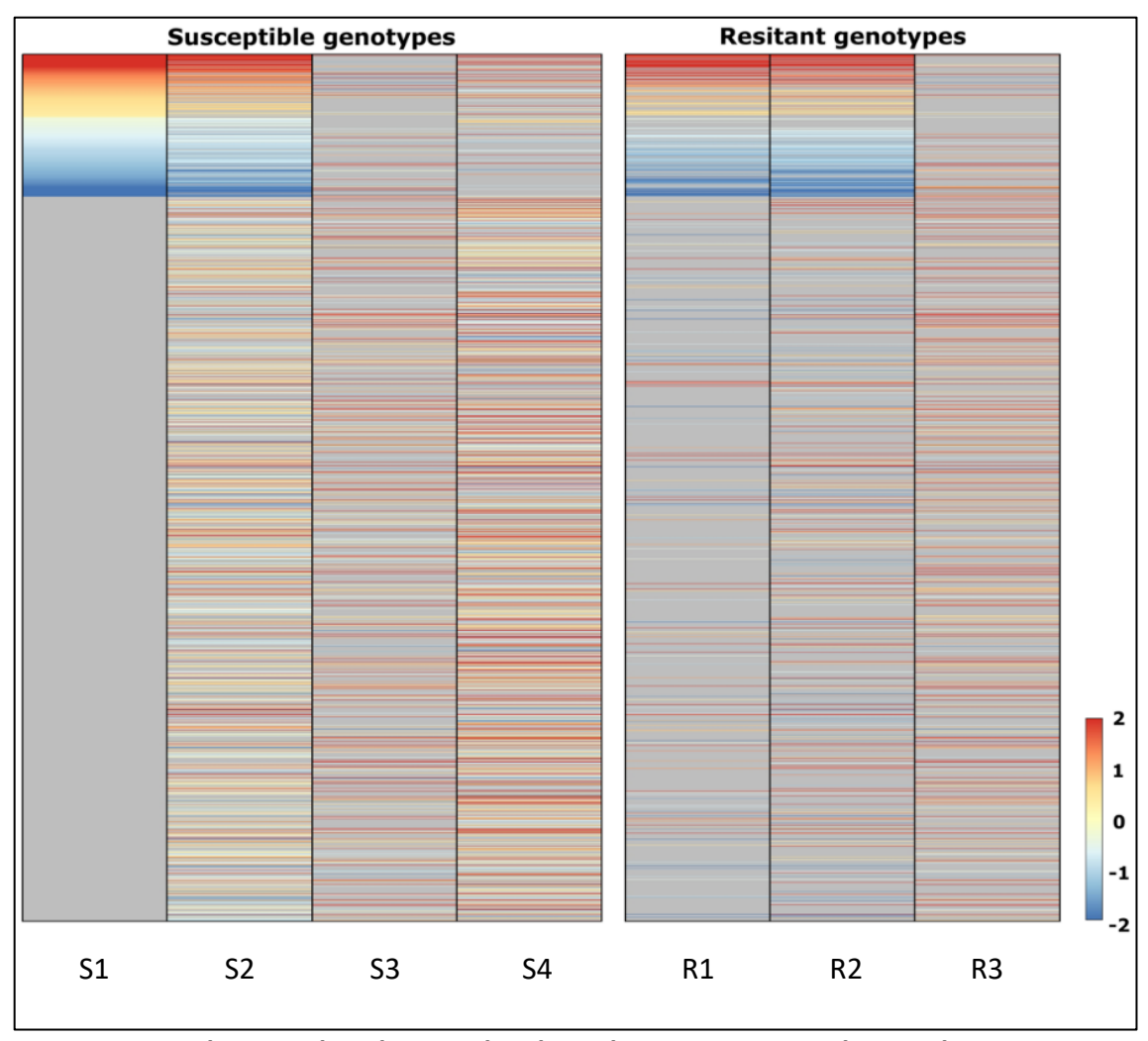


Figure 2. Samples correlated more closely within experiments than within genotypes.

Heatmap illustrating the log2-fold change (Log2 FC) of differentially expressed genes (FDR < 0.05) within each resistant and susceptible genotypes. Heatmap was constructed with R package pheatmap.

a	•

	R1	R2	R3	S1	S2	S3	S4
R1	100.00	72.87	11.47	39.38	56.59	13.64	33.95
R2	41.96	100.00	17.95	22.77	59.29	19.11	46.96
R3	4.30	11.69	100.00	2.79	17.50	70.99	31.69
S1	57.99	58.22	10.96	100.00	70.55	13.24	26.26
S2	23.49	42.73	19.37	19.88	100.00	19.11	30.95
S3	5.66	13.77	78.57	3.73	19.11	100.00	34.17
S4	11.92	28.63	29.67	6.26	26.18	28.91	100.00

b.

	R1	R2	R3	S1	S2	S3	S4
R1	100.00	71.25	4.43	38.30	49.89	5.00	14.55
R2	51.95	100.00	7.79	31.15	61.31	9.78	16.82
R3	6.50	15.67	100.00	7.67	19.67	77.00	7.67
S1	59.02	65.85	8.06	100.00	70.05	8.58	9.98
S2	24.70	41.64	6.64	22.51	100.00	10.69	16.88
S3	5.34	14.32	56.07	5.95	23.06	100.00	11.41
S4	9.48	15.04	3.41	4.22	22.22	6.96	100.00

Table 2. Percentage of differentially expressed genes shared between samples. Values represent the percentage of total DEGs upregulated **(a)** and downregulated **(b)** from each sample in the columns shared by the samples in each row.

MetaRNASeq revealed a potential role of PTI in HA resistance

To better understand tomato defense responses to BWD, we looked for potential immune-related genes shared between the resistant and susceptible responses. One broad category of gene that was highly represented in both groups encode predicted transmembrane pattern recognition proteins (PRRs). PRRs are a class of outer membrane proteins that initiate PTI by recognizing microbe-associated molecular patterns (MAMPs) and transmitting the signal across the membrane, sometimes using an intracellular kinase domain (34). A total of 83

predicted PRRs were differentially regulated in the resistant or susceptible genotypes (Figure 3). Of these, 7 were differentially regulated in all resistant samples, but not in all susceptible samples (Figure 3a), 34 were differentially regulated in all samples (Figure 3b), and 42 were differentially regulated in all susceptible samples but not in all resistant samples (Figure 3c). Of particular interest are 19 predicted PRRs whose response was more intense in the resistant genotypes than in the susceptible genotypes (Figure 3d). These PRR genes may be candidates for further study to understand how resistant tomato varieties overcome *Rs* infection. Thus, our meta-analysis generated specific testable hypotheses to identify mechanisms used by the tomato immune system to recognize and resist *Rs*, as well as the differences between a successful and failed response.

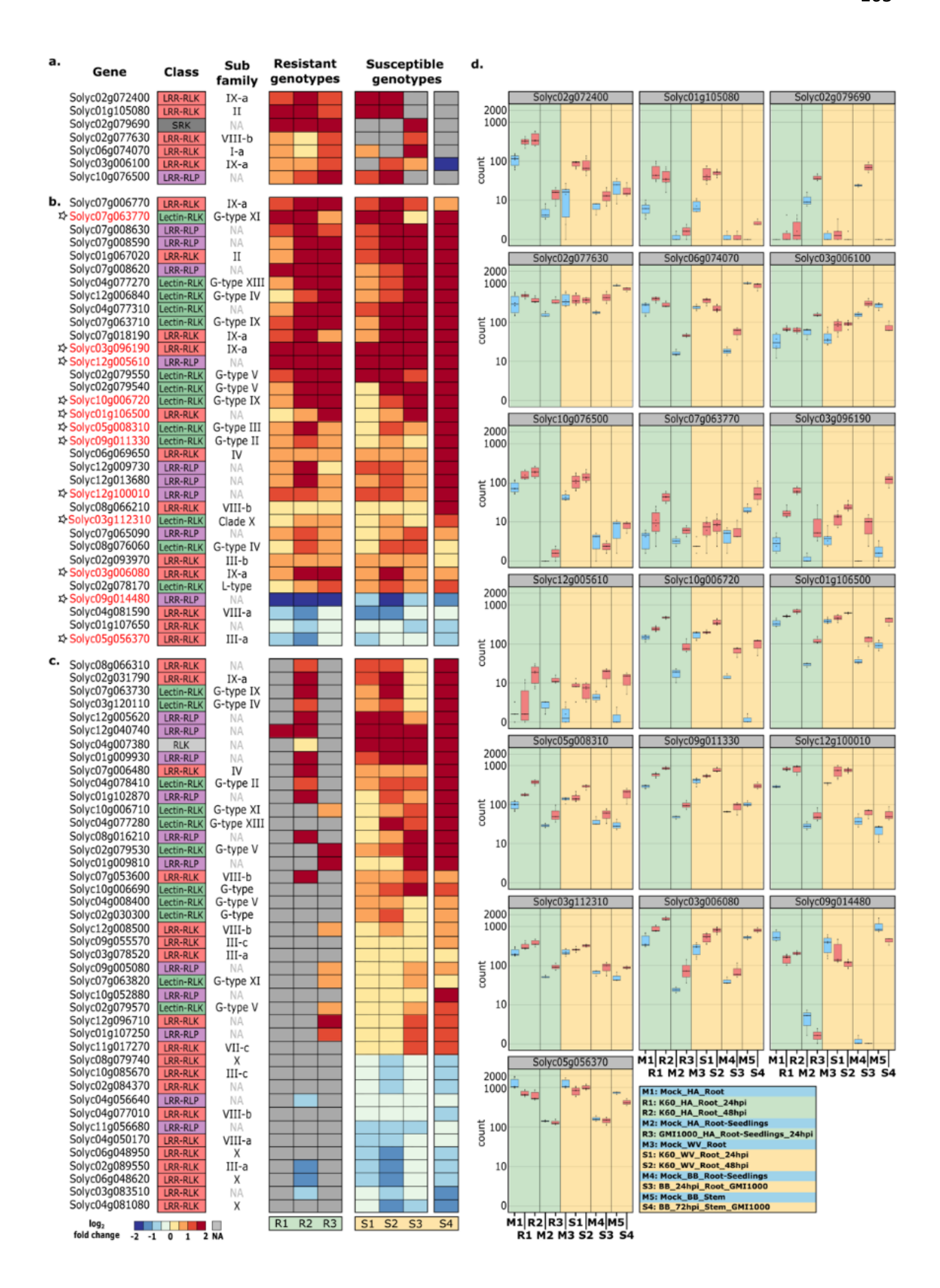


Figure 3. MetaRNASeq revealed membrane-bound Pattern Recognition Receptors that may be involved in tomato defense against bacterial wilt disease. Heatmaps showing the log₂ fold change (LFC) (a., b. and c.) and boxplot showing the counts (d.) of the expression of genes coding for transmembrane putative receptors. Tomato gene locus tags are from the Tomato Genome Consortium 2012 (44). According to the metaRNASeq analysis, genes grouped into 3 clusters. (a) shows the genes induced in every resistant sample, but not in every susceptible sample. (b) shows the genes altered in all resistant and susceptible samples. (c) shows genes altered in every and susceptible sample, but not in every resistant sample. (d) The list of genes selected from the heatmap corresponds to the gene locus tags in panel (a) and the genes in panel (b) labeled with an asterisk. These selected genes show a greater response, either up or down, in the resistant than in the susceptible genotypes.

MetaRNASeq corroborated a role of trehalose and ABA regulation in the tomato response to bacterial wilt disease

If the predictions made by our meta-analysis are valid, the shared resistant and susceptible responses should identify altered expression of pathways that have been independently shown to contribute to tomato responses to BWD. Recent studies found a significant overlap between the physiological and hormonal responses of tomato to BWD and to drought stress (35). The disaccharide trehalose and the hormone abscisic acid (ABA) mediate plant responses to both stressors. Consistent with these functional results, our meta-analysis identified changes across experimental datasets in expression of genes encoding trehalose metabolism, responses to ABA signaling, and plant responses to water stress. For example, five

trehalose-6-phosphate phosphatase genes were significantly downregulated in resistant H7996 under every experimental condition and three predicted ABA-responsive transcription factors were upregulated in all plants in all experimental conditions. In addition, in all conditions the expression of seven genes predicted to encode aquaporins was consistently downregulated. Aquaporins, transmembrane water channel proteins that mediate water homeostasis, play critical roles in plant drought tolerance (36). These observations demonstrate that our meta-analysis can identify independently validated biological responses to BWD.

Discussion

Here, we used a computational method for analyzing multiple transcriptome experiments together to better understand tomato responses to *Rs* infection. Although the three experiments we used had widely varying protocols, covering a range of plant ages, tissue types, inoculation methods, and two different susceptible tomato varieties, metaRNASeq identified common transcriptional changes across both susceptible and resistant varieties as well as changes unique to susceptible or resistant tomato responses (30). That these responses were discerned despite significant experiment-to-experiment noise suggests that they may represent more conserved and possibly more biologically meaningful responses. These results identified a manageable number of potential gene targets for further study.

As a first validation of this analysis, we examined the response of trehalose, ABA, and drought-responsive genes in our analysis. In line with recent work showing that elevated levels of trehalose may help tomato respond to both drought stress and BWD, we found multiple trehalose metabolic genes and ABA responsive genes in our combined resistant and susceptible

responses (35, 37). Interestingly, genes encoding five trehalose-6-phosphate phosphatases, which produce trehalose, were significantly downregulated in resistant HA plants. Future work could measure trehalose levels in root tissue or xylem fluid of HA plants before and after infection to see if this change in gene expression leads to a real change trehalose concentration. Curiously, applying trehalose to susceptible tomato roots increased their resistance to BWD (35). Why resistant plants would downregulate a trehalose synthesis gene in response to *Rs* is unclear, and future experiments could determine if HW resistance is altered by the application of trehalose.

We found a large number of putative PRR genes that respond to *Rs* infection. A subset of these genes had increased expression or induction in the resistant varieties, making them attractive targets for future research. PTI can be an extremely powerful tool for plants responding to pathogens (38). Transferring PRRs between plant families is a useful way of increasing resistance to many pathogens, including *Rs* (39). Transferring the *Arabidopsis* PRR gene EFR, which recognizes the bacterial translation factor Ef-Tu, to tomato not only increased plant recognition of a variety of bacterial pathogens in the lab, but also increased the marketable yield in response to pressure from BWD and bacterial spot disease in the field (6). If experiments show that one or more of the nineteen putative PRRs that respond to *Rs* more strongly in resistant than susceptible tomatoes contribute to HA resistance, these will be promising candidates for future biotechnology applications. However, their function and utility must be validated. First, we can transiently express the putative PRRs in tobacco leaves using *Agrobacterium*. Following expression, we can then test for their ability to produce a ROS burst indicative of PTI after challenge with *Rs*. Should any of the nineteen produce strong responses

to *Rs* in tobacco leaves, we can create composite tomato plant roots overexpressing one or more of the PRRs of interest (40). These plants will can be challenged with *Rs* to see if increasing the expression of the PRR increases their resistance to *Rs*.

Finally, we show that meta-analysis of multiple transcriptomic datasets has the potential to simplify design of future RNA-seq experiments. Increasing the predictive power of individual transcriptomic studies by combining them with existing analyses could be a better use the time and resource costs of each experiment. For example, it would be interesting but resource-intensive to compare the responses of HA plants to resistance-breaking *Rs* strains (such as CMR15 or UW551) to the responses elicited by *Rs* strains that cannot overcome HA resistance (such as GMI1000 and K60). Combined RNA-seq datasets could even reduce the number of samples required in a single experiment, especially if experimental conditions are held constant.

Materials and methods

Plant growth and inoculation

Group A plants were grown and infected as described by French, et al. (26), inoculating 14-17 day old plants by drenching the roots with a suspension of *Rs* strain K60. Group B seedlings were grown and inoculated on agar plates as described by Hamilton, et al. (31), dripping a suspension of *Rs* strain GMI1000 on the seedling root tissue. Group C plants were grown and inoculated as described in Chapter 2 of this thesis by introducing ~2000 CFU of *Rs* strain GMI1000 directly into the xylem of 21-day old tomato plants through a cut petiole. A full list of experimental conditions is detailed in Table 1.

RNA extraction and sequencing

Group A RNA was extracted and sequenced as described by French et al. (26)and Group C RNA was extracted as described in Chapter 2 of this thesis. For Group B, seedling root tissue was ground and used for total RNA extraction using Trizol (Invitrogen, CA). mRNA enrichment, cDNA synthesis, and sequencing on an Illumina HiSeq 2000 were all done by the University of Wisconsin-Madison Biotechnology Center. For all samples, RNA quality was tested using a nanodrop and Agilent Bioanalyzer. A full list of extraction and sequencing conditions can be found in Table 1.

Transcriptome analysis

Raw fastq files from each individual experiment were used in the same analysis pipeline. First, RNA quality was checked using FastQC (v. 0.11.9) and low-quality reads and Illumina sequencing adaptors (TruSeq3-PE-2) were removed using Trimmomatic (v. 0.39). Reads were then mapped onto the *S. lycopersicum* genome using STAR (v. 2.7.4.a) (41). Gene expression was determined using HTSeq (v. 0.11.1) and Samtools (v. 1.10) (42). EdgeR (v. 3.28.0) was used to filter for low counts. Differential gene expression was first calculated using DESeq2 (v. 3.11) using Benjamini-Hochberg FDR multiple testing correction with a P value of 0.05 (33, 43). The P values calculated by DESeq2 were then used in the meta-transcriptomic analysis using metaRNASeq (v. 1.0) with Fisher and inverse normal techniques and a P value of 0.05 (30).

References

- Dong OX, Ronald PC. 2019. Genetic engineering for disease resistance in plants: Recent progress and future perspectives. Plant Physiol 180:26–38.
- 2. Kim BS, French E, Caldwell D, Harrington EJ, Iyer-Pascuzzi AS. 2015. Bacterial wilt disease: Host resistance and pathogen virulence mechanisms. Physiol Mol Plant Pathol 95:37–43.
- 3. Song W, Forderer A, Yu D, Chai J. 2020. Structural biology of plant defence. New Phytol.
- 4. Jones J, Dangl J. 2006. The plant immune system. Nature 444:323–329.
- 5. Thomas NC, Hendrich CG, Gill US, Allen C, Hutton SF, Schultink A. 2020. Roq1 confers resistance to Xanthomonas, Pseudomonas syringae and Ralstonia solanacearum in tomato. Front Plant Sci 11.
- 6. Kunwar S, Iriarte F, Fan Q, Da Silva EE, Ritchie L, Nguyen NS, Freeman JH, Stall RE, Jones JB, Minsavage G V., Colee J, Scott JW, Vallad GE, Zipfel C, Horvath D, Westwood J, Hutton SF, Paret ML. 2018. Transgenic expression of EFR and Bs2 genes for field management of bacterial wilt and bacterial spot of tomato. Phytopathology 108:1402–1411.
- 7. Vasse J, Frey P, Trigalet A. 1994. Microscopic studies of intercellular infection and protoxylem invasion of tomato roots by *Pseudomonas solanacearum*. MPMI 8:241–251.
- 8. Caldwell D, Kim B, Iyer-Pascuzzi AS. 2017. *Ralstonia solanacearum* differentially colonizes roots of resistant and susceptible tomato plants. Phytopathology 107:528–536.
- 9. Hayward AC, Hartman GL. 1994. The hosts of *Pseudomonas solanacearum*, p. 9–24. *In*Bacterial Wilt: The Disease and its Causative Agent, Pseudomonas solanacearum, 1st ed.

 Wallingford, UK.
- 10. Genin S, Denny TP. 2012. Pathogenomics of the Ralstonia solanacearum Species

- Complex. Annu Rev Phytopathol 50:67–89.
- 11. Ailloud F, Lowe TM, Robène I, Cruveiller S, Allen C, Prior P. 2016. In planta comparative transcriptomics of host-adapted strains of Ralstonia solanacearum. PeerJ 2016.
- 12. Huet G. 2014. Breeding for resistances to Ralstonia solanacearum. Front Plant Sci 5:715.
- Mazo-Molina C, Mainiero S, Hind SR, Kraus CM, Vachev M, Maviane-Macia F, Lindeberg M, Saha S, Strickler SR, Feder A, Giovannoni JJ, Smart CD, Peeters N, Martin GB. 2019.
 The Ptr1 locus of Solanum lycopersicoides confers resistance to race 1 strains of Pseudomonas syringae pv. tomato and to Ralstonia pseudosolanacearum by recognizing the type III effectors AvrRpt2 and RipBN. Mol Plant-Microbe Interact 32:946–960.
- 14. Narusaka M, Kubo Y, Hatakeyama K, Imamura J, Ezura H, Nanasato Y, Tabei Y, Takano Y, Shirasu K, Narusaka Y. 2013. Interfamily Transfer of Dual NB-LRR Genes Confers

 Resistance to Multiple Pathogens. PLoS One 8:6–13.
- 15. Grimault V, Prior P, Anaïs G. 1995. A monogenic dominant resistance of tomato to Bacterial Wilt in Hawaii 7996 is associated with plant colonization by *Pseudomonas solanacearum*. J Phytopathol 143.
- 16. Planas-Marquès M, Kressin JP, Kashyap A, Panthee DR, Louws FJ, Coll NS, Valls M. 2019. Four bottlenecks restrict colonization and invasion by the pathogen Ralstonia solanacearum in resistant tomato. J Exp Bot 71:2157–2171.
- 17. Doughty T, Kerkhoven E. 2020. Extracting novel hypotheses and findings from RNA-seq data. FEMS Yeast Res 20:1–7.
- 18. Jiang N, Fan X, Lin W, Wang G, Cai K. 2019. Transcriptome analysis reveals new insights into the bacterial wilt resistance mechanism mediated by silicon in tomato. Int J Mol Sci

- 20:1-21.
- 19. Ghareeb H, Bozsó Z, Ott PG, Repenning C, Stahl F, Wydra K. 2011. Transcriptome of silicon-induced resistance against Ralstonia solanacearum in the silicon non-accumulator tomato implicates priming effect. Physiol Mol Plant Pathol 75:83–89.
- 20. Chen N, Yu B, Dong R, Lei J, Chen C, Cao B. 2018. RNA-Seq-derived identification of differential transcription in the eggplant (Solanum melongena) following inoculation with bacterial wilt. Gene 644:137–147.
- Zuluaga AP, Solé M, Lu H, Góngora-Castillo E, Vaillancourt B, Coll N, Buell CR, Valls M.
 2015. Transcriptome responses to Ralstonia solanacearum infection in the roots of the wild potato Solanum commersonii. BMC Genomics 16:1–16.
- 22. Gao W, Chen R, Pan M, Tang W, Lan T, Huang L, Chi W, Wu W. 2019. Early transcriptional response of seedling roots to Ralstonia solanacearum in tobacco (Nicotiana tabacum L.).

 Eur J Plant Pathol.
- Chen Y, Ren X, Zhou X, Huang L, Yan L, Lei Y, Liao B, Huang J, Huang S, Wei W, Jiang H.2014. Dynamics in the resistant and susceptible peanut (Arachis hypogaea L.) roottranscriptome on infection with the Ralstonia solanacearum. BMC Genomics 15:1–16.
- 24. Prasath D, Karthika R, Habeeba NT, Suraby EJ, Rosana OB, Eapen SJ, Deshpande U, Anandaraj M. 2014. Comparison of the Transcriptomes of Ginger (Zingiber officinale Rosc.) and Mango Ginger (Curcuma amada Roxb.) in Response to the Bacterial Wilt Infection. PLoS One 9:1–12.
- 25. Kelly S, Mun T, Stougaard J, Ben C, Andersen SU. 2018. Distinct Lotus japonicus

 Transcriptomic Responses to a Spectrum of Bacteria Ranging From Symbiotic to

- Pathogenic. Front Plant Sci 9:1–14.
- 26. French E, Kim B-S, Rivera-Zuluaga K, Iyer-Pascuzzi AS. 2018. Whole Root Transcriptomic Analysis Suggests a Role for Auxin Pathways in Resistance to *Ralstonia solanacearum* in Tomato. Mol Plant-Microbe Interact 31:432–444.
- 27. Narancio R, Zorrilla P, Robello C, Gonzalez M, Vilaró F, Pritsch C, Dalla Rizza M. 2013.

 Insights on gene expression response of a characterized resistant genotype of Solanum commersonii Dun. against Ralstonia solanacearum. Eur J Plant Pathol 136:823–835.
- 28. Sinha R, Gupta A, Senthil-Kumar M. 2017. Concurrent Drought Stress and Vascular

 Pathogen Infection Induce Common and Distinct Transcriptomic Responses in Chickpea.

 Front Plant Sci 8:1–18.
- 29. Ishihara T, Mitsuhara I, Takahashi H, Nakaho K. 2012. Transcriptome Analysis of Quantitative Resistance-Specific Response upon Ralstonia solanacearum Infection in Tomato. PLoS One 7.
- 30. Rau A, Marot G, Jaffrézic F. 2014. Differential meta-analysis of RNA-seq data from multiple studies. BMC Bioinformatics 15:1–10.
- 31. Hamilton CD, Steidl OR, Macintyre AM, Hendrich CG, Allen C. 2020. *Ralstonia solanacearum* depends on catabolism of myo-inositol, sucrose, and trehalose for virulence in an infection stage-dependent manner. MPMI.
- 32. Jacobs JM, Babujee L, Meng F, Milling AS, Allen C. 2012. The *in planta* transcriptome of *Ralstonia solanacearum*: conserved physiological and virulence strategies during bacterial wilt of tomato. MBio 3:e00114-12.
- 33. Love MI, Huber W, Anders S. 2014. Moderated estimation of fold change and dispersion

- for RNA-seq data with DESeq2. Genome Biol 15:1–21.
- 34. Macho AP, Zipfel C. 2014. Plant PRRs and the activation of innate immune signaling. Mol Cell 54:263–272.
- 35. Macintyre AM. 2020. The role of trehalose metabolism, signaling, and defense in Ralstonia solanacearum bacterial wilt disease of tomatoes. The University of Wisconsin-Madison.
- 36. Sade N, Vinocur BJ, Diber A, Shatil A, Ronen G, Nissan H, Wallach R, Karchi H, Moshelion M. 2009. Improving plant stress tolerance and yield production: Is the tonoplast aquaporin SITIP2;2 a key to isohydric to anisohydric conversion? New Phytol 181:651–661.
- Lowe-Power TM, Hendrich CG, von Roepenack-Lahaye E, Li B, Wu D, Mitra R, Dalsing BL, Ricca P, Naidoo J, Cook D, Jancewicz A, Masson P, Thomma B, Lahaye T, Michael AJ, Allen C. 2018. Metabolomics of tomato xylem sap during bacterial wilt reveals *Ralstonia solanacearum* produces abundant putrescine, a metabolite that accelerates wilt disease.
 Environ Microbiol 20:1330–1349.
- 38. Huang P-Y, Zimmerli L. 2014. Enhancing crop innate immunity: new promising trends.

 Front Plant Sci 5.
- 39. Lacombe S, Rougon-Cardoso A, Sherwood E, Peeters N, Dahlbeck D, Van Esse HP, Smoker M, Rallapalli G, Thomma BPHJ, Staskawicz B, Jones JDG, Zipfel C. 2010. Interfamily transfer of a plant pattern-recognition receptor confers broad-spectrum bacterial resistance. Nat Biotechnol 28:365–369.
- 40. Hause B, Yadav H. 2020. Creation of composite plants transformation of *Medicago*

- truncatula roots. Model Legum Medicago truncatula 1179–1184.
- 41. Dobin A, Davis CA, Schlesinger F, Drenkow J, Zaleski C, Jha S, Batut P, Chaisson M, Gingeras TR. 2013. STAR: Ultrafast universal RNA-seq aligner. Bioinformatics 29:15–21.
- 42. Li H, Handsaker B, Wysoker A, Fennell T, Ruan J, Homer N, Marth G, Abecasis G, Durbin R.

 2009. The Sequence Alignment/Map format and SAMtools. Bioinformatics 25:2078–

 2079.
- 43. Benjamini Y, Hochberg Y. 1995. Controlling the false discovery rate: A practical and powerful approach to multiple testing. J R Stat Soc Ser B 57:289–300.
- 44. Consortium TG. 2012. The tomato genome sequence provides insights into fleshy fruit evolution. Nature 485:635–641.

Appendix 2

Characterization of seven new phages infecting Ralstonia solanacearum from Bra	
	. i I
	./!!

The material presented in this appendix will be used for the following manuscript in preparation:

Carrión, Y. L. L., Hendrich, C. G., Steidl O., Allen, C. Xavier, A. S. Isolation and characterization of seven novel phages from Brazil.

Contributions: YLLC and ASX isolated the phages. ASX and CGH performed host range experiments and ASX extracted gDNA for sequencing. OS and CGH assembled the genomes. All authors participated in experimental design and data analysis. CGH wrote the text

Abstract

We isolated eight phages that can infect the soil dwelling plant pathogen *Ralstonia* solanacearum (Rs) from tomato fields in the Espírito Santo State of Brazil. All eight phages were able to infect multiple Rs strains but were especially virulent on Brazilian Rs strains. We sequenced the genomes for seven of the eight isolates and found them to be in the family Myoviridae related to the genus Vidavervirus.

Introduction

Bacterial wilt disease caused by members of the *Ralstonia solanacearum* (*Rs*) species complex is a global problem for the production of major crops like potato, tomato, and banana (1, 2). The diversity of the species complex is categorized into four phylotypes, with phylotype I strains originating from Asia, phylotype II strains from the Americas, phylotype III strains from Africa, and phylotype IV strains from Indonesia and Japan (3). While cultural practices like good hygiene and planting resistant varieties can be used to mitigate the damage caused by the disease, there are no viable options for combating the disease once *Rs* has become established in a field (4). Chemical controls like soil fumigation or antibiotic treatment are environmentally destructive, expensive, and generally ineffective (4).

Biocontrol using bacteriophages may provide a method to control bacterial wilt disease. Although many *Rs*-infecting phages have been isolated, none are currently commercially available for use as a biocontrol agents (4, 5). Phage treatment use in real-world settings is often complicated by problems like the evolution of resistance (6, 7). Using a cocktail of multiple phages in a single treatment to reduce the potential for the resistance development

could lead to longer lasting control schemes (6). Isolating and characterizing more *Rs*-infecting phages will provide more options for the choice of biocontrol agents.

Here, we describe the isolation and characterization of eight new phages from the Espírito Santo state of Brazil. We sequenced the genomes of seven of the isolates and found them to be related to the genus *Vidavervirus*.

Results and Discussion

We isolated phages from the soil of tomato fields in the Espírito Santo state of Brazil. We sampled rhizosphere soil from tomato fields known to have high incidence of bacterial wilt disease. Both symptomatic and asymptomatic plants were sampled. Prospective phage isolated from individual plaques formed when filtered soil suspension was applied to a lawn of the *Rs* strain RSB70PC. Plaques were extracted and passaged through RSB70PC three times, each time infecting from a new single plaque to ensure phage purity. We isolated a total of eight phages, and named them F29, F32.2, P36.2, F31, P34.1, F38, and P41.

We characterized the host ranges of these eight phages using a panel of *Rs* isolates from Brazil and around the world, including strains from all four phylotypes (Figure 1). This overlay screen included five phylotype II Brazilian strains that were isolated from the same region of Brazil as the phages. All eight phages were highly virulent on the five Brazilian *Rs* strains, as indicated by large cleared lysis zones on overlay plates at all three phage dilutions (Table 1). We tested these phages ability to lyse four other phylotype II strains. In general, all eight phages were able to infect most of these Phylotype II strains, but to a lesser extent than the Brazilian *Rs* isolates. The only exception was the phylotype IIA strain UW576, originally isolated in the

United States, which was fully resistant to lysis by four of the eight phages (Table 1). Two phylotype I strains were included, GMI1000 and UW672, originally isolated in French Guyana and Cameroon, respectively. While all eight phages could infect GMI1000, UW672 was resistant to four phages. Phylotype III and IV strains were generally more resistant to the Brazilian phages than the other *Rs* test strains. We tested two phylotype III and five phylotype IV isolates. Of these, only one phylotype IV isolate from Japan, UW653, was susceptible to the phages. Overall, these eight phages appeared best adapted to infect and lyse *Rs* phylotype II strains, consistent with the fact that they were isolated from a field in the Americas infested with phylotype II strains.

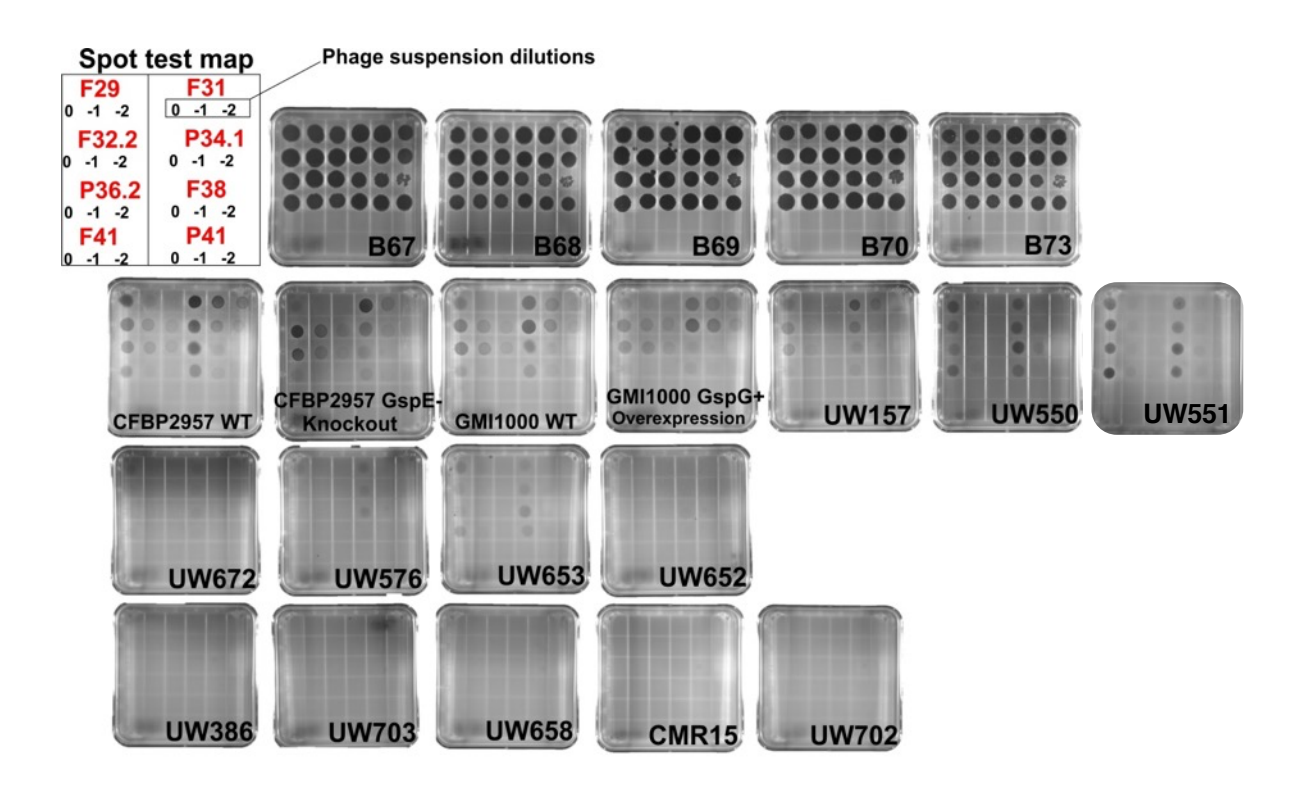


Figure 1. Host range assay. Each test *Rs* strain was grown in a lawn for 24h on rich CPG media plates. Three ten-fold dilutions of each phage were spotted onto the plate in the order shown in the top left. Phylotype identity and origin of each *Rs* candidate host strain is found in Table 1.

Strain	Phylotype	Country of	F29	F32.2	P36.2	F41	F31	P34.1	F38	P41
		origin								
B67	II	Brazil	+++	+++	+++	+++	+++	+++	+++	+++
B68	11	Brazil	+++	+++	+++	+++	+++	+++	+++	+++
B69	II	Brazil	+++	+++	+++	+++	+++	+++	+++	+++
B70	11	Brazil	+++	+++	+++	+++	+++	+++	+++	+++
B73	II	Brazil	+++	+++	+++	+++	+++	+++	+++	+++
CFBP2957	IIA	Martinique,	++	+++	+++	++	+++	+++	++	++
WT		W. Indies								
CFBP2957	IIA		+	+++	+++	+	++	++	+	+
T2SS-										
GMI1000	I	French	+	+++	+++	+	+++	+++	++	++
WT		Guyana								
GMI1000	I		+	+++	+++	-	+++	+++	+	+
T2SS-										
UW157		Peru	+	++	++	-	++	++	+	+

UW550	IIB	The	++	+	+	++	+	+	++	+
		Netherlands								
UW551	IIB	Kenya	++	++	++	++	++	++	++	++
UW672	I	Cameroon	+	-	-	-	+	+	+	-
UW576	IIA	USA	+	-	-	-	+	+	+	-
UW653	IV	Japan	+	+	+	+	+	+	+	+
UW652	IV	Japan	-	-	-	-	-	-	-	-
UW386	III	Nigeria	-	-	-	-	-	-	-	-
UW703	IV	Indonesia	-	-	-	-	-	-	-	-
UW658	IV	Indonesia	-	-	-	-	-	-	-	-
CMR15	III	Cameroon	-	-	-	-	-	-	-	-
UW702	IV		-	-	-	-	-	-	-	-

Table 1. Host range panel details. +++ indicates that all three phage dilutions produced a zone of clearing, ++ the two higher concentrations produced a zone of clearing, + only the highest dilution produced a zone of clearing, and – indicates that no zone of clearing was seen at any concentration.

A previously characterized *Rs*-killing phage from Brazil named phiAP1 requires a functional Type II Secretion System (T2SS) to infect *Rs* (see Chapter 3). To see if any of the eight newly-isolated phages also T2SS-dependent, we tested their ability to lyse two *Rs* mutants that have defective versions of this large cell surface complex. One mutant, CFBP2957 GspE k274a, contains a lysine to alanine mutation in the T2SS inner membrane protein GspE that prevents

GspE from hydrolyzing the ATP that drives the export cargo from the complex. The other mutant, GMI1000 OEgspE, overproduces the major T2SS pseudopilin, GspG, thereby reducing T2SS activity roughly ten-fold. Interestingly, two phage isolates, F29 and F41, had reduced virulence on the GspE mutant (Figure 1). Phage F41 also may be less virulent on the gspG overexpression mutant. Although we have not yet quantified this effect, this suggests that phages F29 and F41 may use the host T2SS during Rs infection.

To genetically characterize the phage isolates, we extracted and sequenced their genomes. We were unable to extract sufficient quantities of gDNA from phage F38, so we excluded it from further analysis. We sequenced and assembled the genomes of the other seven. The sizes of the assembled and polished draft contigs ranged from 80 and 130 kb. All seven contigs were closely related, and each contained over 97.99% bp identity to all other samples (Table 2). Genomes of tailed viruses are linear while in the capsid head, but are often circularized inside their host, often leading to artificially duplicated regions in the sequenced genome (8). Our draft genome sequences contained the same roughly 50 kb sequence repeated twice, suggesting that the true genome size for each phage is much smaller. Further analyses will use restriction digests to determine the true size of the genome, targeted PCR to find potential linearization points, and will predicted ORFs in the draft genomes.

F29	100						
F32.2	98.16	100					
P36.2	99	98.7	100				
F41	99.87	98	99.36	100			
F31	98.19	99.88	98.96	98.01	100		
P34.1	98.62	99.09	99.39	98.79	99.15	100	
P41	99.53	97.99	99.33	99.86	97.99	98.82	100
	F29	F32.2	P36.2	F41	F31	P34.1	P41

Table 2. Bp identity between phage genomes. Values represent percent base pair identity between the two genome sequences as measured by BLAST.

Methods

Bacterial isolates and culture conditions

Rs were routinely cultured in CPG (1g/L casamino acids, 10g/L peptone, 5g/L glucose, 1g/L yeast extract) (9). Unless used for soft agar, 1.6% agar was included for solid plates. Rs were cultured at 28 C. All phages were cultured and propagated as described in (10).

Detection, isolation and propagation of bacteriophages

Soil samples were collected from tomato fields in Venda Nova do Imigrante and Afonso Claúdio municipalities, Espírito Santo state, Brazil. The samples were collected in areas with known incidence of bacterial wilt, sampling rhizosphere soil of both symptomatic and

asymptomatic plants. To detect the presence of bacterial viruses, approximately one gram of soil was resuspended in 2 mL of distilled water. The suspension was then centrifuged at 12,000 rpm for 5 min and then filtered through a 0.22 μm PVDF membrane filter (Analítica). 100 μL of the filtrate were Spot tested using standard soft agar overlay method (11) with the capsuledefective Rs strain RSB70PC used as host. A single lysis plaque was picked and amplified in the presence of RSB70PC in CPG. The bacterial cells were centrifuged, the supernatant filtered, and isolated lysis plaques were obtained using the soft agar overlay method. This procedure was repeated three times to ensure bacteriophage purity. For bacteriophage propagation, 1 L of a RSB70PC culture (optical density at 600 nm of 0.2) was infected at a multiplicity of infection (MOI) of 1.0 and incubated until clear lysis. After incubation cell debris were removed by centrifugation at 4 C for 5 min. The supernatant was passed through a 0.22 µm PVDF membrane filter followed by an overnight precipitation with polyethylene glycol 6000 (5% wt/vol) and 0.5M NaCl. The pellet was recovered by centrifugation at 12,000 rpm at 4 C for 30 minutes and resuspended in SM buffer (50 mM Tris-HCl pH 7.5, 100 mM NaCl, 10 mM MgSO₄, 0.01% gelatin). Partially-purified particles were stored at 4 C.

Phage host-range

Phage susceptibility was determined as described previously (10). Overlay plates were created with top layers of soft CPG containing 0.75% agarose and each *Rs* strain. Then, 4 uL of three ten-fold phage dilutions were spotted onto the top agar. Plaque formation was observed after a 24-hour period of growth at 28°C.

Genomic DNA extraction and sequencing

Cultures of Rs strain CFBP2957 grown in CPG were inoculated with each phage as described previously (10). Once lysis was visible, the solution was passed through a 0.2 um filter to remove live bacterial cells. 1 mL of filtered lysate was used for gDNA extraction with the Norgen Phage DNA Isolation Kit according to the manufacturer's instructions (Norgen, Thorold, ON, Canada). DNA concentration and purity were assessed spectrophotometrically, and the sequencing was done at the Iowa State DNA Sequencing Facility. Quality and fragment size were determined using AATI Fragment Analyzer (Agilent, Santa Clara, CA, USA), and smaller fragments were removed using an AmPure cleanup (Beckman Coulter, Indianapolis, IN, USA). Genome sequencing was done using an Oxford Nanopore GridIONx5 sequencing machine (Oxford Nanopore, Oxford, UK). Sequences were read and bases called using the GridION programs MinKNOW (v 3.6.5), Bream (v 4.3.16), and Guppy (3.2.10). Read quality was assessed using FastQC, and the reads were assembled using Canu (v2.0) (12). The predicted genome size was set to 100 kbp, the corrected error rate set to 0.13, and the corrected output coverage set to 190, with the exception of P41, whose output coverage was set to 250. The assembly was then further refined using Nanopolish (13).

References

- 1. Elphinstone J. 2005. The current bacterial wilt situation: a global overview., p. 9–28. *In* Allen, C, Prior, P, Hayward, AC (eds.), Bacterial Wilt: The Disease and the *Ralstonia solanacearum* Species Complex. Society, American Phytopathological, St Paul, MN.
- 2. Hayward AC, Hartman GL. 1994. The hosts of *Pseudomonas solanacearum*, p. 9–24. *In* Bacterial Wilt: The Disease and its Causative Agent, Pseudomonas solanacearum, 1st ed. Wallingford, UK.
- 3. Genin S, Denny TP. 2012. Pathogenomics of the *Ralstonia solanacearum* species complex. Annu Rev Phytopathol 50:67–89.
- 4. Yuliar, Nion YA, Toyota K. 2015. Recent trends in control methods for bacterial wilt diseases caused by *Ralstonia solanacearum*. Microbes Environ 30:1–11.
- 5. Álvarez B, López MM, Biosca EG. 2019. Biocontrol of the Major Plant Pathogen *Ralstonia* solanacearum in Irrigation Water and Host Plants by Novel Waterborne Lytic Bacteriophages 10:1–17.
- 6. Wang X, Wei Z, Yang K, Wang J, Jousset A, Xu Y, Shen Q, Friman VP. 2019. Phage combination therapies for bacterial wilt disease in tomato. Nat Biotechnol 37:1513–1520.
- 7. da Silva Xavier A, de Almeida JCF, de Melo AG, Rousseau GM, Tremblay DM, de Rezende RR, Moineau S, Alfenas-Zerbini P. 2019. Characterization of CRISPR-Cas systems in the *Ralstonia solanacearum* species complex. Mol Plant Pathol 0:223–239.
- 8. Casjens SR, Gilcrease EB. 2009. Determining DNA packaging strategy by analysis of the termini of the chromosomes in tailed-bacteriophage virions. Methods Mol Biol 502:91–111.
- 9. Hendrick CA, Sequeira L. 1984. Lipopolysaccharide-defective mutants of the wilt pathogen *Pseudomonas solanacearum*. Appl Environ Microbiol 48:94–101.
- da Silva Xavier A, da Silva FP, Vidigal PMP, Lima TTM, de Souza FO, Alfenas-Zerbini P.
 2018. Genomic and biological characterization of a new member of the genus
 Phikmvvirus infecting phytopathogenic *Ralstonia* bacteria. Arch Virol.
- 11. Adams MH. 1959. Bacteriophages. Interscience Publishers, Inc, New York.
- 12. Koren S, Walenz BP, Berlin K, Miller JR, Bergman NH, Phillippy AM. 2017. Canu: scalable and accurate long-read assembly via adaptive k-mer weighting and repeat separation. Genome Res 27:722–736.
- 13. Loman NJ, Quick J, Simpson JT. 2015. A complete bacterial genome assembled de novo

using only nanopore sequencing data. Nat Methods 12:733–735.